Chemical studies on bitter acid oxides derived from hops (*Humulus lupulus* L.) in beer brewing and storage

Yoshimasa Taniguchi

2017

Contents

Introduction

Hops (*Humulus lupulus* L.) are an essential ingredient of beer production that add characteristic bitterness and aroma to beer. The bitter taste and flavor of beer originates from resins and essential oils that accumulate in the lupulin glands of the female inflorescences of hops.[1] Hop resins are further divided into two sub-categories according to their solubility in organic solvent: namely, soft resin (i.e., the fraction that is soluble in low-boiling paraffin hydrocarbons such as *n*-hexane) and hard resin (i.e., the fraction that is insoluble in *n*-hexane but soluble in ether and cold methanol).[2-4] The chemical composition of the resins and essential oils differs depending on the hop variety, and also changes during hop storage.[5-11] Furthermore, the chemical reactions that occur during both the brewing process and beer aging drastically change the composition of substances derived from the resins and essential oils.[12-17] Thus, the nature and reactivity of the compounds related to hop resins and oils are important subjects within the scientific community and have been extensively studied over the years.[18-20]

The α- and β-acids, the most well-studied groups of compounds in hops, are found in the soft resin fraction. Both groups comprise three main congeners, which differ in their acyl side chains [α-acids: cohumulone (**1a**), humulone (**1b**), and adhumulone (**1c**); β-acids: colupulone (**2a**), lupulone (**2b**), and adlupulone (**2c**)] (Figure 1). During the wort boiling process, α-acids thermally isomerize to generate two epimeric isomers: namely, *cis*-iso-α-acids (**3a–c**) and *trans*-iso-α-acids (**4a–c**) (Figure 1).[21] Approximately 50–70% of α-acids are converted to iso-α-acids in this process, and the ratio of the resulting *cis*/*trans* isomers is typically 70/30.[12, 20, 22]

Iso-α-acids are the main contributors to the bitter taste of beer,[5, 23] and the stability of beer foam.[24] However, β-acids form oxidative transformation products, such as hulupones (**5a–c**) (Figure 1), during the wort boiling process that contribute to the bitter taste of beer to a minor extent.[25, 26] The molecular transformation of iso-α-acids during beer aging has received considerable attention, because the degradation of these

compounds strongly influences the bitter taste of beer and generates an off-flavor.[17, 27-29] The stability of iso-α-acids depends on their stereochemistry such that *trans* isomers are more unstable than *cis* isomers. Intelmann *et al.*[30, 31] demonstrated that the instability of *trans* isomers results from a non-oxidative proton-catalyzed cyclization reaction that is specific to *trans* isomers and is driven by the rather low pH (~4.5) of beer, and suggested that the resulting changes are responsible for the harsh and lingering bitter taste of aged beer.

As mentioned above, numerous studies have focused on the soft-resin-derived bitter acids (i.e., α-, β-, and iso-α-acids) and their impact on the properties of beer. In contrast, however, only a little information is available on the components of hard resin, and there has been no consensus on their contribution to beer quality.[9, 23, 32-34] Xanthohumol, a prenyl flavonoid, is a well-known compound of hard resin.[4] Very recently, several novel xanthohumol derivatives were identified in the non-polar fraction of the hard resin from spent hops (i.e., the residue from the supercritical carbon dioxide extraction of hops), and were shown to contribute, together with iso-α-acids, to the bitter taste of pilsner-type beer.[35] In addition to these prenylated flavonoid derivatives, oxidation products derived from α-acids and/or β-acids have been considered to be the main constituents of hard resin, especially in hops not stored under a vacuum state,[4, 36] because, when hops are stored in contact with air, the content of α- and β-acids rapidly decreases due to oxidation together with an increase in the amount of the hard resin fraction.[8, 34]

There have been many reports that oxidized hops containing little or no detectable α-acids had a bittering potential indistinguishable from fresh hops,[32, 37, 38] although other studies have reported that beer brewed with oxidized hops tasted mildly bitter or markedly less bitter.[9, 23, 39] It is considered that detailed information on the chemical composition of oxidized hops used in brewing could help to determine their influence on beer quality. However, there have been very few reports on the oxidation products of

α-acids and β-acids in hops, including changes in their amount during hop storage, because the complexities of the oxidation products hamper identification of each component.

Although many studies have reported the identification of products obtained through chemical oxidation of isolated α-acids or β-acids, their occurrences in oxidized hops have remained uncertain. For example, humulinones (**6a–c**) (Figure 1) can be readily prepared when α-acids are treated with peroxide reagent in a two phase solvent system;[40, 41] however, their occurrence in oxidized hops has not been confirmed due to a lack of suitable analytical methods.[32, 42-45] The presence of certain oxidation products obtained by chemical oxidation of α-acids, such as *cis*- (**7a–c**) and *trans*-humulinic acids (**8a–c**), tricyclodehydroisohumulone (**9**), and Ashurst's compound (**10**) (Figure 1), in oxidized hops have been previously reported,[46-48] however, experimental results using low resolution HPLC or TLC methods should be reconfirmed using high resolution analyses.

Detailed analyses of the chemical composition of the raw hop material are important, however, oxidative transformation of α-acids and β-acids occurring in the raw hop material during its storage are still not clear. Furthermore, the chemical transformations and compositional changes of oxidation products derived from α-acids and β-acids that occur during beer production and aging are totally unknown. To evaluate the influence of oxidation products of α-acids and β-acids on beer quality, such as bitterness character, foam stabilization, and anti-bacterial effects, studies to identify oxidation products in hops and to characterize their chemical changes during the wort boiling process and fermentation, as well as during aging of the finished beer, are essential.

Other than brewing industry, hops have been used for herbal medicines over many years.[49, 50] Among the components in hops, bitter acids have also received considerable attention because of their potential health benefits.[49] The α-acids and β-acids have been

reported to possess various biological activities, such as anti-cancer,[51-53] anti-inflammatory,[54-56] and anti-oxidation activities.[57-59] An isomerized hop extract, which primarily consists of iso-α-acids, was shown to prevent diet-induced obesity by the modulation of lipid metabolism in the liver and inhibition of intestinal lipid absorption.[60] Thus, utilization of hop bitter acids for health promotion may be expected. However, development of functional foods or supplements containing α-, β- and/or iso-α-acids as bioactive ingredients is technically challenging due to the instability of these compounds.

In contrast to bitter acids, there are very few published studies on the physiological effects of oxidized degradation products of bitter acids.[61] In order to evaluate the effects of bitter acid oxides on their potential health benefits as well as beer quality, the chemical structures of the main constituents of bitter acid oxides must be determined. Furthermore, it is essential to develop methods to selectively prepare and analyze the bitter acid oxide fraction, which exclude other hop constituents such as polyphenols, lipids, waxes, and polysaccharides.

The aim of this study was, therefore, to chemically characterize bitter acid oxides in hops and their transformation products occurring during the beer production and aging and to develop analytical and preparative methods for bitter acid oxides, which could lead to evaluating and optimizing the effects of bitter acid oxides on beer quality as well as potential health benefits. First, the author has developed a high resolution HPLC method suitable for simultaneous separation and quantitation of principal bitter acid oxides which occur during the storage of hops and their chemical structures have been elucidated. Then, their further transformations occurring during the wort boiling and beer aging have been investigated by model experiments. Some bitter acid oxides have been shown to be unstable and transformed into more stable compounds in these two processes, and transformation pathways have been found to be different between the two processes. Finally, the author has established a simple liquid-liquid extraction method to obtain the total bitter acid oxide fraction excluding other hop constituents. A quantitative analytical

methodology for whole bitter acid oxides including minor ones has been developed and validated.

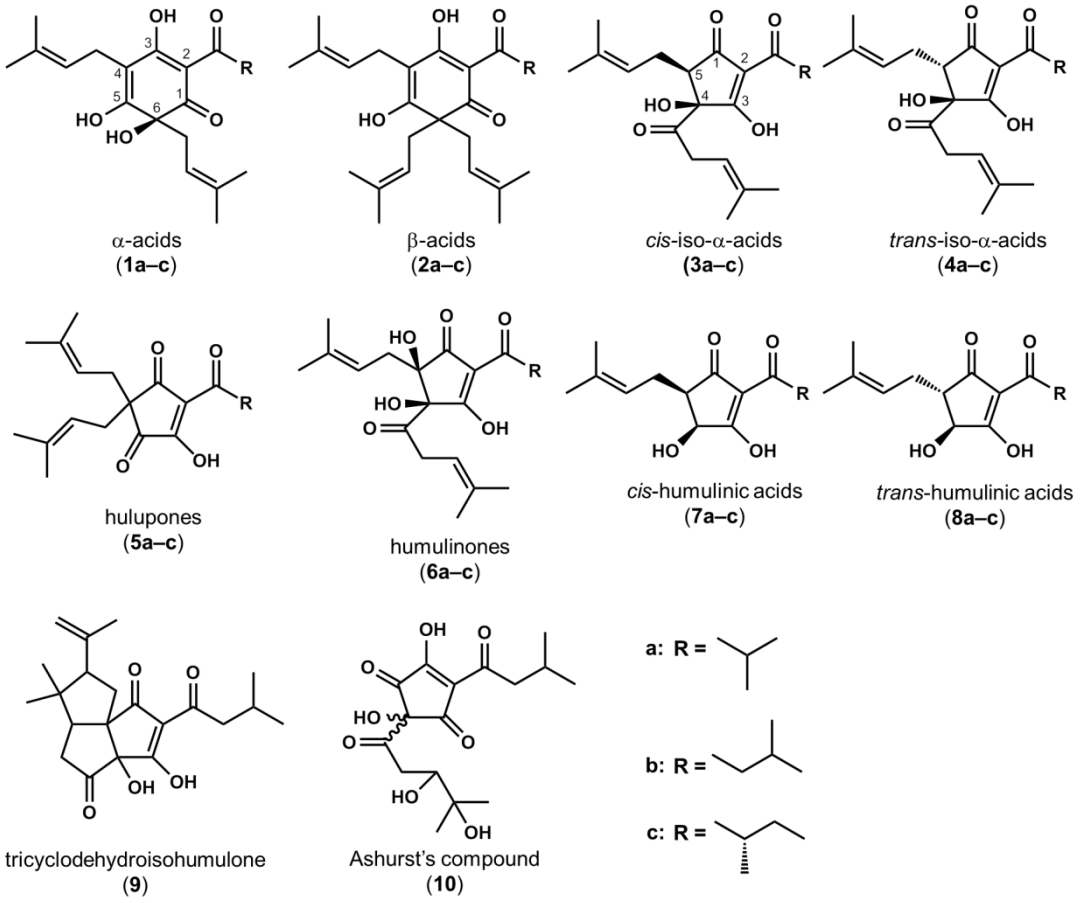

Figure 1. Chemical structures of compounds **1**–**10**.

α-Acids, cohumulone (**1a**), humulone (**1b**), and adhumulone (**1c**); β-acids, colupulone (**2a**), lupulone (**2b**), and adlupulone (**2c**); *cis*-iso-α-acids, *cis*-isocohumulone (**3a**), *cis*-isohumulone (**3b**), and *cis*-isoadhumulone (**3c**); *trans*-iso-α-acids, *trans*-isocohumulone (**4a**), *trans*-isohumulone (**4b**), and *trans*-isoadhumulone (**4c**); hulupones, cohulupone (**5a**), hulupone (**5b**), and adhulupone (**5c**); humulinones, cohumulinone (**6a**), humulinone (**6b**), and adhumulinone (**6c**); *cis*-humulinic acids, *cis*-cohumulinic acid (**7a**), *cis*-humulinic acid (**7b**), and *cis*-adhumulinic acid (**7c**); *trans*-humulinic acids, *trans*-cohumulinic acid (**8a**), *trans*-humulinic acid (**8b**), and *trans*-adhumulinic acid (**8c**); tricyclodehydroisohumulone (**9**); and Ashurst's compound (**10**).

Chapter 1

Identification and quantitation of the major oxidation products derived from α-acids and β-acids during storage of hops

It is well known that α-acids and β-acids are oxidized rapidly during hop storage. However, there have been very few reports on the oxidation products of α-acids and β-acids in hops, including changes in their amount during hop storage, because the complexities of the oxidation products hamper identification of each component. In this chapter, the author has developed a high-performance liquid chromatography (HPLC) analysis method suitable for separation and quantitation of the oxidation products. In addition, the author has succeeded in tracing and identifying the major oxidation products derived from α- and β-acids using this method.

Materials and methods

Chemicals and materials.

The following chemicals were obtained commercially: ethylenediaminetetraacetic acid (EDTA), phosphoric acid, acetonitrile, ethanol, hexane, ethyl acetate, toluene, diethyl ether, *o*-phenylenediamine (Wako Pure Chemicals, Osaka, Japan); dicyclohexylamine (Aldrich, St. Louis, MO, USA); cumene hydroperoxide (Tokyo Chemical Industry, Tokyo, Japan); International Calibration Extract ICE2 (American Society of Brewing Chemists, St. Paul, MN, USA). Deionized water for chromatography was purified by means of a Milli-Q Gradient A10 system (Millipore, Billerica, MA, USA). Hop pellets**,** cultivar Hallertau Perle, supercritical carbon dioxide hop extracts and isomerized hop extracts were purchased from Hopsteiner (Mainburg, Germany).

Preparation of α-acids (mixtures of 1a–c) and pure humulone (1b).

Two hundred g of supercritical carbon dioxide hop extracts [α-acids 55.6% (w/w)

This chapter is reproduced in part with permission from [*J. Agric. Food Chem.* **2013**, *61*, 3121-3130.].

and β-acids 22.6% (w/w)] were dissolved in hexane (1.5 L), and partitioned with 0.24 M disodium carbonate (2 L). In this process, α-acids were selectively extracted into the aqueous solution. The aqueous solution was acidified with 6 N HCl and free α-acids were extracted with hexane. After washing with sat. NaCl, the hexane layer was dried over anhydrous sodium sulfate and concentrated to dryness to give the α-acids fraction (105 g). HPLC analysis confirmed that the purity of α-acids (sum of **1a–c**) in this fraction was more than 90%. Pure humulone (**1b**) was prepared from the above α-acids fraction according to a previously reported method,[40] with small modifications. In brief, 50 g of the α-acids fraction was dissolved in toluene (150 mL). *o*-Phenylenediamine (11.5 g) was added to the solution and heated at 80 °C to dissolve the reagent completely. The solution was then cooled at 4 °C, and the generated precipitate (*o*-phenylenediamine/humulone complex) was collected by filtration and further purified via recrystallization using toluene (8 times) to give pure *o*-phenylenediamine/humulone complex (13.6 g). The complex was added to 2 N HCl (100 mL), and free humulone was extracted with ethyl acetate (250 mL). After washing with sat. NaCl, the ethyl acetate layer was dried over anhydrous sodium sulfate and concentrated to dryness to give humulone (**1b**, 10.1 g). The purity of **1b** was more than 98% by HPLC analysis.

Humulone (**1b**, Figure 1): pale yellow solid; UV (0.1 N HCl-MeOH) λ_{max} 235, 284, 323, and 355 (shoulder) nm, UV (0.1 N NaOH-MeOH) λ_{max} 226, 327, and 358 (shoulder) nm; HRESIMS (negative) *m/z* 361.2015 $[M - H]^-$ (calcd for $C_{21}H_{29}O_5$, 361.2021); ^1H NMR (400 MHz, CD_3OD) and ^{13}C NMR (100 MHz, CD_3OD) spectra were identical to the literature data.[62]

Synthesis of humulinones (mixtures of 6a–c) and pure humulinone (6b).

Humulinones (**6a–c**) and humulinone (**6b**) were prepared from the α-acids fraction described above and humulone, respectively, according to a protocol reported previously.[40] In brief, the α-acids fraction (1.0 g) and cumene hydroperoxide (0.5 mL)

were dissolved in diethyl ether (5 mL). Sat. sodium bicarbonate (35 mL) was added to the diethyl ether solution, and the bi-layer was kept for 4 days at room temperature in a sealed flask. Sodium salts of humulinones were deposited at the border of the bi-layer under these conditions. The sodium salts were filtered and washed with cold diethyl ether and water. The washed sodium salts (600 mg) were then dissolved in MeOH (60 mL) containing 1% phosphoric acid, and 0.5 N HCl (600 mL) was added to the solution. The solution was then partitioned with hexane (600 mL × 2), and the hexane layer was concentrated to dryness to give humulinones (**6a–c**, 550 mg) at a purity of more than 95 % (sum of **6a–c**) by HPLC analysis. Humulinone (**6b**, 480 mg) was prepared from humulone (1.0 g) according to the same procedure described above at a purity of more than 98 % by HPLC analysis.

Humulinone (**6b**, Figure 1): white solid; UV (0.1 N HCl-MeOH) λ_{max} 226, and 282 nm, UV (0.1 N NaOH-MeOH) λ_{max} 254, and 270 (shoulder) nm; HRESIMS (negative) *m/z* 377.1964 $[M - H]^-$ (calcd for $C_{21}H_{29}O_6$, 377.1970); ^{1}H NMR (400 MHz, CD_3OD, COSY) and ^{13}C NMR (100 MHz, CD_3OD, HMQC, HMBC) data are given in Table 1.

Synthesis of hulupones (mixtures of 5a–c) and preparation of pure cohulupone (5a).

Two hundred g of supercritical carbon dioxide hop extracts [β-acids 41.6% (w/w) and trace amounts of α-acids] were dissolved in hexane (1 L), and partitioned with 0.6 M sodium hydroxide (2 L). β-Acids were selectively distributed to the aqueous solution. The aqueous solution was acidified with 6 N HCl, and free β-acids were extracted with hexane. After washing with sat. NaCl, the hexane layer was dried over anhydrous sodium sulfate and concentrated to dryness to give the β-acids fraction (92 g). The purity of the β-acids (sum of **2a–c**) in this fraction was more than 85% by HPLC analysis. Hulupones (**5a–c**) were synthesized from the above β-acids fraction according to a previously reported method.[63] The purity of the prepared hulupones (sum of **5a–c**) was more than 95% by HPLC analysis. Cohulupone (**5a**, 360 mg) was purified from the above

hulupones (800 mg) by preparative HPLC [column: 150 × 10 mm id, 5 μm, Alltima C_{18} column (Systech, Tokyo, Japan); solvent: H_2O/ H_3PO_4 (85%), 100/1 (v/v) (solvent A) and acetonitrile (solvent B), isocratic elution at 60% B; flow rate: 4.7 mL/min; detect: 270 nm; temperature: 40 ˚C; t_R: 10.4 min]. The purity of **5a** was more than 98% by HPLC analysis.

Cohulupone (**5a**, Figure 1): yellow waxy solid; UV (0.1 N HCl-MeOH) λ_{max} 279 nm, UV (0.1 N NaOH-MeOH) λ_{max} 255, and 328 nm; HRESIMS (negative) *m/z* 317.1752 $[M - H]^-$ (calcd for $C_{19}H_{25}O_4$, 317.1759); ^{1}H NMR (400 MHz, CD_3OD) and ^{13}C NMR (100 MHz, CD_3OD) spectra were identical to the literature data.[26]

Preparation of *cis*- and *trans*-iso-α-acids (3a–c and 4a–c).

Each *cis*- and *trans*-iso-α-acid was isolated according to previously reported methods,[62, 64] with small modifications. In brief, 100 mL of isomerized hop extract [iso-α-acids about 30% (w/v)] was added to 1 N HCl (1 L) and partitioned with hexane (250 mL × 2). The hexane layer was concentrated to dryness (36 g), and redissolved in ethyl acetate (100 mL). Dicyclohexylamine (16 g) was added to the solution to precipitate *trans* isomers.

The precipitate (dicyclohexylamine/*trans*-iso-α-acids complex) was collected by filtration and further purified by recrystallization from EtOH, followed by preparative HPLC [column: 150 × 10 mm id, 5 μm, Alltima C_{18} column; solvent: H_2O/ H_3PO_4 (85%), 100/1 (v/v) (solvent A) and acetonitrile (solvent B), isocratic elution at 65% B; flow rate: 4.7 mL/min; detect: 270 nm; temperature: 40 ˚C] as the final step. In the preparative HPLC, the *trans*-iso-α-acids were eluted separately at 9.5 min (**4a**, 218 mg), 12.1 min (**4b**, 188 mg), and 13.2 min (**4c**, 45 mg).

The filtrate of the above precipitation, which contained mainly *cis*-iso-α-acids and dicyclohexylamine, was added to 1 N HCl (300 mL), and partitioned in a separating funnel to remove dicyclohexylamine. The ethyl acetate layer was concentrated to dryness

to yield the mixture of *cis*-iso-α-acids. Each *cis*-iso-α-acid was finally isolated by preparative HPLC (using the same conditions applied to *trans*-iso-α-acids isolation). In the preparative HPLC, the *cis*-iso-α-acids were eluted separately at 10.2 min (**3a**, 193 mg), 13.1 min (**3b**, 254 mg), and 14.4 min (**3c**, 51 mg). The purity of each isolated compound was more than 95% by HPLC analysis.

Cis-isocohumulone (**3a**, Figure 1): pale yellow oil; UV (0.1 N HCl-MeOH) λ_{max} 220, and 264 nm, UV (0.1 N NaOH-MeOH) λ_{max} 254, and 270 (shoulder) nm; HRESIMS (negative) *m/z* 347.1859 $[M - H]^-$ (calcd for $C_{20}H_{27}O_5$, 347.1864); ^{1}H NMR (400 MHz, CD_3OD, COSY) and ^{13}C NMR (100 MHz, CD_3OD, HMQC, HMBC) spectra were identical to the literature data.[62]

Cis-isohumulone (**3b**, Figure 1): pale yellow oil; UV (0.1 N HCl-MeOH) λ_{max} 220, and 273 nm, UV (0.1 N NaOH-MeOH) λ_{max} 254, and 270 (shoulder) nm; HRESIMS (negative) *m/z* 361.2015 $[M - H]^-$ (calcd for $C_{21}H_{29}O_5$, 361.2021); ^{1}H NMR (400 MHz, CD_3OD, COSY) and ^{13}C NMR (100 MHz, CD_3OD, HMQC, HMBC) spectra were identical to the literature data,[62] and are given in Table 1.

Cis-isoadhumulone (**3c**, Figure 1): pale yellow oil; UV (0.1 N HCl-MeOH) λ_{max} 223, and 269 nm, UV (0.1 N NaOH-MeOH) λ_{max} 255, and 273 (shoulder) nm; HRESIMS (negative) *m/z* 361.2015 $[M - H]^-$ (calcd for $C_{21}H_{29}O_5$, 361.2021); ^{1}H NMR (400 MHz, CD_3OD, COSY) and ^{13}C NMR (100 MHz, CD_3OD, HMQC, HMBC) spectra were identical to the literature data.[62]

Trans-isocohumulone (**4a**, Figure 1): colorless crystal; UV (0.1 N HCl-MeOH) λ_{max} 220, and 270 nm, UV (0.1 N NaOH-MeOH) λ_{max} 253, and 270 (shoulder) nm; HRESIMS (negative) *m/z* 347.1860 $[M - H]^-$ (calcd for $C_{20}H_{27}O_5$, 347.1864); ^{1}H NMR (400 MHz, CD_3OD, COSY) and ^{13}C NMR (100 MHz, CD_3OD, HMQC, HMBC) spectra were identical to the literature data.[62]

Trans-isohumulone (**4b**, Figure 1): colorless crystal; UV (0.1 N HCl-MeOH) λ_{max} 220, and 277 nm, UV (0.1 N NaOH-MeOH) λ_{max} 253, and 272 (shoulder) nm; HRESIMS

(negative) *m/z* 361.2014 $[M - H]^-$ (calcd for $C_{21}H_{29}O_5$, 361.2021); ^1H NMR (400 MHz, CD_3OD, COSY) and ^{13}C NMR (100 MHz, CD_3OD, HMQC, HMBC) spectra were identical to the literature data,[62] and are given in Table 1.

Trans-isoadhumulone (**4c**, Figure 1): colorless crystal; UV (0.1 N HCl-MeOH) λ_{max} 220, and 275 nm, UV (0.1 N NaOH-MeOH) λ_{max} 254, and 272 (shoulder) nm; HRESIMS (negative) *m/z* 361.2015 $[M - H]^-$ (calcd for $C_{21}H_{29}O_5$, 361.2021); ^1H NMR (400 MHz, CD_3OD, COSY) and ^{13}C NMR (100 MHz, CD_3OD, HMQC, HMBC) spectra were identical to the literature data.[62]

Isolation of 4′-hydroxyallocohumulinone (11a) and 4′-hydroxyallohumulinone (11b) from oxidized hops.

One hundred g of hop pellets were stored at 60 °C for 120 h (in this process, α- and β-acids in hops decrease to trace amounts), and extracted with EtOH (1 L). The extract (25.5 g) was applied to Diaion HP-20 (Mitsubishi Chemical, Tokyo, Japan) column chromatography (3.0 cm id × 25 cm), and eluted stepwisely with 10% EtOH (2 L; 3.8 g), 30% EtOH (3 L; 4.7 g), 60% EtOH (2 L; 5.6 g), 80% EtOH (2 L; 5.0 g) and 100% EtOH (2 L; 7.7 g). The 30% EtOH fraction was further chromatographed by preparative HPLC [column: 150 × 10 mm id, 5 μm, Alltima C_{18} column; solvent: H_2O/ H_3PO_4 (85%), 1000/0.2 (v/v) containing EDTA (0.02% w/v) (solvent A) and acetonitrile (solvent B), a linear gradient from 15 to 28% B in 0 → 25 min, and 28 to 80% B in 25 → 30 min, then 80% B for 30 → 35 min; flow rate: 8.5 mL/min; detect: 270 nm; temperature: 40 ˚C]. 4′-Hydroxyallocohumulinone (**11a**) and 4′-hydroxyallohumulinone (**11b**) were eluted at 10.2 and 14.4 min, respectively. To remove phosphoric acid and EDTA, each eluate was diluted with H_2O (5 times) and applied to an Oasis HLB column (Waters, Milford, MA, USA) developed with H_2O, and eluted with EtOH. The yield of **11a** and **11b** from the HP-20 30% EtOH fraction (500 mg) was 9.4 and 18.3 mg, respectively.

4′-Hydroxyallocohumulinone (**11a**, Figure 4): pale yellow oil; UV (0.1 N

HCl-MeOH) λ_{max} 230, and 280 (shoulder) nm, UV (0.1 N NaOH-MeOH) λ_{max} 253, and 270 (shoulder) nm; HRESIMS (negative) *m/z* 379.1754 $[M - H]^-$ (calcd for $C_{20}H_{27}O_7$, 379.1762); ^1H NMR (400 MHz, CD_3OD, COSY) and ^{13}C NMR (100 MHz, CD_3OD, HMQC, HMBC) data are given in Table 1.

4'-Hydroxyallohumulinone (**11b**, Figure 4): pale yellow oil; UV (0.1 N HCl-MeOH) λ_{max} 230, and 282 nm, UV (0.1 N NaOH-MeOH) λ_{max} 253, and 270 (shoulder) nm; HRESIMS (negative) *m/z* 393.1912 $[M - H]^-$ (calcd for $C_{21}H_{29}O_7$, 393.1919); ^1H NMR (400 MHz, CD_3OD, COSY) and ^{13}C NMR (100 MHz, CD_3OD, HMQC, HMBC) data are given in Table 1.

High-performance liquid chromatography (HPLC).

A Shimadzu Prominence UFLC system, equipped with a LC-20AD pump, a SIL-20ACHT automated sample injector, a thermostatted column compartment CTO-20AC, and a SPD-M20A photodiode array detector, was used to analyze hop constituents. Data were processed with LCsolution software (Shimadzu, Kyoto, Japan). The used column was 150 × 2.1 mm id, 3 μm, Alltima C_{18} (systech, Tokyo, Japan), and maintained at 40 °C. The method utilized a gradient of H_2O/ H_3PO_4 (85%), 1000/0.2 (v/v) containing EDTA (0.02% w/v) (solvent A) and acetonitrile (solvent B). The elution conditions were 0.6 mL/min, a linear gradient from 10 to 52% B in 0 → 40 min, 52% B for 40 → 45 min, 52 to 75% B in 45 → 49 min, 75 to 85% B in 49 → 55 min, and 85% B for 55 → 56.5 min. The injection volume was 3.0 μL.

Qualitative and quantitative analysis of hop constituents during hop storage.

Fresh hop pellets were ground to a powder and divided into 3 groups. Each group (200 g) was stored at 20, 40, or 60 °C in contact with air under dark conditions. The hop pellets (5.0 g) were sampled at 4, 8, and 24 h and then every other day for the first week, and then once a week for the next 7 weeks in each group. For the 20 and 40 °C groups,

further sampling was undertaken continuously until 40 weeks, at once a week (7 – 12 weeks), once every two weeks (12 – 24 weeks) and once every four weeks (24 – 40 weeks). Each sampled hop pellet (1.0 g) was extracted with 10 mL EtOH for 1 h at room temperature, with agitation, and then centrifuged at 600 × *g* for 5 min. The supernatant (100 μL) was diluted 10 times with EtOH, and the diluted solution (3 μL) was injected into the HPLC.

The International Calibration Extract ICE2 [49.39% (w/w) α-acids, 24.94% (w/w) β-acids] was used for the quantitation of α-acids and β-acids. Humulinones, hulupones, and 4′-hydroxyallohumulinones were quantitated using synthesized or isolated compounds. Cohumulinone (**6a**) and adhumulinone (**6c**) were quantitated using the calibration curve of humulinone (**6b**), hulupone (**5b**) and adhulupone (**5c**) were quantitated using the calibration curve of cohulupone (**5a**), and 4′-hydroxyalloadhumulinone (**11c**) was quantitated using the calibration curve of 4′-hydroxyallohumulinone (**11b**). The wavelengths for quantitative determination of HPLC analysis were 314 nm for α-acids and β-acids, 330 nm for hulupones, and 270 nm for humulinones and 4′-hydroxyallohumulinones.

High-resolution electrospray ionization mass spectrometry (HRESIMS).

HRESIMS of the purified compounds was measured using a Thermo Scientific LTQ Orbitrap mass spectrometer (Thermo Fisher Scientific, San Joes, CA, USA). Before measuring the samples, accurate mass calibration was performed using polytyrosine-1,3,6 calibrant (CS Bio Company, Menlo Park, CA, USA).

Nuclear magnetic resonance spectroscopy (NMR).

^{1}H, ^{13}C, and 2D NMR spectra were measured with a Bruker AVANCE400 spectrometer (Bruker BioSpin, Rheinstetten, Germany). Samples were dissolved in $CDCl_3$ or CD_3OD. Chemical shifts were referenced to tetramethylsilane. Data processing

was performed using TopSpin-NMR software (version 3.0) (Bruker BioSpin, Rheinstetten, Germany).

Results and discussion

Identification of humulinones and hulupones in oxidized hops.

To identify compounds derived from the bitter acids in oxidized hops, the author developed a HPLC method using the Prominence UFLC system (suitable for high pressure analyses) with a gradient program. This method was established to analyze the hydrophilic oxidized compounds, together with α-, β-, and iso-α-acids.

In this method, α-acids (**1a–c**) and β-acids (**2a–c**) in the fresh hops (Figure 2A), and iso-α-acids (**3a–c**, **4a–c**) in the isomerized hop extract (Figure 2B) were eluted separately. In the fresh hops and isomerized hop extract, very few oxidized derivatives derived from α- or β-acids were detected (Figures 2A and B).

To check the separation of the oxidized compounds derived from α- or β-acids, reference standards of humulinones and hulupones prepared from α- and β-acids, respectively, were analyzed using this method. In the chromatography, humulinones [cohumulinone (**6a**), humulinone (**6b**), and adhumulinone (**6c**)] were eluted earlier than iso-α-acids (Figure 2C). In detail, **6a** and **6b** which existed as racemic mixtures (4*R*5*R* and 4*S*5*S*, Figure 3)[42, 65, 66] were detected as single peaks, and **6c** which existed as two diastereomers due to the additional fixed chiral carbon (2‴*S*) in the acyl side chain (**6c**, **6c′**, Figure 3)[30, 66] was detected as two equal intensity peaks (**6c**, **6c′**) (Figure 2C). Thus, it was confirmed that this analytical method could separate all the congeners belonging to humulinones, including the diastereomers of adhumulinone.

The compounds belonging to hulupones [cohulupone (**5a**), hulupone (**5b**), and adhulupone (**5c**)] were eluted at almost the same t_R as the corresponding congeners of humulinones (**6a**, **6b**, **6c**) (Figure 2D). Because hulupones show maximum UV absorption around 330 nm in the solvent used and humulinones do not show significant UV absorption around 330 nm, this wavelength is found to be suitable for the specific detection and quantitation of hulupones.

Analysis of the hops stored at 60 °C for 48 h, to promote the oxidation of α-acids

and β-acids, clearly revealed a decrease in α-acids and β-acids, and the production of many oxidized compounds (Figures 2E and F). Among these, humulinones and hulupones were clearly identified as major oxidized products by their retention time, UV spectra, and molecular formulas determined by the HRESIMS analysis. Although the presence of hulupones in oxidized hops has been previously reported,[67] the presence of humulinones remained controversial.[32, 43-45] The author proved for the first time that humulinones exist as one of the main oxidation products in oxidized hops. In this analysis, adhumulinone was eluted as two equal intensity peaks (**6c, 6c′**) (Figure 2E). This pattern is the same as the reference standards (Figure 2C). Therefore, cohumulinone (**6a**) and humulinone (**6b**) in oxidized hops are suggested to exist as racemic mixtures, and the oxidation mechanism from α-acids to humulinones in hops might resemble the reaction of isolated α-acids with peroxide reagent.[40, 42]

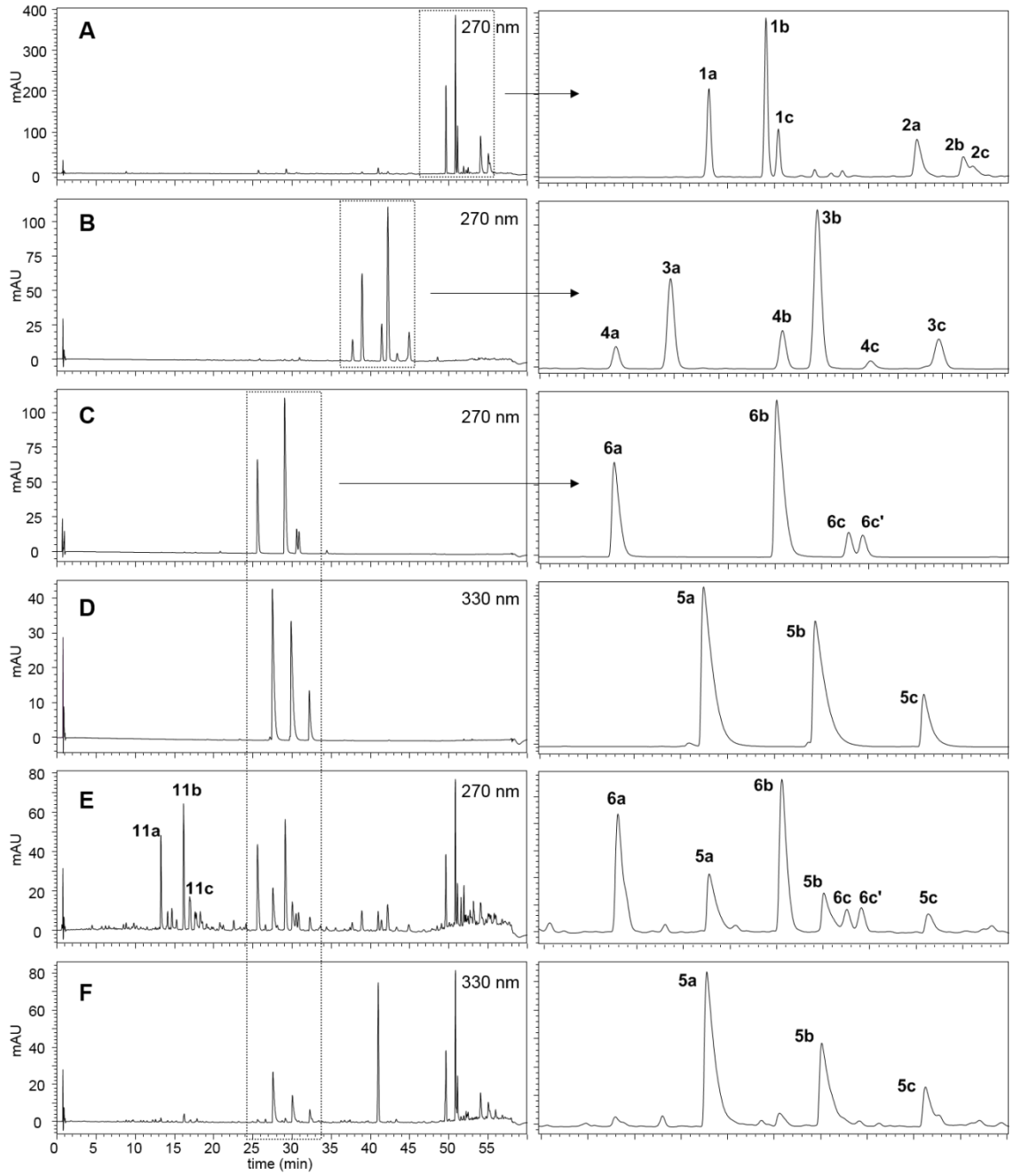

Figure 2. HPLC chromatograms of fresh hops at 270 nm (A), isomerized hop extract at 270 nm (B), reference standards of humulinones at 270 nm (C), reference standards of hulupones at 330 nm (D), and oxidized hops stored at 60 °C for 48 h at 270 nm (E) and 330 nm (F). The right side chromatograms correspond to the enlarged views of the enclosed regions. Structures of compounds are given in Figures 1, 3, and 4.

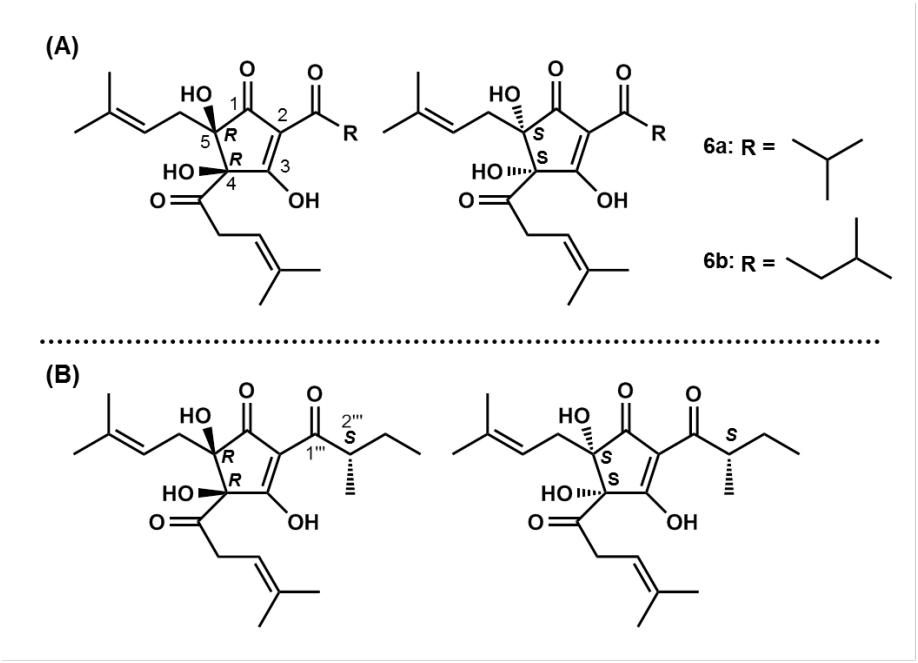

Figure 3. (A) Chemical structures of racemic cohumulinone (**6a**) and racemic humulinone (**6b**). (B) Chemical structures of two diastereomers of adhumulinone, **6c** or **6c′**.

Isolation and structural elucidation of 4′-hydroxyallohumulinones.

In addition to humulinones and hulupones, some unidentified hydrophilic compounds were detected in the oxidized hops. Among these compounds, two major products (**11a** and **11b**) were isolated using Diaion HP-20 column chromatography, followed by preparative ODS HPLC.

Compound **11b** was isolated as pale yellow oil. The UV spectrum of **11b** suggested that this compound possessed the same five-membered ring structure as iso-α-acid derivatives.[68] The HRESIMS of **11b** showed a $[M - H]^-$ peak at *m/z* 393.1912, indicating the molecular formula $C_{21}H_{30}O_7$ [humulinone (**6b**) + O]. The ^1H and ^{13}C NMR spectra of **11b** were closely related to **6b**, and the ^1H and ^{13}C signals due to the five-membered rings (C-1 – C-5) in **6b** were completely preserved in **11b**. In addition, the presence of an isovaleryl side chain at C-2 and prenyl side chain at C-5 in **11b** were confirmed by comparison with the chemical shifts in **6b** (Table 1 and Figure 4). The HMBC experiment

on **11b** proved the long range couplings from H-5′ (δ_H 1.30, singlet methyl) and H-6′ (δ_H 1.30, singlet methyl) to C-4′ (δ_C 71.4) and C-3′ (δ_C 155.5), and from H-3′ (δ_H 6.86, J = 15.6 Hz) and H-2′ (δ_H 6.98, J = 15.6 Hz) to C-1′ (δ_C 200.2), indicating **11b** possesses a *trans*-4-hydroxy-4-methyl-2-pentenoyl structure at C-4. This oxidative side chain is also present in hydroxyalloisohumulones which were recently reported to be oxidation products of iso-α-acids (Figure 5),[69] and their reported ^{1}H and ^{13}C NMR data showed good agreement with those of **11b**, except at position C-5 in the five-membered ring.

The ^{1}H chemical shift difference between H-4″ and H-5″ was Δ0.2 ppm in **11b**, indicating that the relative stereochemistry of the side chains at C-4 and C-5 in **11b** was the same as *trans*-isohumulone (**4b**) and humulinone (**6b**), because the chemical shift difference between H-4″ and H-5″ was greater when the two large side chains at C-4 and C-5 are in the *cis*-position (> Δ0.16 ppm) compared with the *trans*-position (< Δ0.04 ppm) in iso-α-acids and their derivatives.[62, 69, 70] The NOESY experiment also supported this relative configuration because the NOE was detected between H-2′ and H-1″ in **11b**, similar to *trans*-isohumulone (**4b**) and humulinone (**6b**) [the NOE between H-2′ and H-1″ was not observed in *cis*-isohumulone (**3b**)]. From the findings described above, compound **11b** was identified as 4′-hydroxyallohumulinone which has never been reported (Figure 4).

Compound **11a** was isolated as pale yellow oil. The HRESIMS showed a $[M - H]^-$ peak at *m/z* 379.1754, indicating the molecular formula $C_{20}H_{28}O_7$ (**11b** − CH_2). The ^{1}H and ^{13}C NMR spectra of **11a** were almost identical to those of **11b**, except the side chain structure at C-2. The presence of isobutyryl function at C-2 in **11a** was confirmed by the long range couplings from H-3‴ (δ_H 1.03) and H-4‴ (δ_H 1.06) to C-2‴ (δ_C 37.3) and C-1‴ (δ_C 204.3) in the HMBC experiment. Thus, compound **11a** was identified as 4′-hydroxyallocohumulinone which has never been reported (Figure 4).

In addition, the author tentatively identified compound **11c** as 4′-hydroxyalloadhumulinone, on the basis of HRESIMS analysis ($[M - H]^-$ 393.1912,

indicating the molecular formula $C_{21}H_{30}O_7$) together with the typical HPLC elution patterns of the congeners of hop bitter acids.

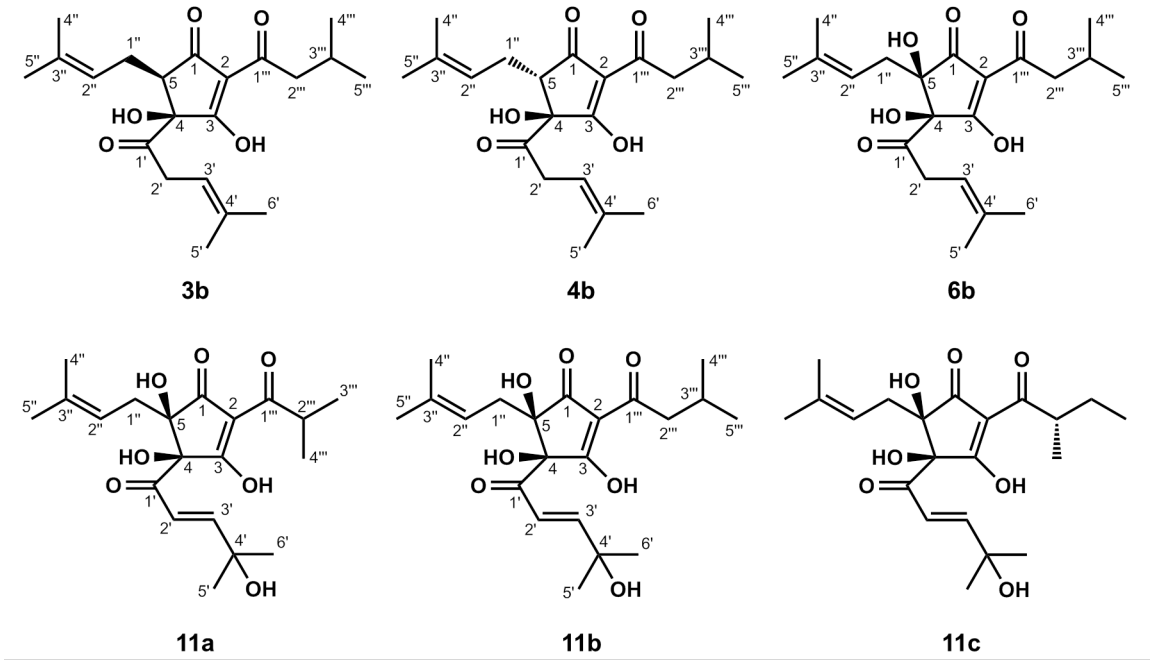

Figure 4. Chemical structures of *cis*-isohumulone (**3b**), *trans*-isohumulone (**4b**), humulinone (**6b**), 4′-hydroxyallocohumulinone (**11a**), 4′-hydroxyallohumulinone (**11b**), and 4′-hydroxyalloadhumulinone (**11c**).

The structures of 4′-hydroxyallohumulinones (**11a–c**) suggested that they were the oxidation products from corresponding humulinones (**5a–c**). Recently, Intelmann *et al.* proposed an oxidation pathway from iso-α-acids (**3a–c** and **4a–c**) to hydroxyalloisohumulones, which is similar to the lipid autoxidation of unsaturated fatty acids (Figure 5).[69] Furthermore, Almedia *et al.* proved that an oxidative reaction between iso-α-acids and 1-hydroxyethyl radicals occurs preferentially through hydrogen atom transfer at allylic positions in the side chain and not through electron transfer from the β-tricarbonyl chromophore. They also detected hydroxyalloisohumulones as the reaction products.[71] On the basis of these reports, the author speculates the reaction pathway from

humulinones (**6a–c**) to 4′-hydroxyallohumulinones (**11a–c**) is identical to that from iso-α-acids (**3a–c** and **4a–c**) to hydroxyalloisohumulones (Figure 5).

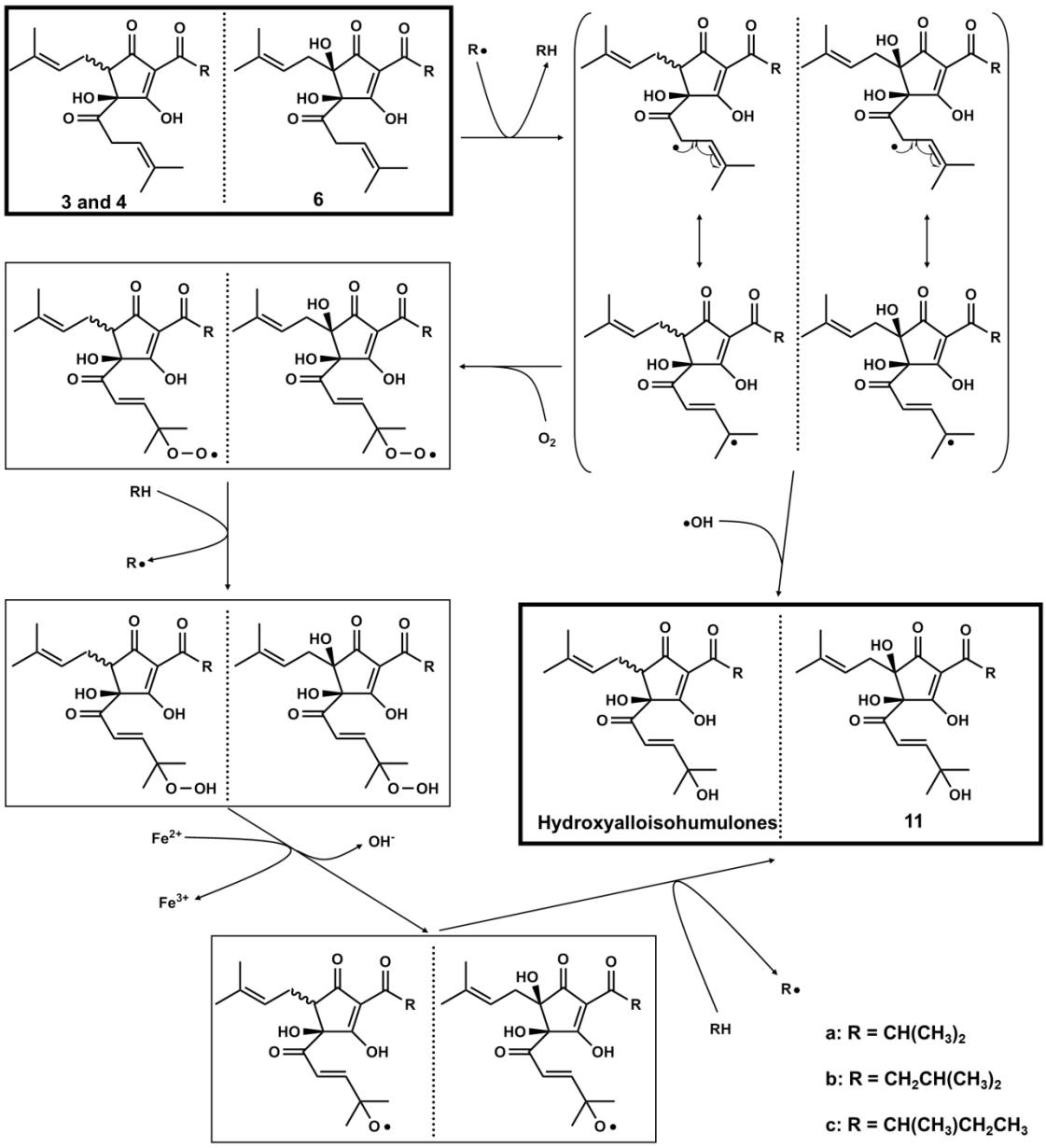

Figure 5. Proposed reaction pathway for the formation of 4′-hydroxyallohumulinones (**11a–c**) from humulinones (**6a–c**). This pathway is the same as the reaction pathway for the formation of hydroxyalloisohumulones from iso-α-acids (**3a–c** and **4a–c**) proposed by Intelmann *et al.*[69] and Almedia *et al.*[71]

Table 1. Assignment of ^{1}H NMR (400 MHz, CD_3OD) and ^{13}C NMR (100 MHz, CD_3OD) signals of compounds **3b**, **4b**, **6b**, **11b**, and **11a**[a]

	cis-isohumulone (**3b**)		*trans*-isohumulone (**4b**)		humulinone (**6b**)		4'-hydroxyallohumulinone (**11b**)		4'-hydroxyallocohumulinone (**11a**)	
pos.	δ_C, type	δ_H, mult. (*J* in Hz)	δ_C, type	δ_H, mult. (*J* in Hz)	δ_C, type	δ_H, mult. (*J* in Hz)	δ_C, type	δ_H, mult. (*J* in Hz)	δ_C, type	δ_H, mult. (*J* in Hz)
1	205.5, C	-	203.9, C	-	201.9, C	-	201.7, C	-	201.6, C	-
2	111.9, C	-	112.4, C	-	111.1, C	-	111.8, C	-	110.9, C	-
3	198.1, C	-	198.5, C	-	198.7, C	-	199.1, C	-	198.9, C	-
4	88.5, C	-	90.7, C	-	91.1, C	-	90.0, C	-	89.7, C	-
5	52.8, CH	3.14, dd (7.6, 5.7)	57.5, CH	2.95, dd (9.9, 5.7)	81.0, C	-	81.6, C	-	81.4, C	-
1'	210.5, C	-	209.9, C	-	210.1, C	-	200.2, C	-	200.5, C	-
2'	38.3, CH_2	3.47, d (6.8)	39.7, CH_2	a: 3.47, dd (19.7, 6.6) b: 3.40, dd (19.7, 6.1)	40.0, CH_2	a: 3.49, dd (20.0, 6.5) b: 3.42, dd (20.0, 6.2)	121.6, CH	6.98, d (15.6)	121.8, CH	6.93, d (15.6)
3'	116.7, CH	5.22, m	116.4, CH	5.23, m	116.5, CH	5.21, m	155.5, CH	6.86, d (15.6)	155.0, CH	6.85, d (15.6)
4'	136.5, C	-	136.2, C	-	136.0, C	-	71.4, C	-	71.3, C	-
5'	18.1, CH_3	1.59, s	18.2, CH_3	1.58, s	18.2, CH_3	1.57, s	29.3, CH_3	1.30, s	29.3, CH_3	1.29, s
6'	25.8, CH_3	1.71, s	25.9, CH_3	1.72, s	25.8, CH_3	1.71, s	29.4, CH_3	1.30, s	29.3, CH_3	1.29, s
1''	26.1, CH_2	a: 2.42, m b: 2.36, m	24.7, CH_2	a: 2.49, m b: 2.25, ddd (15.3, 9.4, 9.4)	30.8, CH_2	2.45, d (6.9)	31.3, CH_2	a: 2.48, m b: 2.37, dd (15.4, 9.0)	31.7, CH_2	a: 2.50, m b: 2.33, dd (15.6, 9.0)
2''	121.8, CH	5.10, m	122.3, CH	5.18, m	119.0, CH	5.33, m	119.3, CH	5.27, m	119.7, CH	5.24, m
3''	135.1, C	-	134.7, C	-	135.5, C	-	135.1, C	-	134.9, C	-
4''	17.9, CH_3	1.59, s	18.0, CH_3	1.51, s	18.1, CH_3	1.46, s	18.1, CH_3	1.42, s	18.2, CH_3	1.42, s
5''	26.0, CH_3	1.63, s	25.8, CH_3	1.67, s	26.0, CH_3	1.66, s	26.1, CH_3	1.62, s	26.1, CH_3	1.61, s
1'''	200.5, C	-	198.7, C	-	199.1, C	-	199.5, C	-	204.3, C	-
2'''	47.0, CH_2	2.71, d (7.0)	45.9, CH_2	a: 2.76, dd (13.8, 7.3) b: 2.69, dd (13.8, 6.9)	46.3, CH_2	a: 2.77, dd (13.8, 7.2) b: 2.69, dd (13.8, 6.9)	47.9, CH_2	a: 2.74, dd (13.7, 7.7) b: 2.69, dd (13.7, 7.4)	37.3, CH	3.64, m
3'''	27.2, CH	2.10, m	27.5, CH	2.11, m	27.6, CH	2.10, m	27.2, CH	2.11, m	18.8, CH_3	1.03, d (6.8)
4'''	22.8, CH_3	0.93, d (6.5)	22.7, CH_3	0.94, d (6.7)	22.7, CH_3	0.93, d (6.7)	23.0, CH_3	0.93, d (7.2)	18.9, CH_3	1.06, d (6.8)
5'''	22.9, CH_3	0.95, d (6.5)	22.9, CH_3	0.97, d (6.7)	22.8, CH_3	0.96, d (6.7)	23.0, CH_3	0.95, d (7.2)		

[a] Arbitrary numbering according to structures **3b**, **4b**, **6b**, **11b**, and **11a** in Figure 4.

Changes in hop bitter acid derivatives during hop oxidation progression.

To evaluate the oxidative changes of α-acids and β-acids during hop storage, hop pellets were stored at 20 or 40 °C for up to 40 weeks, or at 60 °C for up to 8 weeks. The stored hops were extracted with EtOH, and analyzed by HPLC. Figure 6 shows the time dependent decrease in α-acids and β-acids, and compositional changes in the oxidative α-acid derivatives (humulinones and 4′-hydroxyallohumulinones) and oxidative β-acid derivatives (hulupones).

At 20 °C, the initial α-acids (186.9 μmol/g) decreased to 37.0 μmol/g after 40 weeks, while humulinones and 4′-hydroxyallohumulinones reached 32.3 and 27.0 μmol/g (17 and 14% of the initial α-acids), respectively (Figure 6A). β-Acids were decreased from 107.7 to 50.9 μmol/g after 40 weeks, while hulupones increased to 18.6 μmol/g (17% of the initial β-acids) (Figure 6B).

When hops were stored at 40 °C, a rapid decrease in α-acids and β-acids was observed: their concentration decreased to less than 5% of the initial amounts after 8 or 5 weeks, respectively (Figures 6C and D). At this temperature, compositional changes in the oxidation products became clearer. Humulinones reached their maximum (33.2 μmol/g) after 3 weeks storage and then decreased rapidly (Figure 6C). In contrast, the amount of 4′-hydroxyallohumulinones were increased rapidly for 2 – 5 weeks and slowly for 6 – 11 weeks, reaching their maximum (51.3 μmol/g, 27% of the initial α-acids) at 11 weeks, before being degraded very slowly (Figure 6C). From these observations, the author confirmed 4′-hydroxyallohumulinones to be produced by the oxidation of humulinones. Hulupones reached their maximum (32.6 μmol/g, 30% of the initial β-acids) after 4 weeks storage, and existed stably until the 40th week (Figure 6D).

At 60 °C, the observed compositional change curves resembled those at 40 °C, while the reaction speed was about 10 times faster than at 40 °C (Figures 6E and F). α-Acids and β-acids were decreased to less than 5% of the initial amounts after 96 or 72 h, respectively. Humulinones reached their maximum at 48 h before being degraded rapidly,

while 4′-hydroxyallohumulinones reached their maximum at 144 h before being degraded slowly. Hulupones reached their maximum at 72 h and were stable until the 8th week.

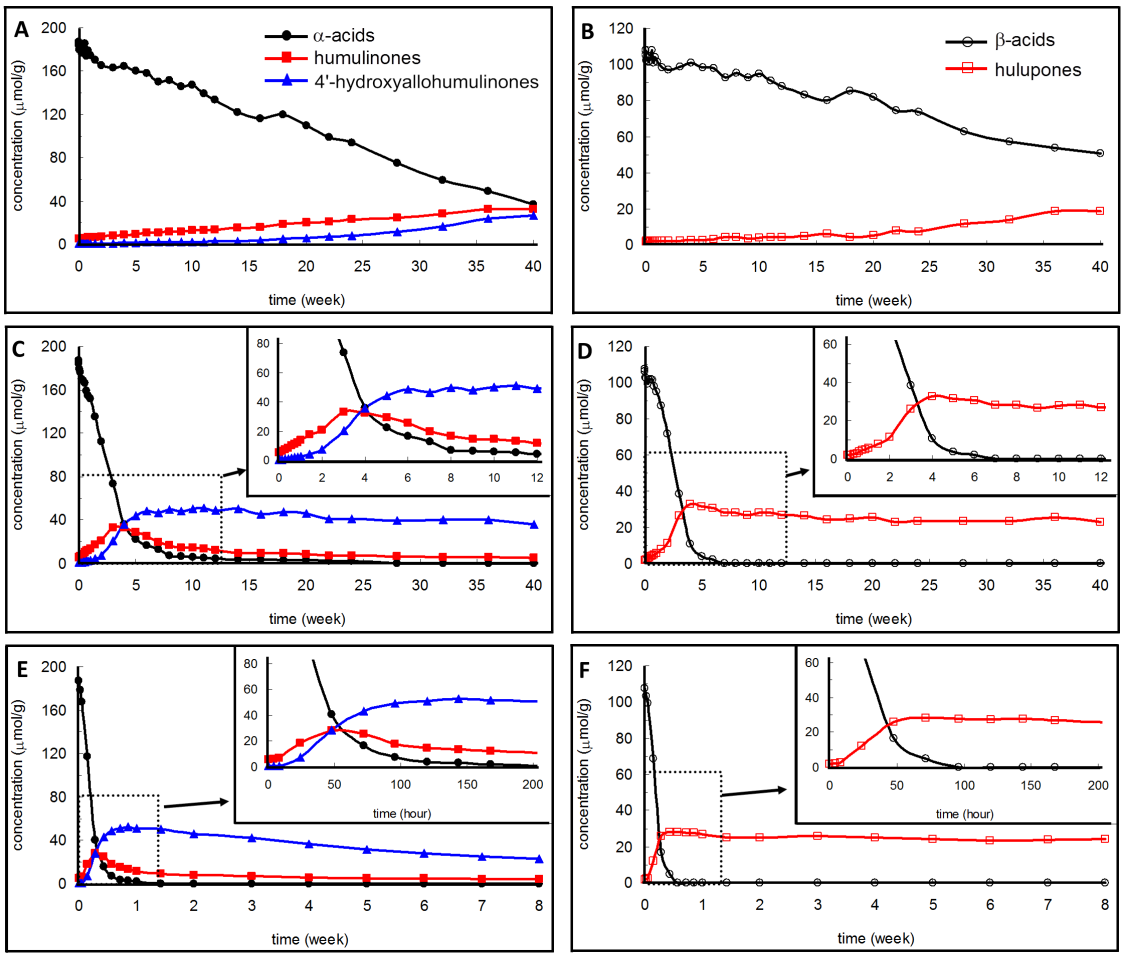

Figure 6. Concentration changes in α-acids, humulinones, 4′-hydroxyallohumulinones, β-acids, and hulupones in hops during storage at 20 °C (A and B), 40 °C (C and D), and 60 °C (E and F).

The results described in this section suggested that the stored temperature affected the oxidative reaction speed, but did not change the composition of generated hydrophilic oxidation products. To confirm this speculation, the author analyzed the hop samples stored at 20, 40, and 60 °C, each of which contained almost the same amounts of α-acids (about 20% of the initial) (40th week for 20 °C, 4th week for 40 °C, and 48 h for 60 °C) by HPLC (Figure 7A–C). The analyses showed that the generated hydrophilic oxidation

products occurring in the stored hops at each temperature were almost identical, including minor peaks, confirming the author's speculation.

The author expects the information will be helpful in more accurately understanding the influence of hop oxidation on beer quality.

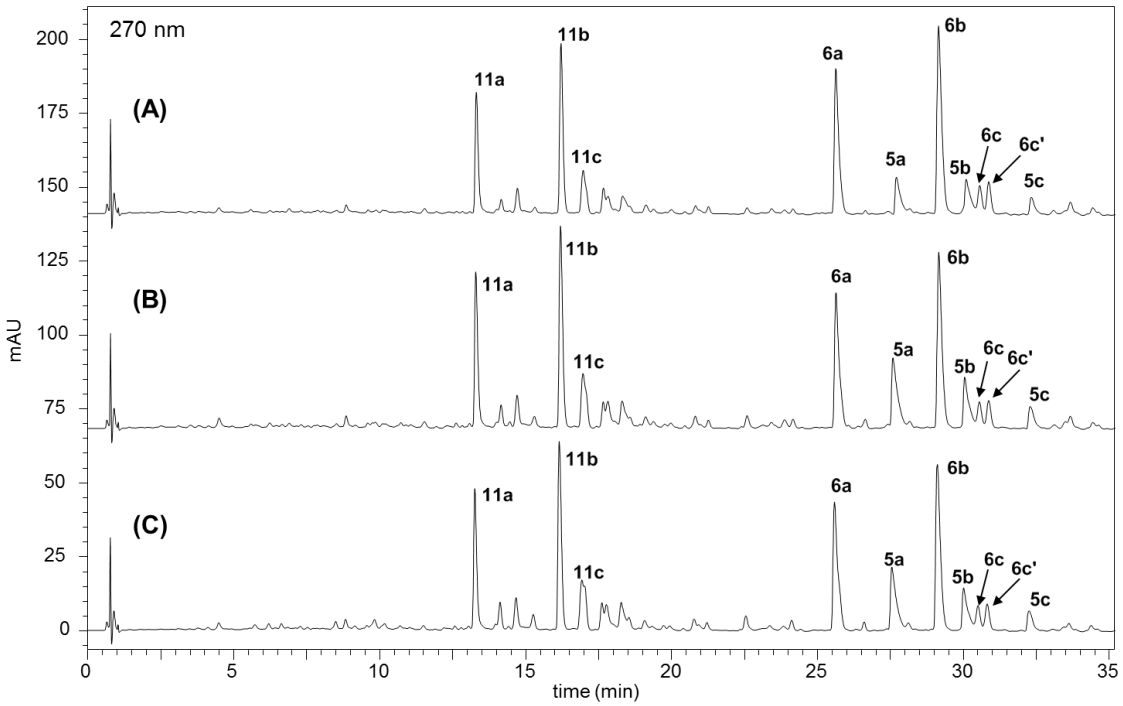

Figure 7. HPLC chromatograms of the hydrophilic oxidation products which were eluted earlier than iso-α-acids in oxidized hops. The hops were analyzed when α-acids decreased to 20% of the initial amounts due to storage at the following temperatures and periods: (A) 20 °C for 40 weeks, (B) 40 °C for 4 weeks, and (C) 60 °C for 48 h.

Summary

The author reported suitable HPLC conditions to analyze α-acids, β-acids, and their oxidation products. This HPLC analysis clearly proved, for the first time, that humulinones and hulupones are major products in oxidized hops. The author is also the first to identify novel 4′-hydroxyallohumulinones, suggested to be oxidative products of humulinones, by means of NMR and HRMS. Using the developed analytical method,

changes in α- and β-acids and their oxidation products during hop storage were clearly revealed for the first time. The author considers that these findings and the aouthor's analytical methods enable precise prediction of the degree of hop oxidation.

Chapter 2

Structural elucidation of tricyclic oxidation products of humulone and analysis of their occurrence in stored hops

In chapter 1, the author developed an HPLC method to investigate the oxidation products in stored hops and demonstrated that humulinones and 4′-hydroxyallohumulinones are the main oxidation products of α-acids. The author also found several other oxidation products derived from α-acids, but these could not be isolated and identified due to their low yields. To determine the structures of these unidentified oxidized compounds, the author developed a simple autoxidation model for α-acids (autoxidation in *n*-hexane) using humulone, a representative congener of α-acids (Figure 1), as the substrate. The use of this model led to the identification of tricyclooxyisohumulones A (**12b**) and B (**13b**), tricycloperoxyisohumulone A (**14b**), deisopropyltricycloisohumulone (**15b**), and the hemiacetal **16b** of tricycloperoxyhumulone A (**16′b**) (Figure 8). The presence of compounds **12b**–**15b** in stored hops was verified using LC/MS/MS analysis. A plausible pathway for the autoxidation of humulone into compounds **12b**–**16b** is proposed.

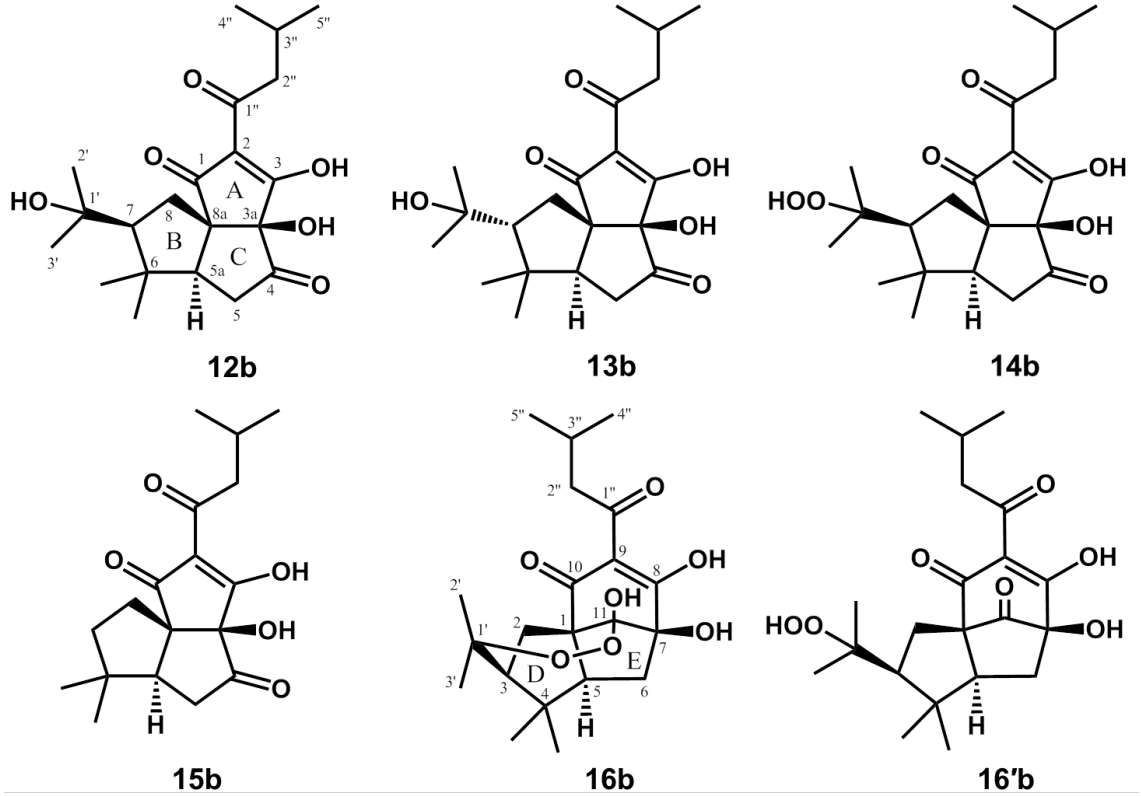

Figure 8. Chemical structures of tricyclooxyisohumulone A (**12b**), tricyclooxyisohumulone B (**13b**), tricycloperoxyisohumulone A (**14b**), deisopropyltricycloisohumulone (**15b**), and the hemiacetal **16b** of tricycloperoxyhumulone A (**16′b**).

Materials and methods

General experimental procedures.

Optical rotations were measured using a P-2200 polarimeter (JASCO, Tokyo, Japan). UV spectra were obtained using an Ultraspec 3100 pro (Amersham biosciences, Bucks, UK). ^{1}H and ^{13}C NMR, ^{1}H-^{1}H COSY, NOESY, HMQC, and HMBC spectra were recorded in methanol-d_4 or acetonitrile-d_3 at 20 °C (compounds **12b**–**15b**) or at 5 °C (compound **16b**) with a Bruker AVANCE400 spectrometer (Bruker BioSpin, Rheinstetten, Germany). Chemical shifts were referenced to the solvent signals (methanol-d_4: δ_H/δ_C 3.30/49.0, acetonitrile-d_3: δ_H/δ_C 1.93/1.3). Data processing was performed using TopSpin-NMR software (version 3.0) (Bruker BioSpin, Rheinstetten,

Germany). HRESIMS of the purified compounds were measured using a Thermo Scientific LTQ Orbitrap mass spectrometer (Thermo Fisher Scientific, San Joes, CA, USA). Before measuring the samples, accurate mass calibration was performed using a polytyrosine-1, 3, 6 calibrant (CS Bio Company, Menlo Park, CA, USA). Preparative HPLC was conducted on a Gilson model HPLC system equipped with a 321 pump and a 171 diode array detector (Gilson, Middleton, WI, USA) and on a Shimadzu Prominence HPLC system (Shimadzu, Kyoto, Japan). Analytical HPLC was conducted on a Shimadzu Prominence UFLC system, and LC/MS/MS was conducted on a 4000 Q-Trap mass spectrometer (AB Sciex, Tokyo, Japan) connected to a Shimadzu Prominence UFLC system.

Material.

Hop pellets (cultivar Hallertau Perle) were purchased from HopSteiner (Mainburg, Germany) and stored in a freezer at −20 °C prior to use.

Autoxidation of humulone and isolation of compounds 12b–16b.

Humulone was prepared according to the method described in chapter 1. Humulone (8.10 g) was dissolved in *n*-hexane (810 mL) and stored at 20 °C for 144 h. The supernatant was collected by decantation and concentrated using a rotary evaporator to afford a yellow oil (3.70 g). A portion of this product (1.78 g) was repeatedly subjected to preparative HPLC [column: 150 × 22 mm id, 5 μm, Alltima C_{18} column (Systech, Tokyo, Japan); solvent: H_2O/H_3PO_4 (85%), 100/1 (v/v) (solvent A) and MeCN (solvent B), a linear gradient from 30 to 75% B in 0 → 30 min, 75 to 90% B in 30 → 30.1 min, and 90% B for 30.1 → 37 min; flow rate: 18.8 mL/min; detector: 270 nm; column temperature: RT], yielding 49 fractions. Fraction 18 (t_R 15.2 – 15.6 min) and fraction 39 (t_R 24.5 – 25.3 min) contained compound **14b** (140 mg) and compound **16b** (330 mg), respectively. Fraction 15 (t_R 13.6 – 13.8 min) and fraction 32 (t_R 20.6 – 20.8 min) were further purified

by a 2nd preparative HPLC [column: 50 × 20 mm i.d., 5 μm, L-column 2 ODS (Chemicals Evaluation and Research Institute, Tokyo, Japan); solvent: 100 mM NH_4HCO_3 (solvent A) and MeCN (solvent B), isocratic elution at 20% B; flow rate: 9.5 mL/min; detector: 270 nm; column temperature: 40 ˚C]. Fraction 15-1 (t_R 3.8 – 4.7 min) and fraction 15-2 (t_R 5.5 – 7.5 min) contained compound **12b** (18.9 mg) and compound **13b** (4.4 mg), respectively. Fraction 32-1 (t_R 6.0 – 6.9 min) contained compound **15b** (11.0 mg).

Tricyclooxyisohumulone A (**12b**, Figure 8): white amorphous solid; $[\alpha]^{20}_D$ +255 (*c* 0.3, MeOH); UV (EtOH) λ_{max} (log ε) 227 (3.93), 256 (4.21), and 276 (sh) (4.11) nm; ^{1}H and ^{13}C NMR data, see Table 3; HRESIMS (negative) *m/z* 377.1963 $[M - H]^-$ (calcd for $C_{21}H_{29}O_6$, 377.1970).

Tricyclooxyisohumulone B (**13b**, Figure 8): pale yellow oil; $[\alpha]^{20}_D$ +173 (*c* 0.3, MeCN); UV (EtOH) λ_{max} (log ε) 228 (4.09), 258 (4.33), and 276 (sh) (4.27) nm; ^{1}H and ^{13}C NMR data, see Table 3; HRESIMS (negative) *m/z* 377.1965 $[M - H]^-$ (calcd for $C_{21}H_{29}O_6$, 377.1970).

Tricycloperoxyisohumulone A (**14b**, Figure 8): white amorphous solid; $[\alpha]^{20}_D$ +242 (*c* 0.3, MeOH); UV (EtOH) λ_{max} (log ε) 227 (4.02), 256 (4.23), and 276 (sh) (4.13) nm; ^{1}H and ^{13}C NMR data, see Table 3; HRESIMS (negative) *m/z* 393.1909 $[M - H]^-$ (calcd for $C_{21}H_{29}O_7$, 393.1919).

Deisopropyltricycloisohumulone (**15b**, Figure 8): white amorphous solid; $[\alpha]^{20}_D$ +245 (*c* 0.3, MeOH); UV (EtOH) λ_{max} (log ε) 224 (4.20), 257 (4.22), and 275 (sh) (4.13) nm; ^{1}H and ^{13}C NMR data, see Table 3; HRESIMS (negative) *m/z* 319.1543 $[M - H]^-$ (calcd for $C_{18}H_{23}O_5$, 319.1551).

*Hemiacetal **16b** of tricycloperoxyhumulone A* (Figure 8): pale yellow oil; $[\alpha]^{20}_D$ +130 (*c* 0.4, MeOH); UV (MeOH) λ_{max} (log ε) 270 (4.14) nm; ^{1}H and ^{13}C NMR data, see Table 4; HRESIMS (negative) *m/z* 393.1911 $[M - H]^-$ (calcd for $C_{21}H_{29}O_7$, 393.1919).

X-ray crystallographic analysis of compound 12b.

Colorless crystals of compound **12b** were obtained from toluene − MeOH (40:1) by slowly removing the solvent. A single crystal (0.30 × 0.30 × 0.10 mm) was separated from the sample and mounted on a glass fiber, and diffraction data were collected using a Rigaku R-AXIS RAPID IP diffractometer with graphite-monochromated Cu Kα radiation (λ =1.54178 Å) at 296 K. Crystal data: $C_{21}H_{30}O_6$, M = 378.46, space group orthorhombic, $P2_12_12_1$, unit cell dimensions: a = 6.0345(3) Å, b =13.0627(6) Å, c = 26.5680(12) Å, V = 2094.3(16) Å^3, Z = 4, $D_{calcd.}$ = 1.200 g/cm^3, μ = 0.7146 mm^{-1}, F(000) = 816. The structure was solved by direct methods using SIR92 and refined using full-matrix least-squares difference Fourier techniques. All non-hydrogen atoms were refined with anisotropic displacement parameters, and a part of the hydrogen atoms were placed in idealized positions and refined as riding atoms with the relative isotropic parameters. The 38599 measurements yielded 3968 independent reflections after equivalent data had been averaged and Lorentz and polarization corrections had been applied. The final refinement gave R_1 = 0.0505, R_w = 0.1536, GOF = 1.028, and Flack = 0.1(3). CCDC 964778 contains the supplementary crystallographic data for compound **12b**. These data can be obtained free of charge from The Cambridge Crystallographic Data Centre via www.ccdc.cam.ac.uk/data_request/cif.

HPLC and LC/MS/MS analysis of compounds 12b–16b in stored hops.

Fresh hop pellets (200 g) were ground to a powder and stored at 40 °C in contact with air under dark conditions. The hop pellet (5.0 g) was sampled over 40 weeks. Each sample (1.0 g) was extracted by agitation in 10 mL of EtOH for 1 h at room temperature and centrifuged at 600 × *g* for 5 min. The supernatant was diluted between 10 and 100 times with EtOH prior to HPLC or LC/MS/MS analysis.

HPLC analysis was performed to quantitate humulone in the stored hops and to monitor the progress of autoxidation of humulone in *n*-hexane using the following

conditions: column: 100 × 2.1 mm id, 3 μm, Alltima C_{18} column (Systech, Tokyo, Japan); solvent: H_2O/H_3PO_4 (85%), 1000/0.2 (v/v) containing EDTA (0.02% w/v) (solvent A) and MeCN (solvent B), a linear gradient from 10 to 52% B in 0 → 26.7 min, 52% B for 26.7 → 30 min, 52 to 75% B in 30 → 32.7 min, 75 to 85% B in 32.7 → 36.7 min, and 85% B for 36.7 → 37.7 min; flow rate: 0.6 mL/min; detector: 270 and 314 nm; column temperature: 40 ˚C. The injection volume was 3.0 μL.

LC/MS/MS analysis was performed for the identification and quantitation of compounds **12b**–**16b** in the stored hops. The LC conditions were as follows: column: 100 × 2.1 mm id, 3 μm, L-column 2 ODS (Chemicals Evaluation and Research Institute, Tokyo, Japan); solvent: 5 mM $HCOONH_4$ (pH 8.5) (solvent A) and MeCN (solvent B), a linear gradient from 10 to 36% B in 0 → 39 min, 36 to 80% B in 39 → 44 min, and 80% B for 44 → 52 min; flow rate: 0.25 mL/min; column temperature: 40 ˚C. The injection volume was 3.0 μL. A 4000 Q-Trap mass spectrometer was equipped with an ESI source operating in the negative ion mode. Nitrogen was used as the turbo gas at 600 °C. The compound-specific mass transition (Q1 → Q3), declustering potential (DP), cell exit potential (CXP), and collision energy (CE) were optimized for each substance prior to analysis by the infusion of pure reference solutions and are summarized in Table 2. The dwell time for each mass transition was 30 ms. The ion spray voltage was set to −4500 V. Data acquisition and processing was performed using the Analyst software version 1.4.2 (AB Sciex, Tokyo, Japan).

The International Calibration Extract ICE2 [49.39% (w/w) α-acids, 24.94% (w/w) β-acids; American Society of Brewing Chemists, St. Paul, MN, USA] was used for the quantitation of humulone. Compounds **12b**, **13b**, **14b**, and **15b** were quantitated using isolated reference compounds.

Table 2. Compound-specific parameters for LC/MS/MS analysis

Compound	Q1 Mass (amu)	Q3 Mass (amu)	DP (V)	CE (V)	CXP (V)
TCOIH A (**12b**)	376.90	124.80	−115.00	−50.00	−19.00
TCOIH B (**13b**)	376.90	124.80	−115.00	−50.00	−19.00
TCPOIH A (**14b**)	392.77	302.90	−45.00	−38.00	−15.00
DeITCIH (**15b**)	318.76	124.80	−90.00	−44.00	−21.00
Hemiacetal **16b** of TCPOH A	392.80	302.90	−60.00	−38.00	−15.00

Results and discussion

Structural elucidation of compounds 12b–16b.

The isolation of α-acid-derived minor oxidation products from stored hops was difficult because of the mixture of congeners (co, *n*-, ad) and the presence of a large number of other constituents, such as polyphenols and waxes. To facilitate the isolation of the minor oxidation products, a model oxidation experiment was conducted using pure humulone (**1b**), the main congener of α-acids. Humulone was dissolved in *n*-hexane and autoxidized at 20 °C for 144 h. The oxidation progress was monitored by HPLC, and the product profile is shown in Figure 9. Preparative HPLC afforded compounds **12b–16b**.

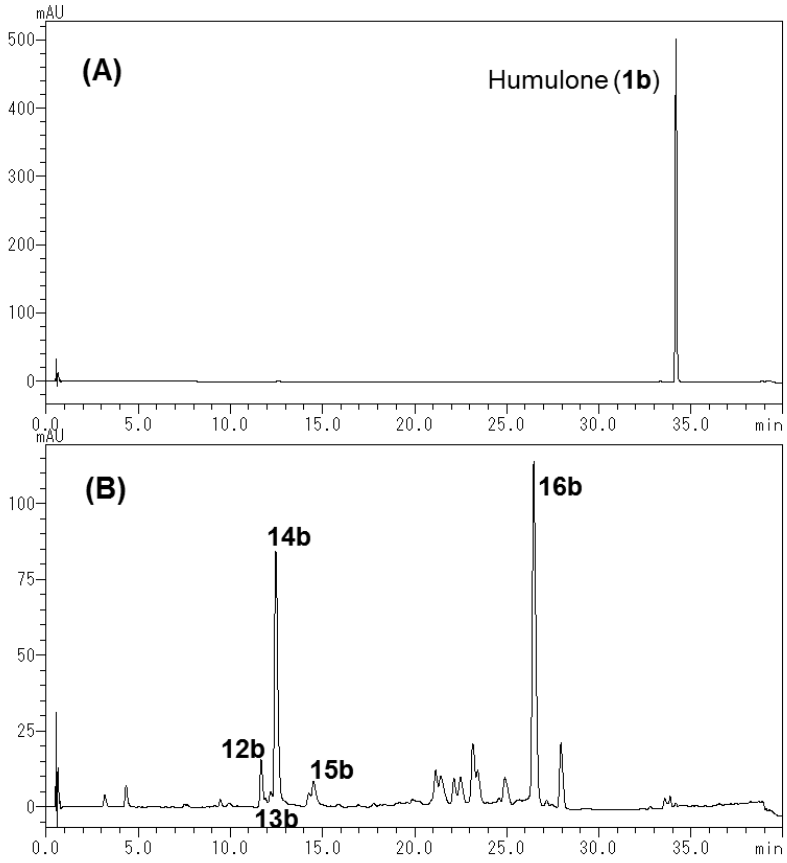

Figure 9. HPLC chromatograms of humulone (A) before and (B) after autoxidation in *n*-hexane for 144 h at 20 °C.

Table 3. NMR spectroscopic data (400 MHz, methanol-d_4) for compounds **12b–15b**

	12b		**13b**		**14b**		**15b**	
pos.	δ_C, type	δ_H, mult. (*J* in Hz)	δ_C, type	δ_H, mult. (*J* in Hz)	δ_C, type	δ_H, mult. (*J* in Hz)	δ_C, type	δ_H, mult. (*J* in Hz)
1	208.3, C	-	208.0, C	-	207.8, C	-	207.8, C	-
2	111.9, C	-	111.7, C	-	111.9, C	-	111.7, C	-
3	196.7, C	-	197.8, C	-	196.1, C	-	196.2, C	-
3a	86.0, C	-	86.5, C	-	85.9, C	-	86.1, C	-
4	213.3, C	-	215.7, C	-	212.1, C	-	212.2, C	-
5	36.2, CH_2	2.42, dd (18.0, 9.2) 2.22, d (18.0)	37.7, CH_2	2.42, dd (17.5, 9.6) 2.24, d (17.5)	36.3, CH_2	2.46, dd (18.0, 9.2) 2.25, d (18.0)	36.7, CH_2	2.48, m 2.27, m
5a	56.3, CH	2.49, d (9.2)	56.1, CH	2.53, d (9.6)	56.1, CH	2.52, d (9.2)	54.4, CH	2.48, m
6	46.3, C	-	46.2, C	-	46.1, C	-	44.4, C	-
6α-Me	29.5, CH_3	1.16, s	26.8, CH_3	1.24, s	29.2, CH_3	1.16, s	28.2, CH_3	1.09, s
6β-Me	17.5, CH_3	0.72, s	27.6, CH_3	0.92, s	18.0, CH_3	0.71, s	21.8, CH_3	0.72, s
7	61.7, CH	2.09, m	60.2, CH	1.65, m	58.9, CH	2.32, m	43.7, CH_2	1.80, ddd (11.8, 11.8, 8.1) 1.65, ddd (11.8, 7.3, 2.3)
8	30.7, CH_2	2.34, dd (13.0, 13.0) 1.98, dd (13.0, 7.2)	30.3, CH_2	2.23, m 2.11, m	30.5, CH_2	2.32, m 2.01, m	27.9, CH_2	2.17, ddd (13.7, 11.8, 7.3) 1.94, ddd (13.7, 8.1, 2.3)
8a	59.4, C	-	62.0, C	-	59.2, C	-	63.5, C	-
1'	73.3, C	-	74.0, C	-	85.0, C	-	-	-
2'	30.6, CH_3	1.27, s	31.3, CH_3	1.30, s	25.3, CH_3	1.30, s	-	-
3'	30.3, CH_3	1.31, s	30.7, CH_3	1.31, s	24.7, CH_3	1.32, s	-	-
1"	201.5, C	-	200.0, C	-	202.0, C	-	202.0, C	-
2"	48.6, CH_2	2.76, dd (14.6, 6.7) 2.72, dd (14.6, 7.0)	50.3, CH_2	2.69, m 2.67, m	48.1, CH_2	2.79, dd (14.9, 7.1) 2.73, dd (14.9, 7.0)	48.2, CH_2	2.78, dd (14.8, 7.0) 2.73, dd (14.8, 7.0)
3"	26.6, CH	2.11, m	26.7, CH	2.08, m	26.5, CH	2.13, m	26.5, CH	2.13, m
4"	23.0, CH_3	0.94, d (6.6)	23.1, CH_3	0.90, d (6.7)	22.9, CH_3	0.95, d (6.6)	22.9, CH_3	0.95, d (6.6)
5"	22.9, CH_3	0.94, d (6.6)	23.1, CH_3	0.90, d (6.7)	22.8, CH_3	0.96, d (6.6)	22.8, CH_3	0.96, d (6.6)

Compound **12b** was obtained as a white amorphous solid. The HRESIMS data showed an $[M - H]^-$ ion at *m/z* 377.1963, and together with the ^{13}C NMR data, indicated a molecular formula of $C_{21}H_{30}O_6$. The ^1H, ^{13}C NMR and HMQC spectra showed the presence of six methyls [δ_H/δ_C: 0.72/17.5, 0.94/22.9, 0.94/23.0, 1.16/29.5, 1.27/30.6, and 1.31/30.3], three sp^3 methylenes [δ_H/δ_C: (2.34 and 1.98)/30.7, (2.42 and 2.22)/36.2, and (2.76 and 2.72)/48.6], three sp^3 methines [δ_H/δ_C: 2.09/61.7, 2.11/26.6, and 2.49/56.3], four sp^3 quaternary carbons (two hydroxylated) [δ_C: 46.3, 59.4, 73.3, and 86.0], one sp^2 quaternary carbon [δ_C: 111.9], one enolic carbon [δ_C: 196.7], and three carbonyl carbons [δ_C: 201.5, 208.3, and 213.3]. The characteristic ^{13}C NMR quaternary chemical shift set at δ_C 59.4, 86.0, 111.9, 196.7, 201.5, and 208.3 strongly suggested that compound **12b** possesses a 2-acyl-3-hydroxycyclopent-2-enone structure composed of C-1″ – C-1 – C-2 – C-3 – C-3a – C-8a (ring A) based on comparison with the corresponding ^{13}C NMR chemical shifts of iso-α-acids and their derivatives (Table 3).[62, 69]

The molecular formula of compound **12b** required seven indices of hydrogen deficiency, four of which were accounted for by the 2-acyl-3-hydroxycyclopent-2-enone structure and a further one by the remaining carbonyl group (δ_C: 213.3). This indicated that compound **12b** possesses a tricyclic structure.

Three structural fragments (C-5 − C-5a, C-7 − C-8, and C-2″ – C-5″) were established from the correlations in the ^1H-^1H COSY spectrum (bold lines in Figure 10). The HMBC correlations of H-2″ (δ_H 2.72) and H-3″ (δ_H 2.11) to C-1″ (δ_C 201.5) and the ^{13}C NMR chemical shifts of C-1″ and C-2 (δ_C 111.9)[62, 69] indicated the presence of an isovaleryl side chain (C-1″ – C-5″) at C-2. The attachment of the 1-hydroxy-1-methylethyl function at C-7 was confirmed by the HMBC correlations of H-2′ (δ_H 1.27) and H-3′ (δ_H 1.31) to C-1′ (δ_C 73.3) and C-7 (δ_C 61.7) (Figure 10).

The connectivities of C-5a – C-6 – C-7 were established from the HMBC correlations of 6α-Me (δ_H 1.16) and 6β-Me (δ_H 0.72) to C-5a (δ_C 56.3), C-6 (δ_C 46.3), and C-7. The HMBC correlations of H-8 (δ_H 1.98) to C-8a (δ_C 59.4) and C-5a suggested

a cyclopentane structure composed of C-5a − C-6 − C-7 − C-8 − C-8a (ring B). Furthermore, the HMBC correlations of H-5a (δ_H 2.49) to C-3a (δ_C 86.0) and C-8a and of H-5 (δ_H 2.22) to C-4 (δ_C 213.3) and C-3a established the presence of a cyclopentane ring composed of C-3a − C-4 − C-5 − C-5a − C-8a (ring C) and its fusion to ring B at C-5a and C-8a (Figure 10). Because C-3a and C-8a were common to rings A and C, the fusion of these rings was confirmed. From these findings, the planar structure of compound **12b** was established, as shown in Figure 10.

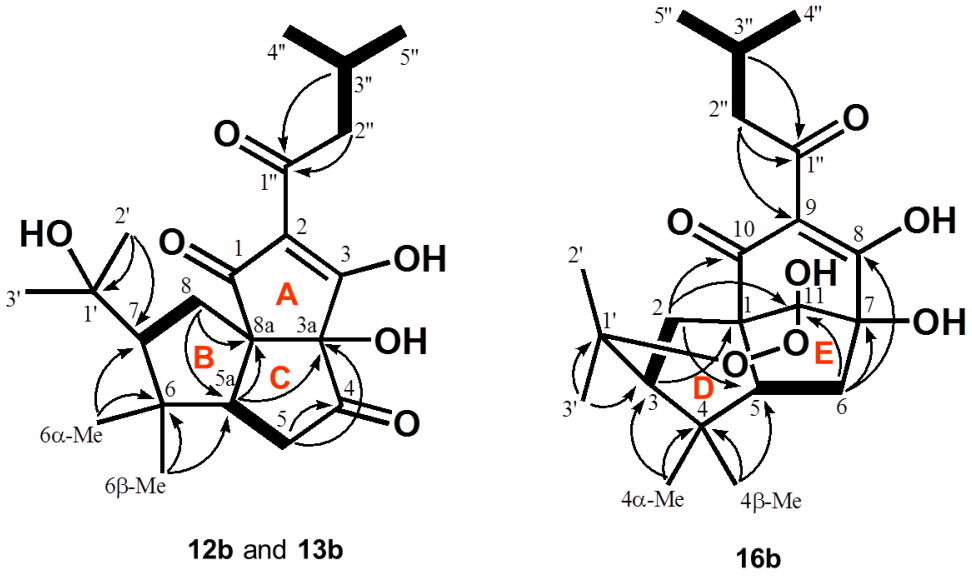

Figure 10. Selected HMBC (arrow) and ^{1}H-^{1}H COSY (bold) correlations for compounds **12b**, **13b**, and **16b**.

The 1-hydroxy-1-methylethyl moiety at C-7 was confirmed to be β-oriented from the correlations between H-5a(α), H-7(α), and 6α-Me in the NOESY experiment (Figure 11). Considering the mechanism of formation of compound **12b** from humulone (Figure 15), the absolute configurations of C-5a and C-8a are both likely to be *S*. It was demonstrated that natural humulone isomerizes via an acyloin rearrangement, resulting in *cis*- and *trans*-isohumulone, both with a (4*S*) absolute configuration (Figure 1).[21] Therefore, the C-3a absolute configuration in compound **12b** is also *S*. Thus, the absolute

configuration of compound **12b** was defined as (3a*S*, 5a*S*, 7*S*, 8a*S*). This configuration was confirmed by a single-crystal X-ray diffraction study, and a perspective ORTEP plot is shown in Figure 12. From the aforementioned findings, compound **12b** was defined as (3a*S*,5a*S*,7*S*,8a*S*)-3,3a-dihydroxy-7-(1-hydroxy-1-methylethyl)-6,6-dimethyl-2-(3-methylbutyryl)-5a,6,7,8-tetrahydro-3a*H*,5*H*-cyclopenta[*c*]pentalene-1,4-dione and named tricyclooxyisohumulone A (TCOIH A).

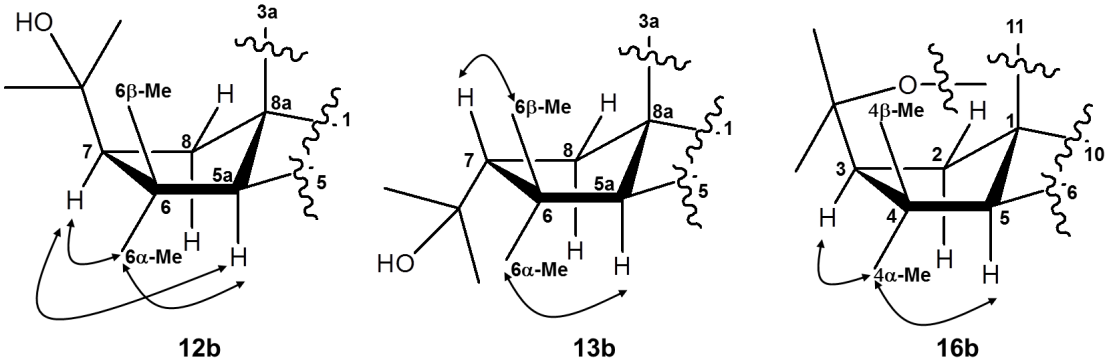

Figure 11. Key NOESY correlations for compounds **12b**, **13b**, and **16b**.

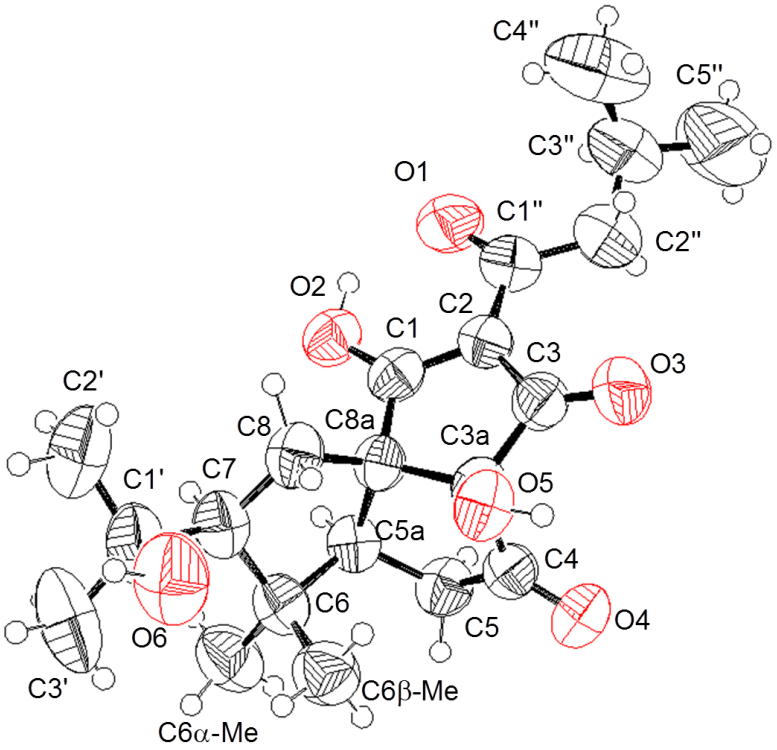

Figure 12. X-ray crystallographic structure of TCOIH A (**12b**).

Compound **13b** was obtained as a pale yellow oil. The HRESIMS data showed an $[M - H]^-$ ion at *m/z* 377.1965, and together with the ^{13}C NMR data, indicated a molecular formula of $C_{21}H_{30}O_6$, which is the same as that of compound **12b**. Analysis of the ^1H, ^{13}C NMR, ^1H-^1H COSY, HMQC, and HMBC spectra indicated that compounds **13b** and **12b** possess the same planar structure (Figure 10). However, the chemical shift of the C-7 methine proton was shielded by 0.44 ppm [δ_H 1.65 (**13b**) vs δ_H 2.09 (**12b**)], and the ^1H and ^{13}C NMR chemical shifts for the 6β-Me were strongly deshielded [δ_H 0.92, δ_C 27.6 (**13b**) vs δ_H 0.72, δ_C 17.5 (**12b**)] (Table 3). Thus, compound **13b** is the C-7 epimer of compound **12b**.[25, 26, 72, 73] This was confirmed by a NOESY experiment, showing correlations between H-5a(α) and 6α-Me and between H-7(β) and 6β-Me (Figure 11). Based on these findings, compound **13b** was defined as (3a*S*,5a*S*,7*R*,8a*S*)-3,3a-dihydroxy-7-(1-hydroxy-1-methylethyl)-6,6-dimethyl-2-(3-meth ylbutyryl)-5a,6,7,8-tetrahydro-3a*H*,5*H*-cyclopenta[*c*]pentalene-1,4-dione and named tricyclooxyisohumulone B (TCOIH B).

Compound **14b** was obtained as a white amorphous solid. The HRESIMS data showed an $[M - H]^-$ ion at *m/z* 393.1909, and together with the ^{13}C NMR data, indicated a molecular formula of $C_{21}H_{30}O_7$ (compound **12b** + O). Analysis of its ^1H and ^{13}C NMR data showed resonances similar to those of compound **12b**, except for the chemical shifts of C-7, 1′, 2′, and 3′ (Table 3). When compared to compound **12b**, the oxygenated C-1′ was strongly deshielded [δ_C 85.0 (**14b**) vs 73.3 (**12b**)] and the two methyl carbons C-2′ and C-3′ were shielded [C-2′/3′: δ_C 25.3/24.7 (**14b**) vs 30.6/30.3 (**12b**)]. These observations indicated that in compound **14b**, a 1-hydroperoxy-1-methylethyl fragment was present at C-7 rather than the 1-hydroxy-1-methylethyl fragment found in compound **12b**.[26, 69] The spontaneous generation of compound **12b** during the storage of compound **14b** (Figure 13) supports the existence of a hydroperoxy structure and indicates that the absolute configuration of compound **14b** is identical to that of compound **12b**. Thus, compound **14b** was defined as

(3a*S*,5a*S*,7*S*,8a*S*)-3,3a-dihydroxy-7-(1-hydroperoxy-1-methylethyl)-6,6-dimethyl-2-(3-methylbutyryl)-5a,6,7,8-tetrahydro-3a*H*,5*H*-cyclopenta[*c*]pentalene-1,4-dione and named tricycloperoxyisohumulone A (TCPOIH A).

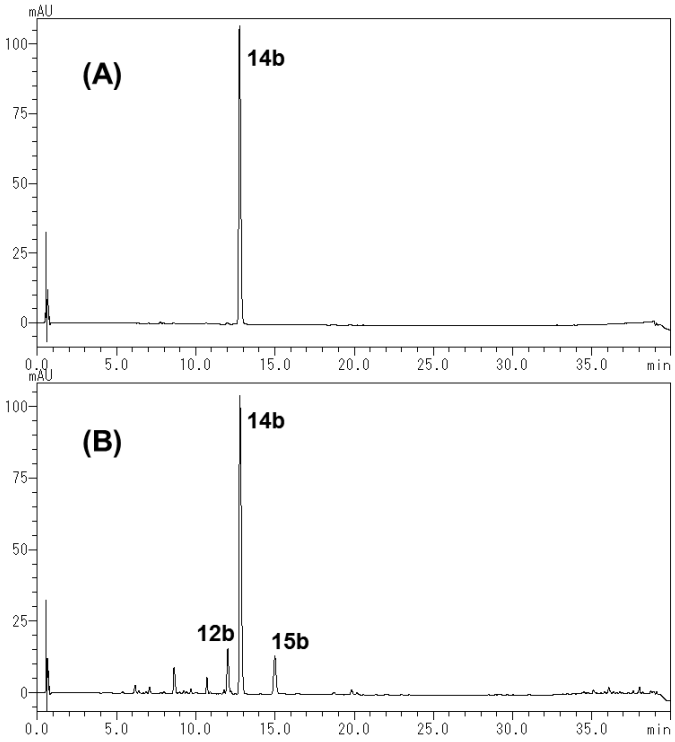

Figure 13. HPLC chromatograms of the isolated compound **14b** (A) before and (B) after storage in MeOH for 3 days at ambient temperature.

Although the structure of TCPOIH A (**14b**) was not previously known, a compound with a planar structure identical to that of TCOIH A (**12b**) and B (**13b**) has been previously reported.[74] However, the ^{1}H and ^{13}C NMR data in the aforementioned report were different from those of TCOIH A (**12b**) and B (**13b**) in this study but were identical to that of TCPOIH A (**14b**). Therefore, the isolated compound in the previous study[74] was neither TCOIH A (**12b**) nor B (**13b**) but TCPOIH A (**14b**). The author thus reports the correct structures and ^{1}H and ^{13}C NMR data (Table 3) for compounds **12b**–**14b** for the first time.

Compound **15b** was obtained as a white amorphous solid. The HRESIMS data showed an $[M - H]^-$ ion at *m/z* 319.1543, and together with the ^{13}C NMR data, indicated a molecular formula of $C_{18}H_{24}O_5$ (compound **12b** − C_3H_6O). The ^1H and ^{13}C NMR data of compound **15b** were similar to those of compounds **12b**–**14b**, except for the absence of the resonances derived from the side chain (C-1′– C-3′) at C-7 in compounds **12b**–**14b** (Table 3). From these observations, the structure of compound **15b** was proposed to be that shown in Figure 8. Analysis of the ^1H-^1H COSY, HMQC, and HMBC spectra also supported this structure. The spontaneous generation of compound **15b** during the storage of **14b** (Figure 13) indicated that these compounds had the same absolute configuration. Therefore, compound **15b** was defined as (3a*S*,5a*S*,8a*S*)-3,3a-dihydroxy-6,6-dimethyl-2-(3-methylbutyryl)-5a,6,7,8-tetrahydro-3a*H*,5*H*-cyclopenta[*c*]pentalene-1,4-dione and named deisopropyltricycloisohumulone (DeITCIH), which has not been previously reported.

Compound **16b** was obtained as a pale yellow oil. The HRESIMS data showed an $[M - H]^-$ ion at *m/z* 393.1911, and together with the ^{13}C NMR data, indicated a molecular formula of $C_{21}H_{30}O_7$, which is the same as that for compound **14b**. Compound **16b** rapidly and quantitatively isomerized into TCPOIH A (**14b**) in EtOH (Figure 14), suggesting a structure such as **16′b** or **16b** (Figure 8) that can readily undergo an acyloin rearrangement to yield compound **14b**. The molecular formula of compound **16b** required seven indices of hydrogen deficiency, three of which were accounted for by the one enolic and two carbonyl carbons (Table 4). Because no other carbonyl resonances were observed in the ^{13}C NMR spectroscopic data, compound **16b** must be a tetracyclic compound, and the structure of compound **16b** was proposed to be that shown, and not the structure of **16′b**.

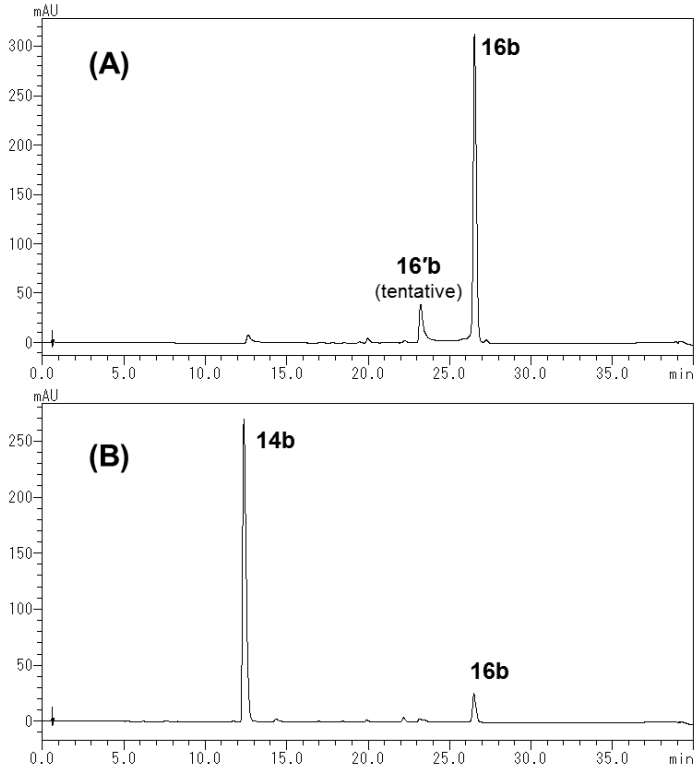

Figure 14. HPLC chromatograms of the isolated compound **16b** (A) before and (B) after storage in EtOH for 24 h at ambient temperature.

Table 4. NMR spectroscopic data (400 MHz, methanol-d_4) for compound **16b**

	16b	
pos.	δ_C, type	δ_H, mult. (*J* in Hz)
1	68.3, C	-
2	27.4, CH_2	2.75, dd (13.9, 8.0) 2.37, d (13.9)
3	60.8, CH	1.98, d (8.0)
4	48.3, C	-
4α-Me	39.8, CH_3	1.17, s
4β-Me	25.7, CH_3	1.35, s
5	55.7, CH	1.94, dd (10.5, 5.1)
6	34.1, CH_2	2.18, dd (13.2, 5.1) 1.74, dd (13.2, 10.5)
7	86.4, C	-
8	196.4, C	-
9	109.5, C	-
10	204.2, C	-
11	108.0, C	-
1'	88.2, C	-
2'	29.4, CH_3	1.13, s
3'	26.4, CH_3	1.55, s
1"	202.2, C	-
2"	46.9, CH_2	2.95, dd (13.1, 6.6) 2.89, dd (13.1, 7.1)
3"	27.8, CH	2.10, m
4"	22.9, CH_3	0.97, d (6.4)
5"	23.1, CH_3	0.98, d (6.4)

To confirm the proposed structure for compound **16b**, a detailed NMR spectroscopic analysis was performed. The ^1H, ^{13}C NMR and HMQC spectra showed the presence of six methyls [δ_H/δ_C: 0.97/22.9, 0.98/23.1, 1.13/29.4, 1.17/39.8, 1.35/25.7, and 1.55/26.4], three sp^3 methylenes [δ_H/δ_C: (2.18 and 1.74)/34.1, (2.75 and 2.37)/27.4, and (2.95 and 2.89)/46.9], three sp^3 methines [δ_H/δ_C: 1.94/55.7, 1.98/60.8, and 2.10/27.8], five sp^3 quaternary carbons [δ_C: 48.3, 68.3, 86.4 (mono-oxygenated), 88.2 (mono-oxygenated), and 108.0 (di-oxygenated)], and four sp^2 quaternary carbons [δ_C: 109.5, 196.4, 202.2, and 204.2]. The characteristic four sp^2 quaternary ^{13}C NMR

resonances strongly indicated that compound **16b** possessed a β-tricarbonyl (one enolic moiety) unit (C-8, C-9, C-10, C-1″), similar to TCPOIH A (**14b**).

Several structural fragments (C-2 − C-3, C-5 − C-6, and C-2″ − C-5″) were confirmed by the correlations in the ^{1}H-^{1}H COSY spectrum (bold lines in Figure 10). The HMBC correlations of H-2″ (δ_H 2.95) and H-3″ (δ_H 2.10) to C-1″ (δ_C 202.2) and of H-2″ to C-9 (δ_C 109.5) revealed the presence of the isovaleryl side chain at C-9, whereas the correlations of H-2′ (δ_H 1.13) and H-3′ (δ_H 1.55) to C-1′ (δ_C 88.2) and C-3 (δ_C 60.8) confirmed the attachment of the 1-methyl-1-oxyethyl function at C-3 (Figure 10).

The connectivities of C-3 − C-4 − C-5 were established by the HMBC correlations of 4α-Me (δ_H 1.17) and 4β-Me (δ_H 1.35) to C-3, C-4 (δ_C 48.3), and C-5 (δ_C 55.7) (Figure 10). The HMBC correlations of H-3 (δ_H 1.98) to C-1 (δ_C 68.3) and of H-2 (δ_H 2.75) to C-5 established the presence of a cyclopentane structure (ring D) composed of C-1 − C-5 (Figure 10). The HMBC correlations of H-2 to C-11 (δ_C 108.0) and of H-6 (δ_H 2.18) to C-7 (δ_C 86.4) and C-11 indicated the presence of another cyclopentane structure (ring E), composed of C-1 − C-5 − C-6 − C-7 − C-11, which was fused with ring D at C-1 and C-5. Ring E was shown to be part of a bicyclo[3.2.1]octane ring by the HMBC correlations of H-2 to C-10 (δ_C 204.2) and of H-6 to C-8 (δ_C 196.4), as C-8 and C-10 were contained within the β-tricarbonyl (one enolic moiety) unit (Figure 10).

The tetracyclic structure of compound **16b** and the large differences in the ^{1}H and ^{13}C NMR chemical shifts between 2′ and 3′ (geminal dimethyl at C-1′) and the ^{13}C NMR chemical shifts of C-1′ (δ_C 88.2) and C-11 (δ_C 108.0)[75, 76] suggested a peroxide bridge between C-1′ and C-11. Thus, the planar structure of compound **16b** shown in Figure 10 is proposed.

The *R*-configuration at C-7 in compound **16b** is derived from the C-6 carbon in humulone (Figure 1).[21] Because the C-1 – C-11 – C-7 bridge in the bicyclo ring is only possible in the *cis* form,[72, 77] C-1 must have an *R*-configuration. In addition, the (5*S*) absolute configuration should be identical to that of C-5a in TCPOIH A (**14b**). Because

the NOESY correlations between H-5(α) and 4α-Me and between 4α-Me and H-3(α) confirmed that H-3 was in the α-orientation (Figure 11), the absolute configuration at C-3 was determined to be *S*. The configuration at the C-11 hemiacetal carbon could not be established. Therefore, compound **16b** was identified as the hemiacetal of 7,8-dihydroxy-4,4-dimethyl-9-(3-methylbutyryl)-3β-(1-hydroperoxy-1-methylethyl)-5α -H-tricyclo[5.3.1.$0^{1,5}$]undec-8-ene-10,11-dione and named the hemiacetal of tricycloperoxyhumulone A (TCPOH A), which has not previously been reported.

An autoxidation reaction cascade from humulone to compounds **12b**–**16b**, related to the previously reported β-acid oxidation pathway,[26, 77] was proposed, as shown in Figure 15. The reaction presumably starts via a single-electron oxidation at C-4 in humulone to afford the stabilized α-keto radical intermediate 1. Stereoselective cyclization of 1 onto the prenyl group at C-6 would afford the bicyclic [3.2.1] tertiary radical 2, which could undergo a second cyclization onto the C-4 prenyl group to give tertiary radical intermediate 3 (as a mixture of C-3 epimers). Upon the addition of triplet oxygen, 3 would form a hydroperoxy radical, which could abstract a hydrogen from a donor molecule to afford epimers TCPOH A (**16′b**) and B (**16′′b**). Although only TCPOH A (**16′b**) could isomerize to the rather stable, isolable hemiacetal product (**16b**), both TCPOH A (**16′b**) and B (**16′′b**) would rapidly isomerize to their corresponding epimers TCPOIH A (**14b**) and B (**14′b**) via an acyloin rearrangement. TCPOIH A (**14b**) and B (**14′b**), which would be unstable, would be transformed to the corresponding alkoxy radical 4, which could either be saturated via hydrogen abstraction to give the corresponding alcohols, TCOIH A (**12b**) and B (**13b**), or lose one molecule of acetone, leading to DeITCIH (**15b**). In the author's study, it appears that the humulone in *n*-hexane preferably autoxidized to the epimer (intermediate 3) with the 3β-orientation, affording a larger amount of TCOIH A (**12b**) than TCOIH B (**13b**). Although the author could not isolate TCPOIH B (**14′b**), the presence of TCOIH B (**13b**) strongly suggested its existence.

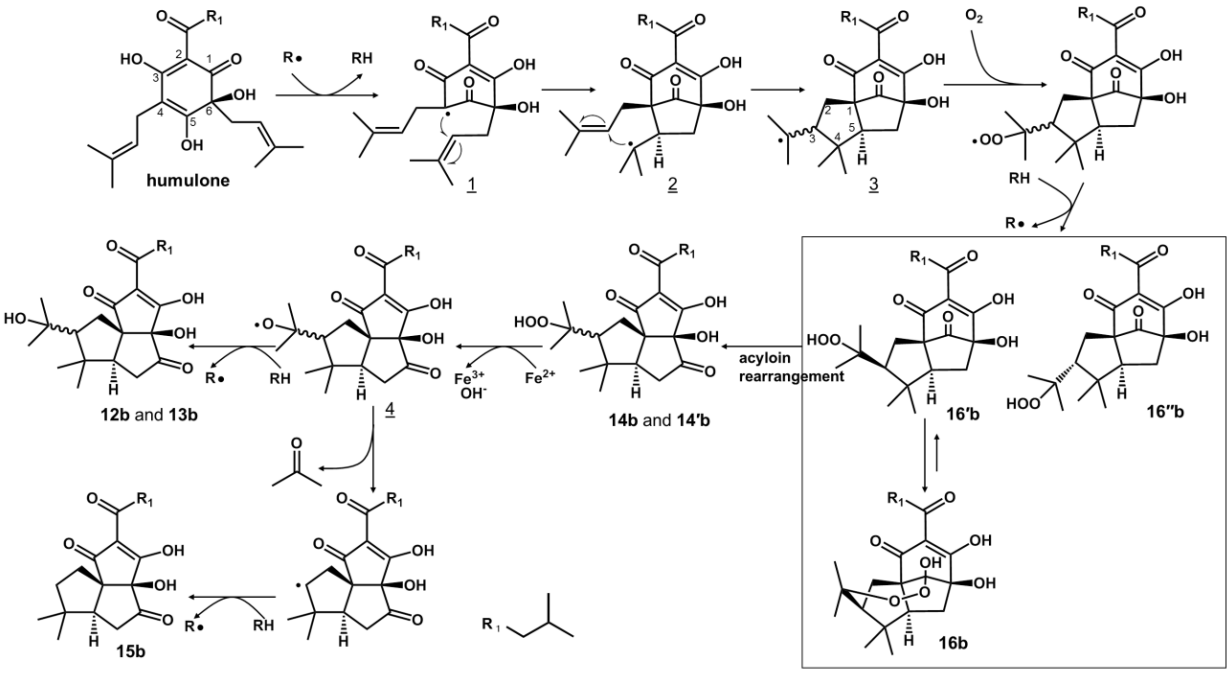

Figure 15. Proposed autoxidation pathway of humulone.

Analysis of compounds 12b–16b in stored hops.

To verify the presence of compounds **12b–16b**, hops stored at 40 °C for up to 40 weeks were analyzed sequentially by LC/MS/MS (for compounds **12b–16b**) and HPLC (for humulone). Compounds **12b–15b** were detected in the stored hops, but compound **16b** was not. Next, their concentrations during storage of the hops were examined. Figure 16 shows the time-dependent decrease in humulone and the compositional changes in the oxidation products **12b–15b**. Humulone concentration rapidly decreased during the first 5 weeks (94.7 → 10.1 μmol/g). TCPOIH A (**14b**) reached a maximum after 4 weeks of storage and then decreased rapidly. In contrast, the amounts of TCOIH A (**12b**) and B (**13b**) and of DeITCIH (**15b**) increased rapidly during the first 5 weeks and were then rather stable until the 40th week. The total amount of oxidation products **12b–15b** generated after 5 weeks of storage was 7.70 μmol/g, which accounted for 9.1% of the humulone that decomposed. Because the amounts of TCOIH A (**12b**) and B (**13b**) produced were nearly equal, the stereoselectivity of the oxidation of humulone in hops

may be different from that in *n*-hexane. From the auhor's results, the author believes that compounds **12b–15b** could serve as indicators for the hop oxidation progress, similar to humulinones and 4′-hydroxyallohumulinones as described in chapter 1.

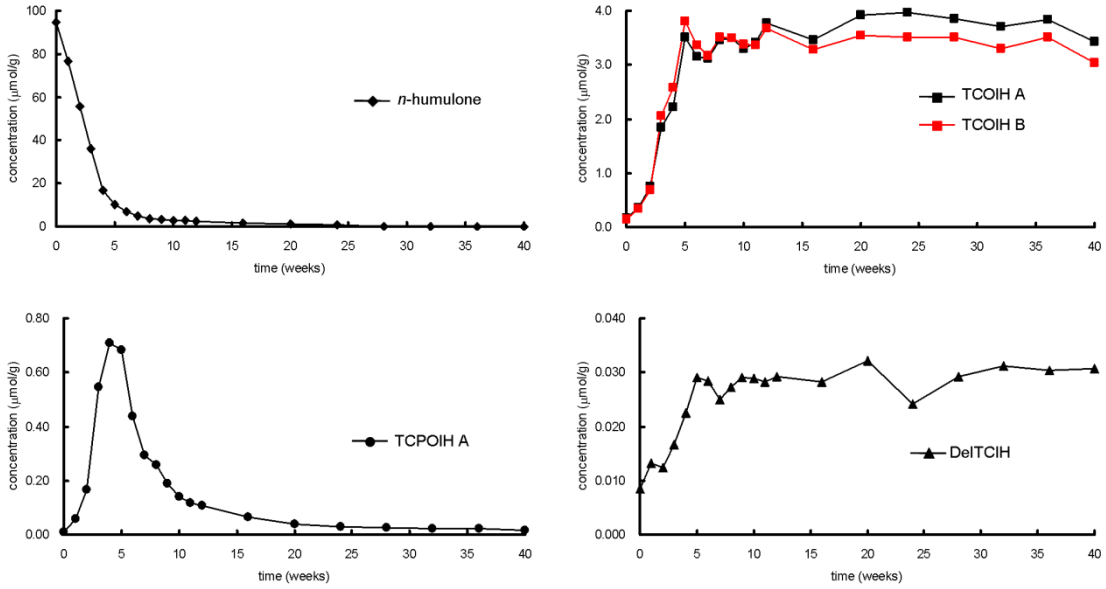

Figure 16. Concentration changes in humulone, TCOIH A (**12b**) and B (**13b**), TCPOIH A (**14b**), and DeITCIH (**15b**) in hops during storage at 40 °C over 40 weeks.

Summary

Because an understanding of α-acid oxides is essential to optimize the effects of oxidized hops on the quality of beer, the author investigated the autoxidation products of humulone (a representative congener of α-acids) using a simplified autoxidation model. Humulone was dissolved in *n*-hexane and autoxidized at 20 °C for 144 h. Among the oxidation products, TCOIH A (**12b**) and B (**13b**), TCPOIH A (**14b**), DeITCIH (**15b**), and the hemiacetal **16b** of TCPOH A (**16′b**) were isolated, and their structures were elucidated for the first time. The occurrence of compounds **12b–15b** in stored hops was verified using LC/MS/MS analysis. The levels of compounds **12b–15b** during hop storage were monitored using LC/MS/MS analysis. When hops were stored at 40 °C, humulone decreased to 10% during the first 5 weeks. TCPOIH A (**14b**) reached a

maximum after 4 weeks of storage and then decreased rapidly. In contrast, the amounts of TCOIH A (**12b**) and B (**13b**) and of DeITCIH (**15b**) increased rapidly during the first 5 weeks and were then rather stable until the 40th week.

Chapter 3

Analysis of the components of hard resin in hops and structural elucidation of their transformation products formed during the brewing process

The lupulin glands from female inflorescences of hops are known to accumulate resins and essential oils. The resins are composed of many different substances and are responsible for the fine bitter taste of beer. According to the European Brewery Convention and the American Society of Brewing Chemists, resins in hops can be divided into two main sub-fractions; namely soft resin (i.e., the fraction soluble in low-boiling paraffin hydrocarbons such as hexane) and hard resin (i.e., the fraction insoluble in hexane but soluble in ether and cold MeOH). [2-4, 78]

There have been numerous published studies that have focused on the soft resin components and their impact on the properties of beer. By contrast, however, there is a lack of information concerning the hard resin components and their effect on beer quality. Xanthohumol, a prenyl chalcone, is a well-known constituent of hard resin.[4, 36] However, other components of hard resin have not, until now, been identified.[4, 36] It has been reported that the α- and β-acids undergo rapid oxidation during the storage of hops, and the amount of hard resin fraction increases.[8, 34] Thus, the hard resin is considered to be mainly composed of the oxidation products derived from α-acids and/or β-acids.[4, 36]

The organoleptic properties and functionality of the hard resin have received considerable attention over the years. However, opinion concerning the effect of the hard resin accumulated in stored hops on the bitterness quality of beer remains contentious.[9, 23, 32, 37-39] Previous studies using hard resin enriched extracts for brewing proved inconclusive and failed to explain the effect of the hard resin on the quality of the beer.[33, 34] The apparent inconsistency in the results of these studies could be due to the lack of chemical analysis of materials used in the experiments. Recently, Alamaguer *et al.* reported that the hard resin positively contributed to the foam stability of beer and

produced a more pleasant bitter taste as opposed to the sharper bitterness of iso-α-acids. However, the hard resin enriched extracts used in the study were not subjected to rigorous chemical compositional analysis.[36] Thus, a suitable method to fully analyze the chemical composition of the hard resin was needed to properly examine its effect on the properties of beer. Furthermore, transformation of the hard resin components during the wort boiling process, which is known to have a significant effect on beer taste, was not understood, except for the conversion of xanthohumol into isoxanthohumol.[79] Knowledge of the transformation of hard resin components during the wort boiling process is also essential to evaluate and optimize the effect of the hard resin on beer quality.

In chapters 1 and 2, the author reported an HPLC method suitable for investigation of the oxidation products in stored hops, which showed that α-acids are oxidized into humulinones (**6a–c**), 4′-hydroxyallohumulinones (**11a–c**) and tricyclooxyisohumulones A (**12a–c**) and B (**13a–c**), and that β-acids are oxidized into hulupones (**5a–c**) (Figure 17). These oxidation products are thought to be components in the soft or hard resins. In this study, the author analyzed the soft and hard resins derived from stored hops using the author's newly developed analytical method and clarified the existence of these oxidation compounds for the first time. The author also investigated the transformation of the hard resin components through wort boiling by utilizing model boiling experiments, and successively isolated and determined the structures of the transformation products. The concentration changes of these products and their precursors during the boiling process were also investigated.

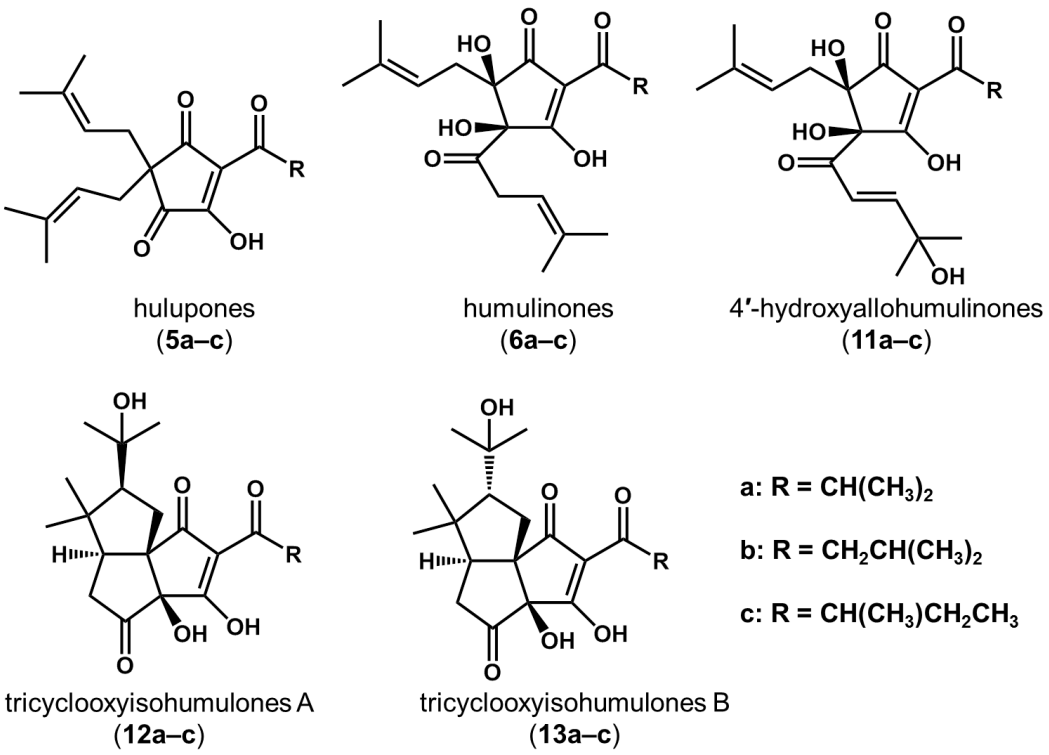

Figure 17. Structures of hulupones, cohulupone (**5a**), hulupone (**5b**), and adhulupone (**5c**); humulinones, cohumulinone (**6a**), humulinone (**6b**), and adhumulinone (**6c**); 4′-hydroxyallohumulinones, 4′-hydroxyallocohumulinone (**11a**), 4′-hydroxyallohumulinone (**11b**), and 4′-hydroxyalloadhumulinone (**11c**); tricyclooxyisohumulones A, tricyclooxyisocohumulone A (**12a**), tricyclooxyisohumulone A (**12b**), and tricyclooxyisoadhumulone A (**12c**); and tricyclooxyisohumulones B, tricyclooxyisocohumulone B (**13a**), tricyclooxyisohumulone B (**13b**), and tricyclooxyisoadhumulone B (**13c**).

Materials and methods

Chemicals and materials.

The following chemicals were obtained commercially: ethylenediaminetetraacetic acid (EDTA), H_3PO_4, MeCN, EtOH, hexane, diethyl ether, CH_2Cl_2 (Wako Pure Chemicals, Osaka, Japan); xanthohumol and isoxanthohumol (Funakoshi, Tokyo, Japan). Deionized water for chromatography was purified by means of a Milli-Q Gradient A10

system (Millipore, Billerica, MA, USA). Hop pellets, cultivar Hallertau Perle, were purchased from Hopsteiner (Mainburg, Germany).

Preparation of humulinones (6a–c), hulupones (5a–c), and tricyclooxyisohumulones A (12b) and B (13b).

Humulinones (**6a–c**) and hulupones (**5a–c**) were prepared according to a protocol reported in chapter 1. Tricyclooxyisohumulones A (**12b**) and B (**13b**) were isolated from the autoxidation products of humulone as described in chapter 2.

Preparation of 4′-hydroxyallohumulinones (11a–c and 11c′) from stored hops.

Hop pellets (850 g) were stored at 60 °C for 120 h and extracted with H_2O (8.5 L) at 50 °C for 1 h. The extract was filtered and then lyophilized to yield a brown powder (176 g). A portion of this powder (120 g) was dissolved in H_2O (8.1 L) and partitioned with CH_2Cl_2 (16.2 L) after adding 1 N HCl (810 mL) to the solution. The CH_2Cl_2 layer containing 4′-hydroxyallohumulinones was collected and dried over anhydrous Na_2SO_4 and concentrated to dryness *in vacuo* to give a yellowish brown oil (22 g). This oil was dissolved in EtOH and repeatedly subjected to preparative HPLC [column: 150 × 22 mm id, 5 μm, Alltima C_{18} column (Systech, Tokyo, Japan); solvent: H_2O/H_3PO_4 (85%), 100/1, (v/v) (solvent A) and MeCN (solvent B), a linear gradient from 30 to 90% B in 0 → 40 min and 90% B for 40 → 45 min; flow rate: 18.8 mL/min; detector: 270 nm; column temperature: RT], and divided into 11 fractions depending on their elution times. Compounds **11a**, **11b**, and **11c/c′** were contained in fractions 3 (t_R 8.6 – 9.5 min), 6 (t_R 11.0 – 12.1 min) and 7 (t_R 12.1 – 12.9 min), respectively. Compound **11a** in fraction 3 and compound **11b** in fraction 6 were further purified by repeatedly subjecting them to a second preparative HPLC step [column: 50 × 20 mm id, 5 μm, L-column 2 ODS (Chemicals Evaluation and Research Institute, Tokyo, Japan); solvent: 10 mM NH_4HCO_3 (solvent A) and MeCN (solvent B), isocratic elution at 20% B; flow rate: 9.5

mL/min; detector: 270 nm; column temperature: 40 ˚C]. Compounds **11a** and **11b** were eluted at 3.8 – 4.7 min and at 5.5 – 7.5 min, respectively. Each eluate was immediately diluted two times with H_2O, adjusted to pH 2.0 with 1 N HCl, and partitioned with CH_2Cl_2 (1/2 volume of the diluted eluate × 2 times). The respective CH_2Cl_2 layer was dried over anhydrous Na_2SO_4 and concentrated to dryness to yield pure **11a** (814 mg) and **11b** (1.2 g). Similarly, compounds **11c/c′** in fraction 7 were further purified by repeatedly subjecting them to a second preparative HPLC [column: 150 × 20 mm id, 5 μm, L-column 2 ODS (Chemicals Evaluation and Research Institute, Tokyo, Japan); solvent: 100 mM NH_4HCO_3 (solvent A) and MeCN (solvent B), isocratic elution at 20% B; flow rate: 18.8 mL/min; detector: 270 nm; column temperature: RT]. Compounds **11c** and **11c′** were eluted separately at 9.8 – 10.8 min and at 10.8 – 11.8 min, respectively. Pure **11c** (40.3 mg) and **11c′** (37.2 mg) were recovered from each eluate in the same way as that described for **11a** and **11b**.

4′-Hydroxyalloadhumulinone A (**11c**): pale yellow oil; $[\alpha]^{20}_{D}$ +4.01 (*c* 0.4, MeOH); ^{1}H and ^{13}C NMR data, see Table 6; HRESIMS (negative) *m/z* 393.1916 $[M - H]^-$ (calcd for $C_{21}H_{29}O_7$, 393.1919).

4′-Hydroxyalloadhumulinone B (**11c′**): pale yellow oil; $[\alpha]^{20}_{D}$ +12.1 (*c* 0.3, MeOH); ^{1}H and ^{13}C NMR data, see Table 6; HRESIMS (negative) *m/z* 393.1914 $[M - H]^-$ (calcd for $C_{21}H_{29}O_7$, 393.1919).

Preparation of soft and hard resins.

Soft and hard resins from hops were prepared according to Analytica EBC[78] with some modification. Hop pellets (100 g) were stored at 60 °C for 48 h, and a portion (10 g) was extracted with MeOH (100 mL) by stirring at room temperature for 1 h and then filtered. The filtrate was kept at 4 °C for 1 day, and a waxy precipitate that formed was removed by filtration. To a portion of the filtrate (20 mL), MeOH (10 mL), hexane (80 mL) and 1 N HCl (20 mL) were added, and the two layer solution (hexane/acidic

MeOH-H_2O) was partitioned in a separating funnel. The hexane layer, prepared by repeating the above partition four times (320 mL), was evaporated to dryness to give a yellowish brown oil (250 mg, soft resin).

The residual acidic MeOH-H_2O layer was partitioned with diethyl ether (80 mL × 2 times). The diethyl ether layer (160 mL) was washed with sat. NaCl solution (160 mL), dried over anhydrous Na_2SO_4, and concentrated to dryness to give a brown solid (200 mg, hard resin).

Boiling test for the hard resin.

To 500 μL of 10 mM citrate buffer (pH 5.5) pre-heated to 100 °C was added a 25 μL solution of the hard resin in EtOH (5.0 mg/mL). The combined solution was kept at 100 °C and analyzed by HPLC at 30, 60, 90 and 120 min.

Boiling test of 4′-hydroxyallohumulinones (11a–c, c′).

To a 500 μL aliquot of 10 mM citrate buffer (pH 5.5) pre-heated to 100 °C was added 25 μL solution of either 4′-hydroxyallocohumulinone (**11a**), 4′-hydroxyallohumulinone (**11b**), 4′-hydroxyalloadhumulinones A (**11c**) or B (**11c′**) (1.0 mg/mL in EtOH). Each combined solution was kept at 100 °C, and analyzed by HPLC at 30, 60, 90, and 120 min.

Isolation of the transformation products produced by boiling of 4′-hydroxyallocohumulinone (11a) and 4′-hydroxyallohumulinone (11b).

4′-Hydroxyallocohumulinone (**11a**) (200 mg) was dissolved in EtOH (50 mL) and added to 10 mM citrate buffer (pH 5.5, 1 L) pre-heated to 100 °C and maintained at this temperature for 90 min. After cooling to room temperature, the solution was acidified with 1 N HCl (100 mL) and partitioned with CH_2Cl_2 (250 mL × 3 times). The CH_2Cl_2 layer (750 mL) was washed with sat. NaCl solution (400 mL), dried over anhydrous

Na_2SO_4, and concentrated to dryness to give a yellowish brown oil (150 mg).

The oil was dissolved in EtOH and repeatedly subjected to preparative HPLC [column: 150 × 10 mm id, 5 μm, Alltima C_{18} column (Systech, Tokyo, Japan); solvent: H_2O/H_3PO_4 (85%), 100/1, (v/v) (solvent A) and MeCN (solvent B), a linear gradient from 30% B for 0 → 15 min, 30 to 90% B in 15 → 18 min, and 90% B for 18 → 22 min; flow rate: 4.7 mL/min; detector: 270 nm; column temperature: 40 °C]. In this preparative HPLC, 4′-hydroxyallo-*cis*-cohumulinone (**17a**) was eluted at 8.6 – 10.0 min and *cis*-oxycohumulinic acid (**18a**) was eluted at 10.0 – 10.6 min. Each eluate was diluted with H_2O to lower the concentration of MeCN to less than 10%, and extracted with CH_2Cl_2 (1/4 volume of the diluted eluate × 3 times). The CH_2Cl_2 layer was dried over anhydrous Na_2SO_4 and concentrated to dryness to yield **17a** (33.4 mg) and **18a** (4.0 mg).

The transformation products (**17b** and **18b**) of 4′-hydroxyallohumulinone (**11b**) were prepared and purified in almost the same way as described for **17a** and **18a**. In summary, 4′-hydroxyallohumulinone (**11b**) (200 mg) was boiled and partitioned between CH_2Cl_2 and acidic H_2O. The CH_2Cl_2 layer was concentrated to give an oil (167 mg). The oil was repeatedly subjected to preparative HPLC (column, flow rate, detector, and column temperature are identical to those used for the isolation of **17a** and **18a**; solvent: H_2O/H_3PO_4 (85%), 100/1, (v/v) (solvent A) and MeCN (solvent B), a linear gradient from 30 to 48% B in 0 → 12 min, 48 to 90% B in 12 → 18 min, and 90% B for 18 → 21 min). In this preparative HPLC, 4′-hydroxyallo-*cis*-humulinone (**17b**) and *cis*-oxyhumulinic acid (**18b**) were eluted at 9.0 – 9.6 min and at 10.0 – 10.3 min, respectively. Pure **17b** (41.3 mg) and **18b** (5.9 mg) were recovered from each eluate in the same way as described for **17a** and **18a**.

4′-Hydroxyallo-cis-cohumulinone (**17a**): pale yellow oil; $[\alpha]^{20}_D$ ±0 (*c* 0.7, MeOH); ^1H and ^{13}C NMR data, see Table 5; HRESIMS (negative) *m/z* 379.1753 $[M - H]^-$ (calcd for $C_{20}H_{27}O_7$, 379.1762).

4′-Hydroxyallo-cis-humulinone (**17b**): pale yellow oil; $[\alpha]^{20}_D$ ±0 (*c* 0.4, MeOH); ^1H

and ^{13}C NMR data, see Table 5; HRESIMS (negative) *m/z* 393.1911 $[M - H]^-$ (calcd for $C_{21}H_{29}O_7$, 393.1919).

cis-Oxycohumulinic acid (**18a**): white, amorphous solid; $[\alpha]^{20}_D$ ±0 (*c* 0.1, MeOH); ^1H and ^{13}C NMR data, see Table 5; HRESIMS (negative) *m/z* 267.1230 $[M - H]^-$ (calcd for $C_{14}H_{19}O_5$, 267.1238).

cis-Oxyhumulinic acid (**18b**): pale yellow oil; $[\alpha]^{20}_D$ ±0 (*c* 0.1, MeOH); ^1H and ^{13}C NMR data, see Table 5; HRESIMS (negative) *m/z* 281.1390 $[M - H]^-$ (calcd for $C_{15}H_{21}O_5$, 281.1395).

Preparation of *cis*- (18b) and *trans*-oxyhumulinic acids (19b) by hydrolysis of humulinone (6b).

Both *cis*- and *trans*-oxyhumulinic acids were prepared by alkaline hydrolysis of humulinone (**6b**) according to the previous report[80] with some modification.

Humulinone was prepared according to a protocol reported in chapter 1. To 2 M aqueous NaOH (300 mL) pre-heated at 100 ˚C, 30 mL solution of humulinone in MeOH (10 mg/mL) was added and mixed well. The temperature was maintained at 100 ˚C for 10 min before cooling the solution to room temperature, acidifying with 6 N HCl (120 mL) and partitioning with CH_2Cl_2 (200 mL × 2 times). The CH_2Cl_2 layer was dried over anhydrous Na_2SO_4 and concentrated to dryness to give a yellow oil (270 mg). The oil was dissolved in EtOH and repeatedly subjected to preparative HPLC [column: 150 × 22 mm id, 5 μm, Alltima C_{18} column (Systech, Tokyo, Japan); solvent: H_2O/H_3PO_4 (85%), 100/1, (v/v) (solvent A) and MeCN (solvent B), isocratic elution at 45% B; flow rate: 22.8 mL/min; detector: 270 nm; column temperature: RT]. In this preparative HPLC, *cis*- (**18b**) and *trans*-oxyhumulinic acids (**19b**) were eluted at 5.1 – 5.5 min and at 6.7 – 7.2 min, respectively. Pure **18b** (74.6 mg) and **19b** (94.6 mg) were recovered from each eluate in the same way as described for **17a** and **18a**.

trans-Oxyhumulinic acid (**19b**): white, amorphous solid; $[\alpha]^{20}_D$ ±0 (*c* 0.3, MeOH);

^{1}H and ^{13}C NMR data, see Table 5; HRESIMS (negative) *m/z* 281.1389 $[M - H]^-$ (calcd for $C_{15}H_{21}O_5$, 281.1395).

HPLC.

A Shimadzu Prominence UFLC system (Shimadzu, Kyoto, Japan) was used for all HPLC analysis. Data were processed with LCsolution software (Shimadzu, Kyoto, Japan). HPLC analyses were performed to investigate the constituents in the soft and hard resins of hops and to analyze compositional changes in the hard-resin components in the boiling tests using the following conditions: column: 100 × 2.1 mm id, 3 μm, Alltima C_{18} column (Systech, Tokyo, Japan); solvent: H_2O/H_3PO_4 (85%), 1000/0.2, (v/v) containing EDTA (0.02% w/v) (solvent A) and MeCN (solvent B), a linear gradient from 10 to 52% B in 0 → 26.7 min, 52% B for 26.7 → 30 min, 52 to 75% B in 30 → 32.7 min, 75 to 85% B in 32.7 → 36.7 min, and 85% B for 36.7 → 37.7 min; flow rate: 0.6 mL/min; detector: 270 nm; and column temperature: 40 ˚C. The injection volume was 3.0 μL. In the boiling tests, transformation products were quantified using isolated reference compounds. 4′-Hydroxyallo-*cis*-adhumulinones A (**17c**) and B (**17c′**) were quantified using the calibration curve of 4′-hydroxyallo-*cis*-humulinone (**17b**) and *cis*-oxyadhumulinic acids A (**18c**) and B (**18c′**) were quantified using the calibration curve of *cis*-oxyhumulinic acid (**18b**).

To separate and check the purity of 4′-hydroxyalloadhumulinones A (**11c**) and B (**11c′**) by HPLC (Figure 25), the following LC conditions were used: column: 100 × 2.1 mm id, 3 μm, L-column 2 ODS (Chemicals Evaluation and Research Institute, Tokyo, Japan); solvent: 5 mM $HCOONH_4$ (pH 8.5) (solvent A) and MeCN (solvent B), a linear gradient from 10 to 36% B in 0 → 39 min, 36 to 80% B in 39 → 44 min, and 80% B for 44 → 52 min; flow rate: 0.25 mL/min; detector: 270 nm; and column temperature: 40 ˚C. The injection volume was 3.0 μL.

HRESIMS.

HRESIMS of the purified compounds was measured using a Thermo Scientific LTQ Orbitrap mass spectrometer (Thermo Fisher Scientific, San Joes, CA, USA). Before measuring the samples, accurate mass calibration was carried out using polytyrosine-1,3,6 as a mass standard (CS Bio Company, Menlo Park, CA, USA).

NMR.

^{1}H, ^{13}C, and 2D NMR spectra were measured with a Bruker AVANCE400 spectrometer (Bruker BioSpin, Rheinstetten, Germany). Samples were dissolved in methanol-d_4. Chemical shifts were referenced to the solvent signals (δ_H/δ_C 3.30/49.0). Data processing was performed using TopSpin-NMR software (version 3.0) (Bruker BioSpin). *J*-Resolved HMBC experiments were conducted on a Varian INOVA-500 NMR spectrometer (Agilent, Santa Clara, CA, USA) using the previously reported method.[81]

Results and discussion

Identification of the components in the soft and hard resins derived from stored hops.

In chapters 1 and 2, the author reported the transformation of α-acids to humulinones (humulinones were further transformed to 4′-hydroxyallohumulinones) and to tricyclooxyisohumulones A and B due to oxidation. During these studies, the author also developed a HPLC method that is suitable for the analysis of α- and β-acid-derived oxidation compounds. Using this HPLC method, the author analyzed a MeOH extract of the stored hops, and soft and hard resins prepared from the MeOH extract. The results are shown in Figure 18 (18A: MeOH extract of the stored hops, 18B: the soft resin, 18C: the hard resin).

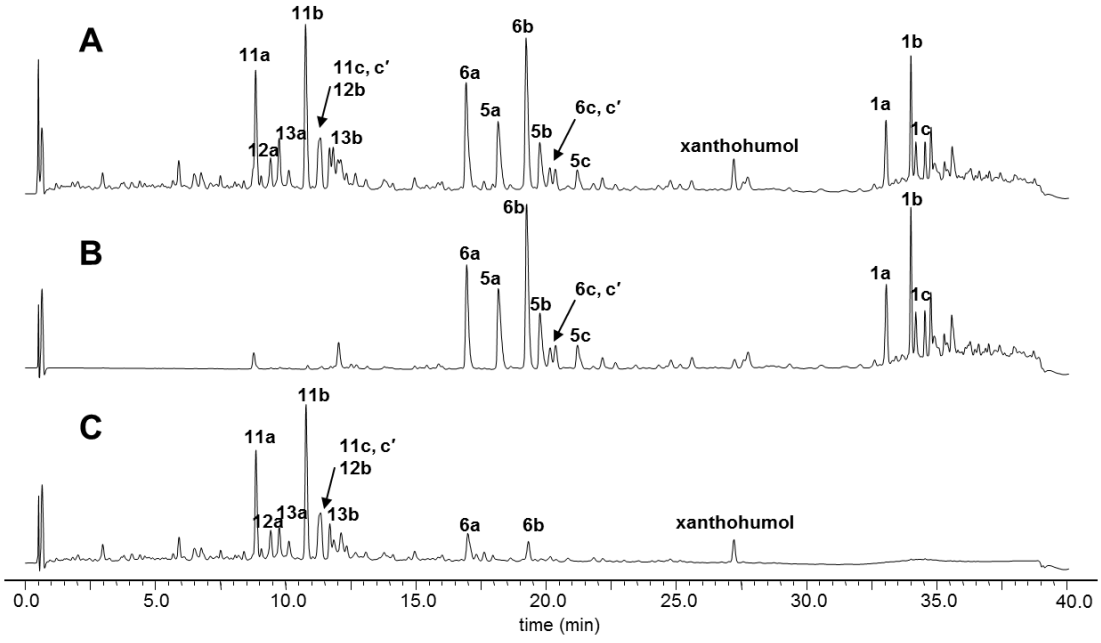

Figure 18. HPLC chromatograms of the MeOH extract of hops stored at 60 °C for 48 h (A), the soft resin fraction prepared from the MeOH extract (B), and the hard resin fraction prepared from the MeOH extract (C). Structures of the compounds are given in Figures 1, 17, and 24.

As shown in Figure 18B, the presence of humulinones (**6a–c**, **c′**), hulupones (**5a–c**) in addition to α-acids (**1a–c**) in the soft resin can clearly be observed. This is the first study reporting the presence of humulinones (**6a–c**, **c′**) and hulupones (**5a–c**) in soft resin.

The compounds contained in the soft resin were barely detectable in the hard resin (Figure 18C). Indeed, xanthohumol and the hydrophilic α-acid-derived oxidation products such as tricyclooxyisohumulones A (**12a**, **12b**) and B (**13a**, **13b**), and 4′-hydroxyallohumulinones (**11a–c**, **c′**) were found only in the hard-resin extract. This is the first study to report the existence of these α-acid-derived oxidation products in hard resin.

These findings also verify changes in the composition of the soft and hard resin constituents of hops caused by oxidation, because the concentration changes in α- and β-acid-derived oxidation products in soft and hard resins detected in this study during oxidation of hops have been clarified in chapters 1 and 2.

Transformation of the constituents of hard resin during the wort boiling process.

There has been little reported data on the compositional changes in hard resin during the wort boiling process. Thus, the author investigated the constituents in the hard resin after wort boiling. Changes in the chemical composition of hard resin constituents were determined by using a model boiling experiment conducted in an aqueous buffer (pH 5.5). HPLC analysis of the hard resin after 90 min of boiling (Figure 19B) clearly showed the transformation of xathohumol into isoxanthohumol, which was reported previously.[79] In addition, the HPLC analysis also detected a decrease in the concentration of 4′-hydroxyallohumulinones [4′-hydroxyallocohumulinone (**11a**), 4′-hydroxyallohumulinone (**11b**) and 4′-hydroxyalloadhumulinone (**11c/c′**)], and the appearance of some new compounds (Figure 19B). These findings suggested, for the first time, further transformation of 4′-hydroxyallohumulinones in the hard resin during the wort boiling process.

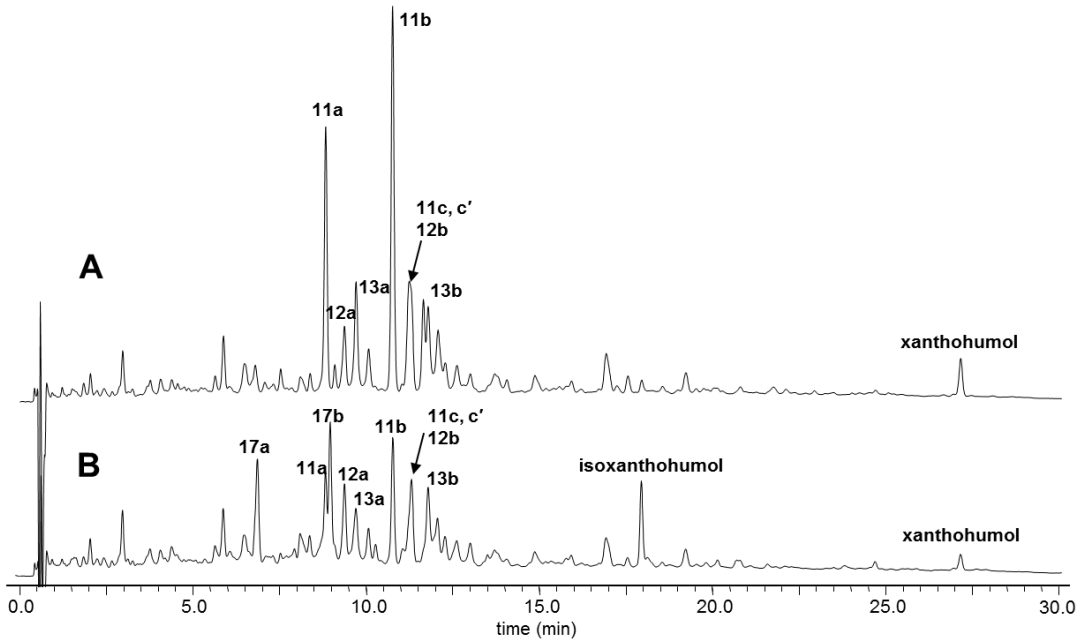

Figure 19. HPLC chromatograms of the hard resin (A) before and (B) after boiling in an aqueous buffer (pH 5.5) for 90 min. Structures of the compounds are given in Figures 17, 21, and 24.

Isolation and structural elucidation of the transformation products of 4′-hydroxyallocohumulinone (11a) and 4′-hydroxyallohumulinone (11b).

To verify the transformation of 4′-hydroxyallohumulinones into new compounds, isolated 4′-hydroxyallocohumulinone (**11a**) and 4′-hydroxyallohumulinone (**11b**) were boiled in the same buffer. The HPLC analyses clearly showed the transformation of **11a** into **17a** and **18a** (Figure 20A1 and A2) and of **11b** into **17b** and **18b** (Figure 20B1 and B2). The author also boiled tricyclooxyisohumulones A (**12b**) and B (**13b**), but the compounds were stable (i.e., unchanged) under these conditions (data not shown).

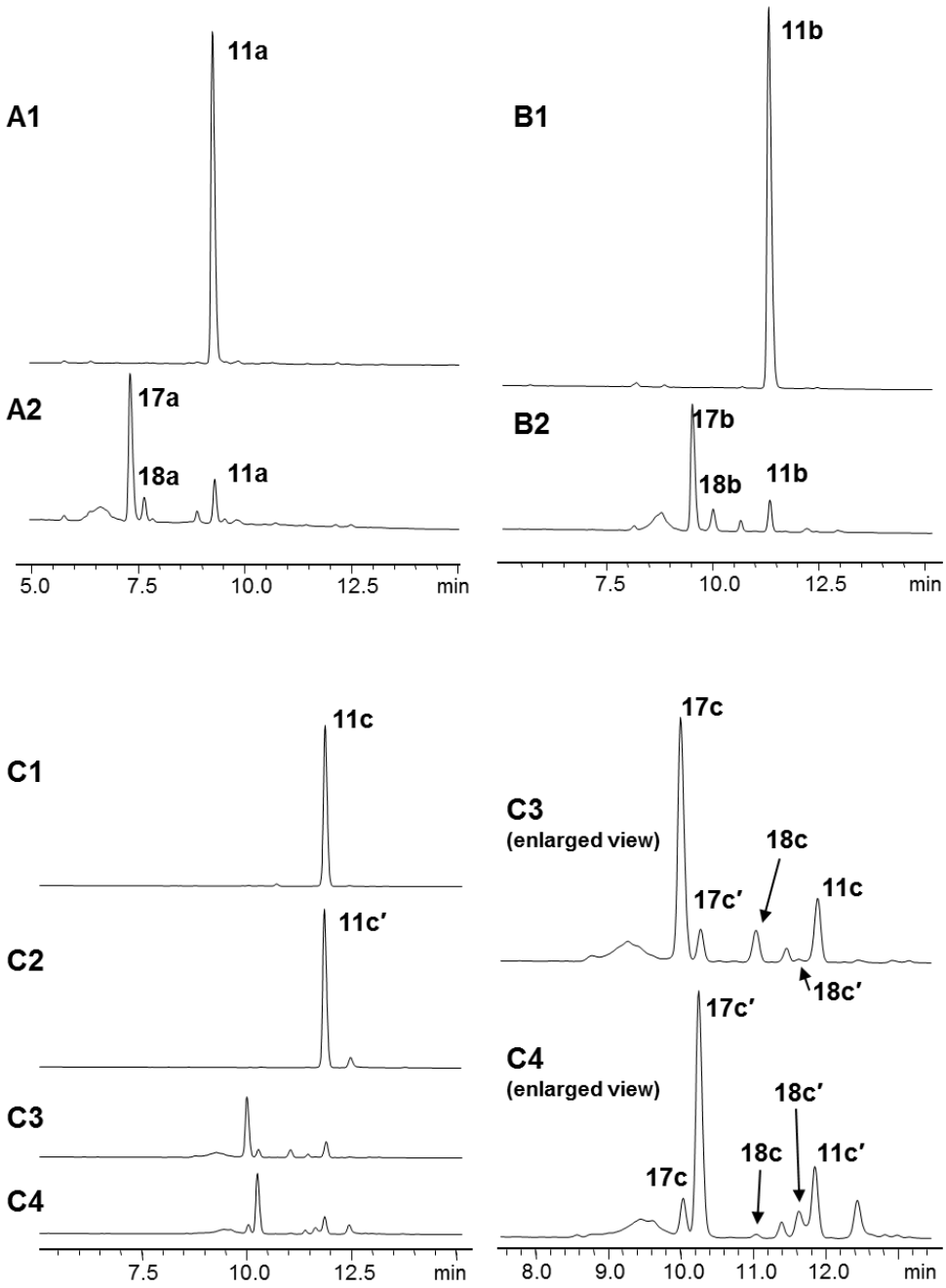

Figure 20. HPLC chromatograms of the isolated compounds before and after boiling in an aqueous buffer (pH 5.5) for 90 min. 4′-Hydroxyallocohumulinone (**11a**) (A1) before and (A2) after boiling; 4′-hydroxyallohumulinone (**11b**) (B1) before and (B2) after boiling; 4′-hydroxyalloadhumulinones A (**11c**) and B (**11c′**) (C1 and C2, respectively) before and (C3 and C4, respectively) after boiling.

To identify the transformation products of 4′-hydroxyallocohumulinone (**11a**) and 4′-hydroxyallohumulinone (**11b**), each 200 mg sample of isolated **11a** and **11b** was subjected to the boiling test. The compounds in the reaction products were purified using two phase solvent partition and preparative ODS HPLC, affording **17a** (33.4 mg) and **18a** (4.0 mg) from **11a**, and **17b** (41.3 mg) and **18b** (5.9 mg) from **11b**.

Compound **17b** was obtained as a pale yellow oil. The HRESIMS data showed an $[M - H]^-$ ion at *m/z* 393.1911, and together with the ^{13}C NMR data, indicated a molecular formula of $C_{21}H_{30}O_7$, which is identical to that of **11b**. Analysis of the ^1H, ^{13}C NMR, ^1H-^1H COSY, HMQC and HMBC spectra of **17b** in methanol-d_4 established that **17b** and **11b** possessed the same planar structure, whereas the ^{13}C NMR chemical shifts of C-5 and C-1″ were different between **17b** [δ 85.1 (C-5) and δ 36.7 (C-1″)] and **11b** [δ 81.6 (C-5) and δ 31.3 (C-1″)] (Tables 1 and 5). Furthermore, the NOE observed between H-2′ and H-1″ in **11b** was not observed in **17b**. From these results, **17b** was determined to be the C-5 epimer of **11b**, and named 4′-hydroxyallo-*cis*-humulinone, which has not been previously reported (Figure 21).

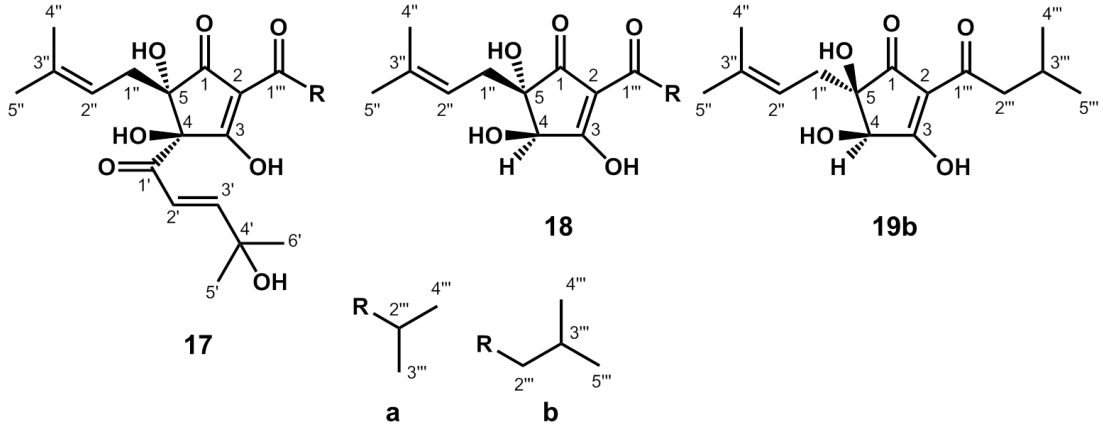

Figure 21. Chemical structures of 4′-hydroxyallo-*cis*-cohumulinone (**17a**), 4′-hydroxyallo-*cis*-humulinone (**17b**), *cis*-oxycohumulinic acid (**18a**), *cis*-oxyhumulinic acid (**18b**), and *trans*-oxyhumulinic acid (**19b**).

Table 5. NMR spectroscopic data (400 MHz, methanol-d_4) for compounds **17a**, **17b**, **18a**, **18b**, and **19b**[a]

	17a		**17b**		**18a**		**18b**		**19b**	
pos.	δ_C, type	δ_H, mult. (*J* in Hz)	δ_C, type	δ_H, mult. (*J* in Hz)	δ_C, type	δ_H, mult. (*J* in Hz)	δ_C, type	δ_H, mult. (*J* in Hz)	δ_C, type	δ_H, mult. (*J* in Hz)
1	200.9, C	-	201.6, C	-	199.6, C	-	200.2, C	-	200.5, C	-
2	113.3, C	-	114.1, C	-	111.6, C	-	112.6, C	-	112.8, C	-
3	195.4, C	-	196.0, C	-	197.8, C	-	198.3, C	-	199.8, C	-
4	92.0, C	-	92.3, C	-	80.6, CH	4.35, s	80.9, CH	4.35, s	74.2, CH	4.14, s
5	84.9, C	-	85.1, C	-	82.2, C	-	82.4, C	-	77.7, C	-
1'	198.2, C	-	198.3, C	-	-	-	-	-	-	-
2'	121.9, CH	6.78, d (15.5)	121.9, CH	6.79, d (15.5)	-	-	-	-	-	-
3'	155.9, CH	6.92, d (15.5)	156.0, CH	6.92, d (15.5)	-	-	-	-	-	-
4'	71.4, C	-	71.4, C	-	-	-	-	-	-	-
5'	29.1, CH_3	1.27, s	29.1, CH_3	1.28, s	-	-	-	-	-	-
6'	29.1, CH_3	1.29, s	29.1, CH_3	1.29, s	-	-	-	-	-	-
1"	36.79, CH_2	2.63, dd (13.9, 8.7) 2.48, dd (13.9, 6.6)	36.7, CH_2	2.62, dd (14.0, 8.5) 2.45, dd (14.0, 6.7)	34.8, CH_2	2.61, dd (13.5, 9.2) 2.45, dd (13.5, 6.4)	34.8, CH_2	2.60, dd (13.6, 9.1) 2.43, dd (13.6, 6.4)	34.6, CH_2	2.54, dd (14.0, 7.7) 2.48, dd (14.0, 6.9)
2"	119.1, CH	5.10, m	119.0, CH	5.10, m	119.3, CH	5.03, m	119.2, CH	5.02, m	118.3, CH	5.03, m
3"	136.6, C	-	136.6, C	-	136.5, C	-	136.4, C	-	137.6, C	-
4"	17.9, CH_3	1.52, s	17.9, CH_3	1.53, s	17.8, CH_3	1.52, s	17.9, CH_3	1.52, s	18.1, CH_3	1.65, s
5"	26.2, CH_3	1.60, s	26.2, CH_3	1.61, s	26.1, CH_3	1.58, s	26.1, CH_3	1.58, s	26.1, CH_3	1.68, s
1"'	203.5, C	-	197.8, C	-	205.2, C	-	199.9, C	-	201.9, C	-
2"'	36.75, CH	3.50, sep (6.9)	46.6, CH_2	2.74, dd (13.6, 7.2) 2.69, dd (13.6, 7.2)	37.3, CH	3.49, sep (6.9)	47.7, CH_2	2.77, dd (13.8, 7.0) 2.64, dd (13.8, 7.1)	48.4, CH_2	2.78, dd (14.5, 7.0) 2.73, dd (14.5, 6.9)
3"'	18.0, CH_3	1.10, d (6.9)	27.6, CH	2.11, m	17.8, CH_3	1.09, d (6.9)	27.1, CH	2.11, m	26.7, CH	2.13, m
4"'	18.6, CH_3	1.14, d (6.9)	22.86, CH_3	0.95, d (6.7)	18.7, CH_3	1.12, d (6.9)	22.8, CH_3	0.94, d (6.2)	22.8, CH_3	0.96, d (6.7)
5"'	-	-	22.94, CH_3	0.97, d (6.7)	-	-	22.9, CH_3	0.96, d (6.2)	22.9, CH_3	0.96, d (6.7)

[a] Arbitrary numbering according to structures **17a**, **17b**, **18a**, **18b** and **19b** shown in Figure 21.

Compound **18b** was obtained as a pale yellow oil. The HRESIMS data showed an $[M - H]^-$ ion at *m/z* 281.1390, and together with the ^{13}C NMR data, indicated a molecular formula of $C_{15}H_{22}O_5$ (**17b** − $C_6H_8O_2$). Analysis of the ^1H, ^{13}C NMR, ^1H-^1H COSY, HMQC, and HMBC spectra of **18b** in methanol-d_4 established that the *trans*-4-hydroxy-4-methyl-2-pentenoyl side chain attached at C-4 in **17b** was absent in **18b** (Table 5). Thus, the planar structure of **18b** was determined as oxyhumulinic acid (Figure 21). To determine relative configurations at C-4 and C-5 in **18b**, the author prepared *cis*- and *trans*-oxyhumulinic acids (epimers at C-5) by alkaline hydrolysis of humulinone (**6b**)[80] as a mixture, and then isolated each isomer using ODS preparative HPLC. By ^1H and ^{13}C NMR analysis (Table 5), one of the two isomeric compounds was identified to be **18b** and thus the other (**19b**) was determined to be the C-5 epimer of **18b**. In the NOESY experiments on **18b** and **19b**, the NOE between H-4 and H-1″ (the prenyl CH_2 attached at C-5) was clearly observed in **19b**, but was barely detected in **18b** (Figure 22). Furthermore, *J*-resolved HMBC experiments[81] on **18b** and **19b** showed that the absolute value of the two-bond ^{13}C-^1H coupling constant between H-4 and C-5 was greater in **18b** than in **19b** [^2J(C5, 4H) = 5.9 Hz in **18b**, ^2J(C5, 4H) $\leqq$ 3.0 Hz in **19b**] (Figure 23), indicating a larger dihedral angle between H-4 and 5-OH in **19b** than **18b**.[82] These observations clearly indicated that H-4 and 5-OH were in the α-orientation in **18b**, and that H-4 and the prenyl group attached at C-5 were in the α-orientation in **19b**. Thus, **18b** was determined as *cis*-oxyhumulinic acid and **19b** was determined as *trans*-oxyhumulinic acid (Figure 21). Although the structures of **18b** and **19b** were reported about 50 years ago,[80] the author presents their NMR data for the first time (Table 5).

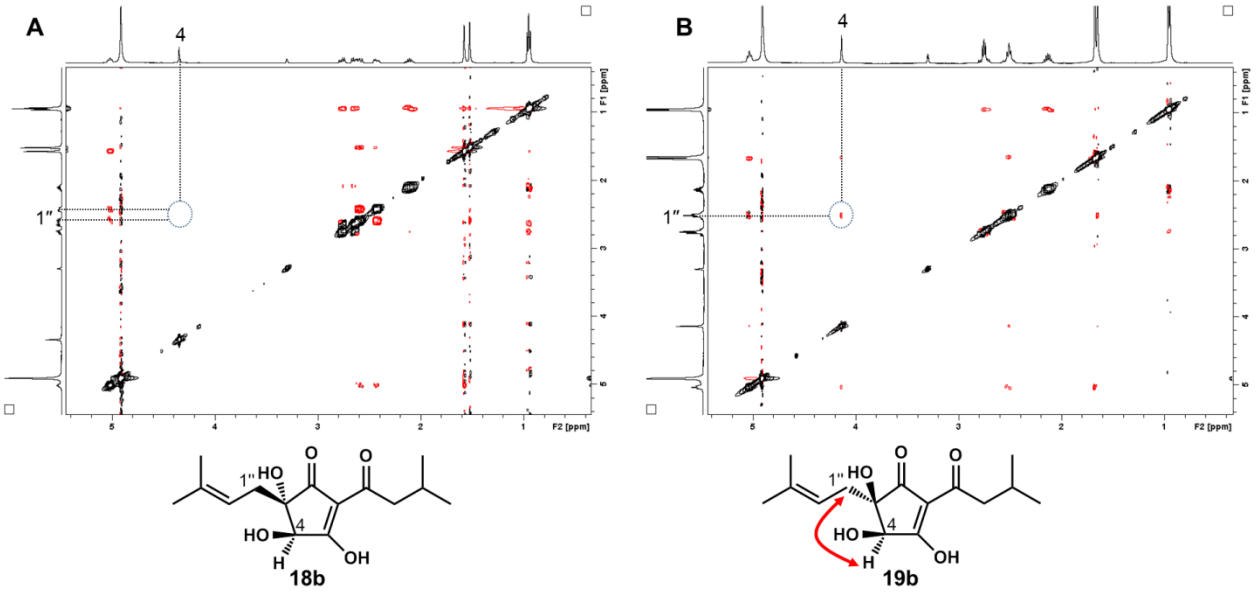

Figure 22. The NOESY spectra of compounds **18b** (A) and **19b** (B).

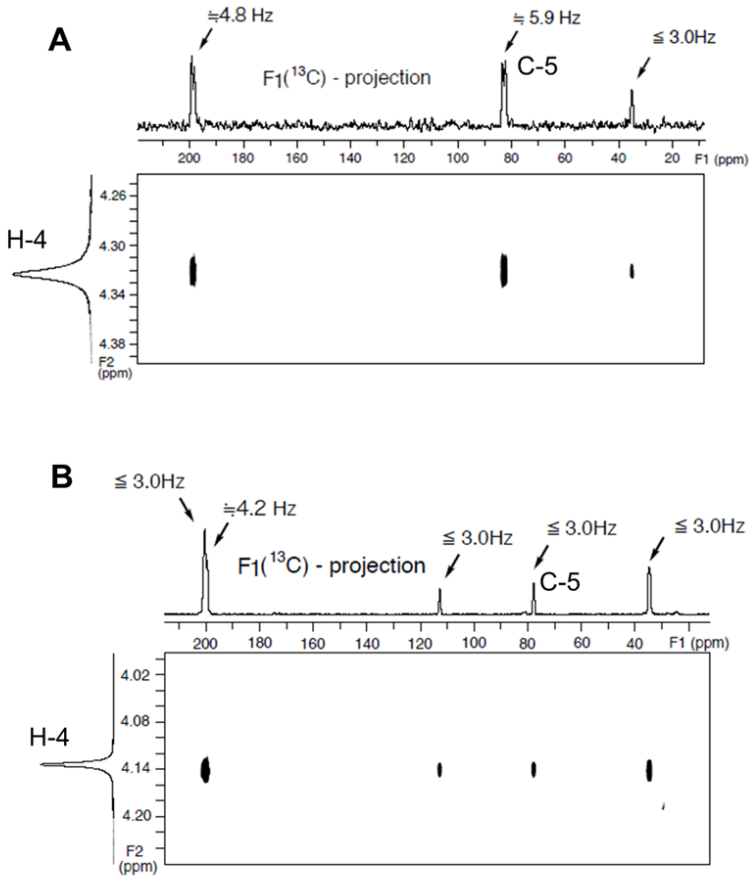

Figure 23. The *J*-resolved HMBC spectra of compounds **18b** (A) and **19b** (B).

Compound **17a** was obtained as a pale yellow oil. The HRESIMS data showed an $[M - H]^-$ ion at *m/z* 379.1753, and together with the ^{13}C NMR data, indicated a molecular formula of $C_{20}H_{28}O_7$, which was the same as for **11a**. Analysis of the ^1H, ^{13}C NMR, ^1H-^1H COSY, HMQC, and HMBC spectra established that **17a** possessed an isobutyryl side chain at C-2 instead of an isovaleryl side chain in **17b** (Table 5). Thus, **17a** was identified as 4′-hydroxyallo-*cis*-cohumulinone, which has not been previously reported (Figure 21).

Compound **18a** was obtained as a white, amorphous solid. The HRESIMS data showed an $[M - H]^-$ ion at *m/z* 267.1230, and together with the ^{13}C NMR data, indicated a molecular formula of $C_{14}H_{20}O_5$ (**17a** − $C_6H_8O_2$). Analysis of the ^1H, ^{13}C NMR, ^1H-^1H COSY, HMQC, and HMBC spectra established that **18a** also possessed an isobutyryl side chain at C-2 instead of an isovaleryl side chain in **18b** (Table 5). Thus, **18a** was identified as *cis*-oxycohumulinic acid, which has not been previously reported (Figure 21).

Compounds **17a**, **17b**, **18a** and **18b** were determined to be racemates because none of these compounds showed optical activity. Moreover **17a**, **17b**, **18a** and **18b** were formed *via* a simple thermal reaction in aqueous solution from the precursors **11a** and **11b**, which do exist as racemates.

Analyses of the transformation products of 4′-hydroxyalloadhumulinone (11c/c′).

Adhumulinone, a precursor of 4′-hydroxyalloadhumulinone, is a mixture of two diastereomers (**6c** and **6c′**) (Figure 24) as described in chapter 1. Thus, 4′-hydroxyalloadhumulinone in hard resin is also a mixture of two diastereomers (**11c** and **11c′**) (Figure 24). Although ODS HPLC analysis using an acidic buffer could not separate the diastereomers (**11c** and **11c′**) (Figure 20C1 and C2), the author successfully separated them through ODS HPLC analysis using a basic buffer (Figure 25). By employing a mobile phase containing the basic buffer, the author isolated each diastereomer successively, and named the former eluate in analytical HPLC (t_R 16.6 min)

as 4′-hydroxyalloadhumulinone A (**11c**) and the latter eluate (t_R 17.5 min) as 4′-hydroxyalloadhumulinone B (**11c′**) (Figure 25). The ^{1}H and ^{13}C NMR data of **11c** and **11c′** were almost identical (Table 6), and the author could not analyze the respective stereochemistries of **11c** and **11c′**.

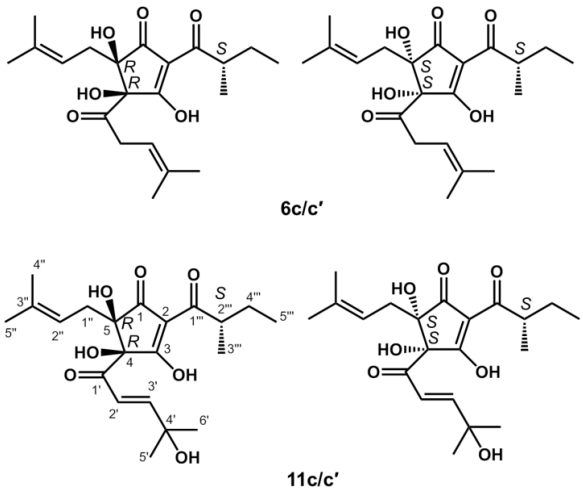

Figure 24. Chemical structures of adhumulinone diastereomers (**6c** and **6c′**) and 4′-hydroxyalloadhumulinones A and B (**11c** and **11c′**).

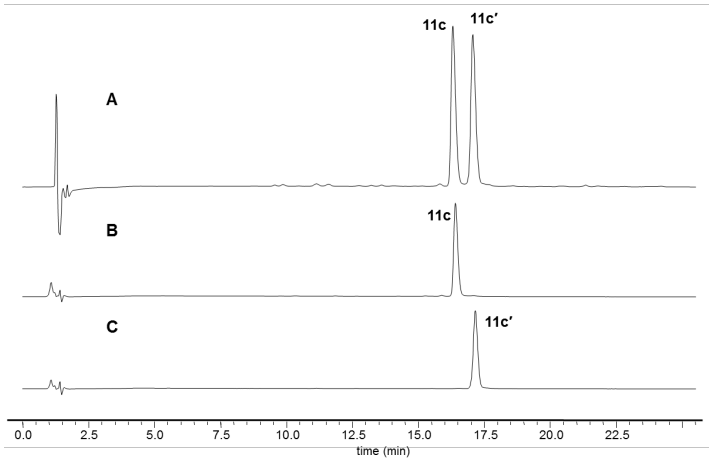

Figure 25. HPLC chromatograms of 4′-hydroxyalloadhumulinones A and B (**11c** and **11c′**, respectively) in the mobile phase using a basic aqueous buffer before (A) and after (B and C) their isolation.

Table 6. NMR spectroscopic data (400 MHz, methanol-d_4) for compounds **11c** and **11c′**[a]

	11c		**11c′**	
pos.	δ_C, type	δ_H, mult. (*J* in Hz)	δ_C, type	δ_H, mult. (*J* in Hz)
1	201.8, C	-	201.6, C	-
2	111.3, C	-	111.3, C	-
3	198.9, C	-	199.0, C	-
4	90.1, C	-	89.9, C	-
5	81.6, C	-	81.6, C	-
1'	200.0, C	-	200.0, C	-
2'	121.4, CH	7.03, d (15.7)	121.4, CH	7.04, d (15.7)
3'	155.8, CH	6.87, d (15.7)	155.8, CH	6.87, d (15.7)
4'	71.4, C	-	71.4, C	-
5'	29.3, CH_3	1.31, s	29.3, CH_3	1.31, s
6'	29.4, CH_3	1.31, s	29.4, CH_3	1.31, s
1"	31.0, CH_2	2.47, dd (14.8, 4.7) 2.42, dd (14.8, 8.9)	31.1, CH_2	2.47, dd (15.1, 5.5) 2.41, dd (15.1, 8.5)
2"	118.9, CH	5.30, m	118.9, CH	5.30, m
3"	135.5, C	-	135.5, C	-
4"	18.1, CH_3	1.41, s	18.1, CH_3	1.41, s
5"	26.1, CH_3	1.62, s	26.1, CH_3	1.62, s
1"'	204.1, C	-	204.2, C	-
2"'	42.6, CH	3.46, ddq (6.8, 6.8, 6.8)	42.7, CH	3.44, ddq (6.8, 6.8, 6.8)
3"'	16.0, CH_3	1.13, d (6.8)	15.9, CH_3	1.09, d (6.8)
4"'	27.3, CH_2	1.64-1.74, m 1.36-1.46, m	27.3, CH_2	1.70-1.80, m 1.40-1.50, m
5"'	11.9, CH_3	0.87, dd (7.4, 7.4)	12.0, CH_3	0.92, dd (7.4, 7.4)

[a] Arbitrary numbering according to structures **11c** and **11c′** shown in Figure 24.

The yield of isolated **11c** and **11c′** was too low to enable the separation of their transformation products in the boiling tests and perform structural determination by NMR analyses. Thus, the author tentatively identified **17c** (main transformed product of **11c**) as 4′-hydroxyallo-*cis*-adhumulinone A and **18c** (minor transformed product of **11c**) as *cis*-oxyadhumulinic acid A, by comparison with the transformation products from 4′-hydroxyallocohumulinone (**11a**) and 4′-hydroxyallohumulinone (**11b**) (Figure 20C3). Similarly, **17c′** and **18c′** (transformed products of **11c′**) were tentatively identified as

4′-hydroxyallo-*cis*-adhumulinone B and *cis*-oxyadhumulinic acid B, respectively (Figure 20C4).

The HPLC analysis of isolated **11c** demonstrated that it did not contain **11c′** (Figure 25B). Moreover, HPLC analysis of isolated **11c′** also showed that it did not contain **11c** (Figure 25C). However, the boiling test on **11c** afforded a small amount of **17c′** and **18c′** in the HPLC analysis (Figure 20C3). A small quantity of **17c** and **18c** was also obtained in the boiling test of **11c′** (Figure 20C4). These results suggested that the configuration at C-2‴ in **11c**, **11c′**, **17c**, **17c′**, **18c** and **18c′** may convert through proton exchange of H-2‴ during the boiling process. Figure 26 shows a plausible thermally induced epimerization of **17c** into the enantiomer of **17c′** and of **17c′** into the enantiomer of **17c**.

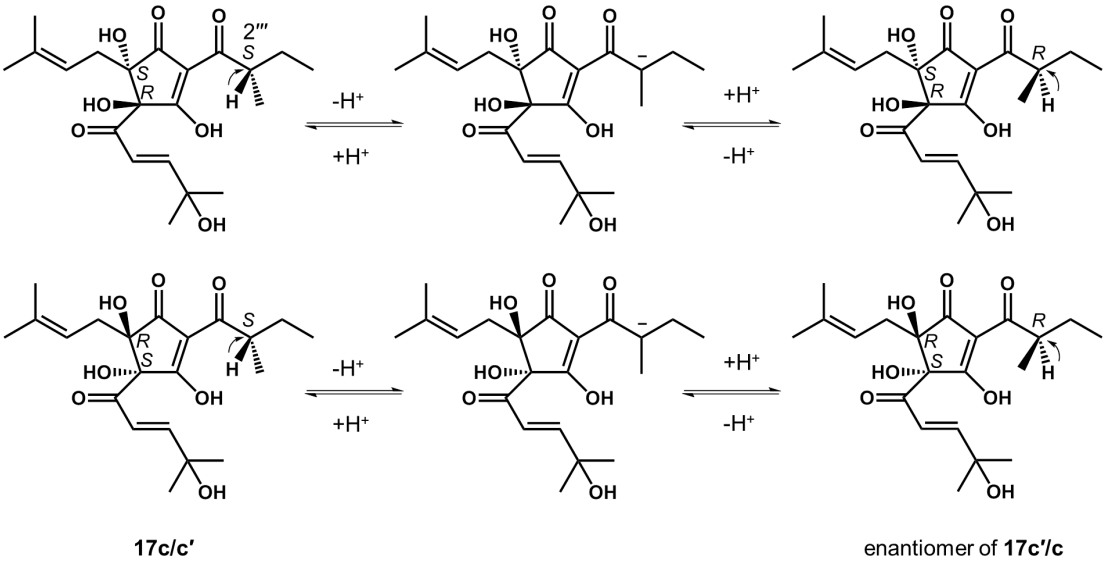

Figure 26. Proposed epimerization of 4′-hydroxyallo-*cis*-adhumulinones A and B (**17c** and **17c′**) through the proton exchange at C-2‴ as a result of boiling the sample.

Quantitative analyses of 4′-hydroxyallohumulinones and their transformation products during the boiling process.

The author aimed to quantitatively evaluate the changes in 4′-hydroxyallohumulinones and their transformation products during boiling. Thus, boiling solutions of **11a**, **11b**, and **11c**/**c′** were sampled at 30, 60, 90 and 120 min and

analyzed by HPLC. Figure 27 shows the time dependent decrease in 4′-hydroxyallohumulinones, and compositional changes in the transformation products. The degree of conversion of 4′-hydroxyallo-*cis*-humulinones (**17a**, **17b**, and **17c/c′**) increased until around 60 min and then slowly decreased thereafter. By contrast, the amount of *cis*-oxyhumulinic acids (**18a**, **18b**, and **18c/c′**) increased in inverse proportion to the decrease in the amount of 4′-hydroxyallo-*cis*-humulinones.

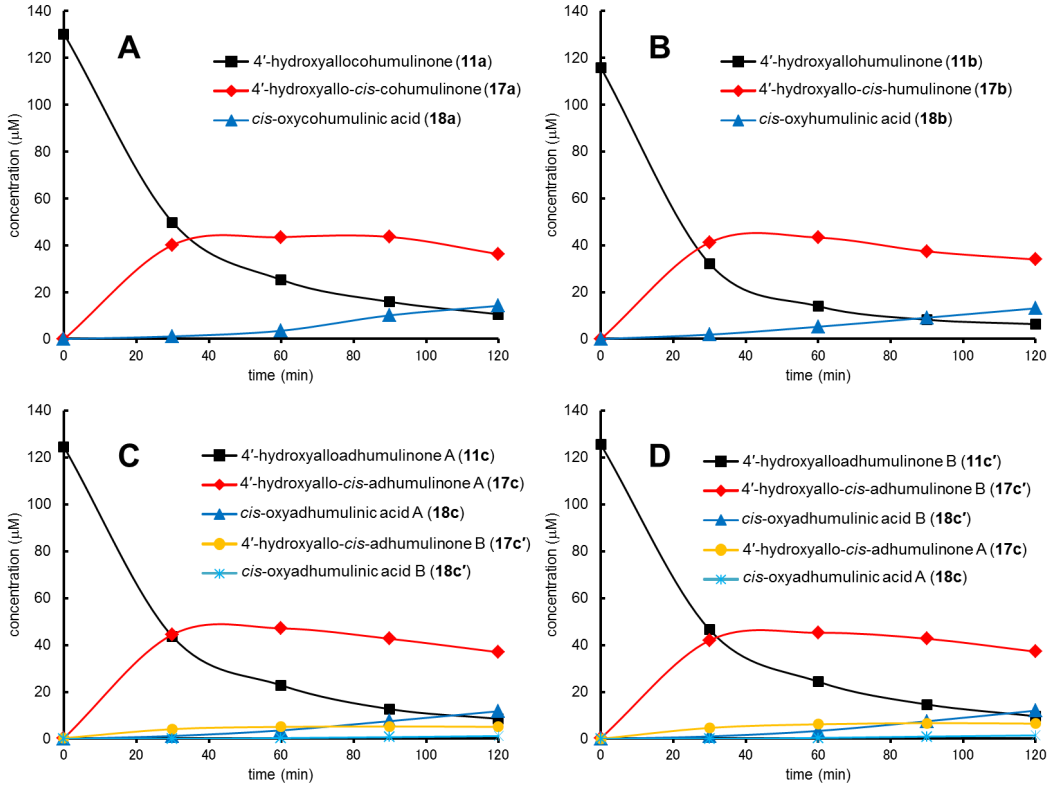

Figure 27. Concentration changes in 4′-hydroxyallocohumulinone (**11a**), 4′-hydroxyallo-*cis*-cohumulinone (**17a**), and *cis*-oxycohumulinic acid (**18a**) (A) and in 4′-hydroxyallohumulinone (**11b**), 4′-hydroxyallo-*cis*-humulinone (**17b**), and *cis*-oxyhumulinic acid (**18b**) (B) and in 4′-hydroxyalloadhumulinone A (**11c**), 4′-hydroxyallo-*cis*-adhumulinones A and B (**17c** and **c′**), and *cis*-oxyadhumulinic acids A and B (**18c** and **c′**) (C) and in 4′-hydroxyalloadhumulinone B (**11c′**), 4′-hydroxyallo-*cis*-adhumulinones A and B (**17c** and **c′**), and *cis*-oxyadhumulinic acids A and B (**18c** and **c′**) (D) during boiling in an aqueous buffer (pH 5.5).

These results suggested that during boiling, 4′-hydroxyallohumulinones (**11a–c**, **c′**) primarily isomerized into 4′-hydroxyallo-*cis*-humulinones (**17a–c**, **c′**), which then decomposed to *cis*-oxyhumulinic acids (**18a–c**, **c′**). The hydrolysis reaction from compound **17** to compound **18** was proposed as shown in Figure 28. The reaction starts via protonation of the carbonyl group of the hydroxyisohexenoyl side chain at C-4 in compound **17**, followed by addition of H_2O to the carbonyl carbon. Then, carbon-carbon bond cleavage would occur leading to the carbanion stabilized by resonance. Protonation of the carbanion would lead to compound **18**.

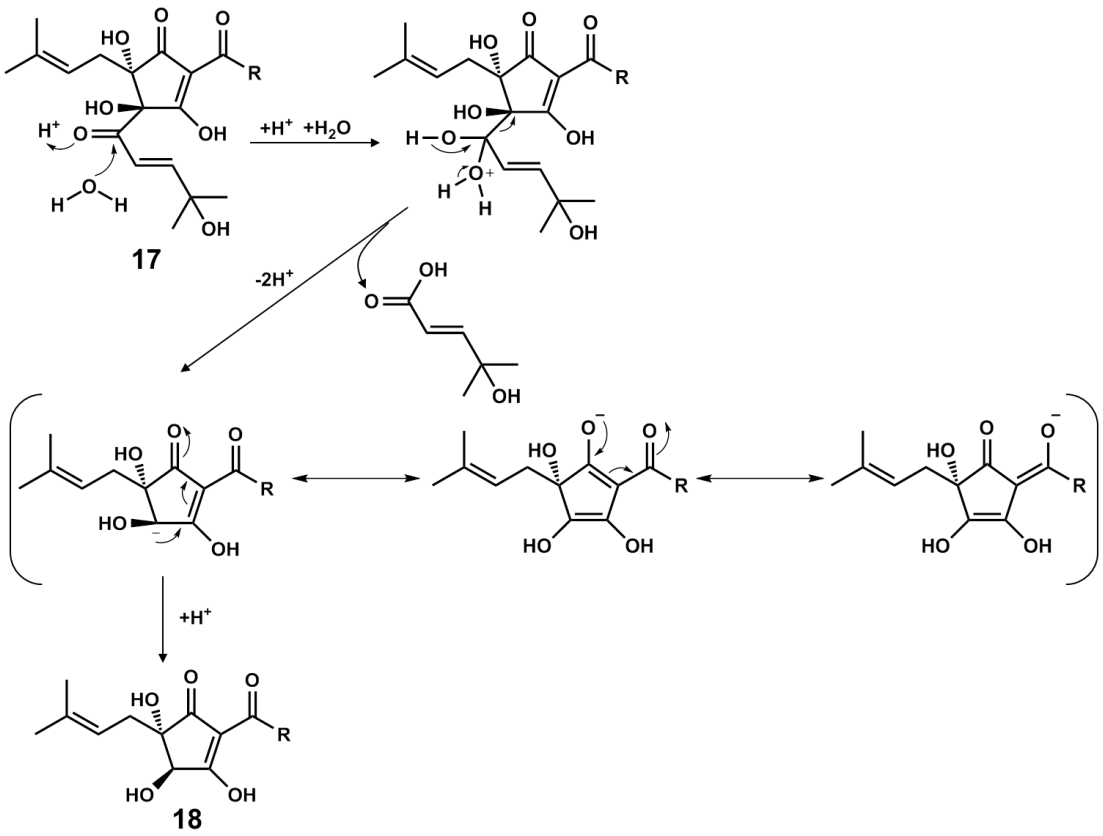

Figure 28. Proposed hydrolysis reaction from **17** to **18**.

The total amount of generated 4′-hydroxyallo-*cis*-humulinones and *cis*-oxyhumulinic acids accounted for 40 to 50% of the decomposed 4′-hydroxyallohumulinones. The author's analysis indicates that under these experimental

conditions about 10–15% of ad-congener substrates (**11c** and **11c′**) are epimerized through proton exchange at C-2‴ [calculated from the ratio of **17c** and **17c′** generated from **11c** (Figure 27C) and of **17c′** and **17c** generated from **11c′** (Figure 27D)]. This is the first study to report time-dependent changes of α-acid-derived oxidation products in the hard resin during boiling. The author believes these findings will be extremely valuable when evaluating effects of the hard resin generated through the oxidation of hops on beer properties.

Summary

α-Acids and β-acids in soft resin and their transformation during the wort boiling process are well-studied, however, other constituents in resins, especially hard resin, have been unidentified. In this study, the author identified humulinones and hulupones as soft resin components, in addition to 4′-hydroxyallohumulinones and tricyclooxyisohumulones A and B as hard resin components. These compounds are all oxidation products derived from α-acids or β-acids. The author also investigated compositional changes in the hard resin during the wort boiling process, which has a significant effect on the taste of the beer, by utilizing model boiling experiments. The major changes were identified to be isomerization of 4′-hydroxyallohumulinones into 4′-hydroxyallo-*cis*-humulinones followed by decomposition into *cis*-oxyhumulinic acids. These findings will be helpful in systematically evaluating and optimizing the effect of the hard resin on beer quality.

Chapter 4

Chemical characterization of beer aging products derived from hard resin components in hops

In chapter 3, the author identified the α-acid oxides, 4′-hydroxyallohumulinones (**11a–c**) [oxidation products of humulinones (**6a–c**)] and tricyclooxyisohumulones A (**12a–c**) and B (**13a–c**), as principal constituents of hard resin in stored hops. Furthermore, the transformation of 4′-hydroxyallohumulinones (**11a–c**) into 4′-hydroxyallo-*cis*-humulinones (**17a–c**) followed by degradation into *cis*-oxyhumulinic acids (**18a–c**) during wort boiling has been revealed. However, the compositional changes in these hard resin components that occur during beer aging are still unknown. Therefore, the objective of the present study was to characterize the transformation of hop oxidation-derived hard resin (i.e., stored hard resin) components during the beer aging process. Transformation products generated specifically under beer aging conditions were successfully isolated using model experiments of beer storage. Their structures were determined by means of high-resolution MS, and 1D and 2D NMR analyses, which enabled the author to propose the reaction mechanism that leads to these transformation products. Lastly, the time-dependent changes in the concentration of these products and their precursors were investigated under beer aging conditions.

Materials and methods

Chemicals and materials.

The following chemicals were obtained commercially: ethylenediaminetetraacetic acid (EDTA), H_3PO_4, MeCN, EtOH, *n*-hexane, diethyl ether, CH_2Cl_2 (Wako Pure Chemicals, Osaka, Japan); xanthohumol and isoxanthohumol (Funakoshi, Tokyo, Japan). Deionized water for chromatography was purified by means of a Milli-Q Gradient A10 system (Millipore, Billerica, MA, USA). Hop pellets, cultivar Hallertau Perle, were

purchased from Hopsteiner (Mainburg, Germany).

HPLC.

A Shimadzu Prominence UFLC system (Shimadzu, Kyoto, Japan) was used for all HPLC analysis. Data were processed with LCsolution software (Shimadzu, Kyoto, Japan). The column used was a 100 mm × 2.1 mm i.d., 3 μm, Alltima C_{18} (Systech, Tokyo, Japan). Analyses were performed under the following conditions: solvent: H_2O/H_3PO_4 (85%), 1000/0.2, (v/v) containing EDTA (0.02% w/v) (solvent A) and MeCN (solvent B), linear gradient from 10 to 52% B in 0 → 26.7 min, 52% B for 26.7 → 30 min, 52 to 75% B in 30 → 32.7 min, 75 to 85% B in 32.7 → 36.7 min, and 85% B for 36.7 → 37.7 min; flow rate: 0.6 mL/min; detector: 270 nm; column temperature: 40 ˚C. The sample injection volume was 3.0 μL. Transformation products were quantitated by using isolated reference compounds.

HRMS.

The purified compounds were analyzed by HRESIMS using a Thermo Scientific LTQ Orbitrap mass spectrometer (Thermo Fisher Scientific, San Joes, CA, USA). Before measuring the samples, accurate mass calibration was carried out by using polytyrosine-1,3,6 as a mass standard (CS Bio Company, Menlo Park, CA, USA).

NMR.

^{1}H, ^{13}C, and 2D NMR spectra were measured with a Bruker AVANCE400 spectrometer (Bruker BioSpin, Rheinstetten, Germany). Samples were dissolved in methanol-d_4 or pyridine-d_5. Chemical shifts were referenced to the solvent signals (methanol-d_4: δ_H/δ_C 3.30/49.0, pyridine-d_5: δ_H/δ_C 8.70/149.9). Data processing was performed with TopSpin-NMR software (version 3.0) (Bruker BioSpin). Molecular models were generated by ChemBio3D Ultra 13.0 software (Cambridge Soft, Cambridge,

MA, USA) using MM2 force field calculations.

Standard compounds.

4′-Hydroxyallocohumulinone (**11a**), 4′-hydroxyallohumulinone (**11b**), 4′-hydroxyallo-*cis*-cohumulinone (**17a**), 4′-hydroxyallo-*cis*-humulinone (**17b**), *cis*-oxycohumulinic acid (**18a**), and *cis*-oxyhumulinic acid (**18b**) were prepared as described in chapter 3. Tricyclooxyisohumulones A (**12b**) and B (**13b**) were isolated from the autoxidation products of humulone as described in chapter 2.

Preparation of hard resin.

Hard resin was prepared by a method described in chapter 3 from hop pellets stored for 3 years at 4 °C in contact with air in the dark. In brief, hop pellets (10 g) were extracted with MeOH (100 mL), and the extract was filtered and kept at 4 °C for 1 d. The waxy precipitate generated was removed by filtration. A portion of the filtrate (20 mL) was mixed with MeOH (10 mL) and 1 M HCl (20 mL), and then partitioned with *n*-hexane (80 mL × 5 times) to extract and remove the soft resin. The residual aqueous phase was partitioned with diethyl ether (80 mL × 2 times). Lastly, the diethyl ether layer was collected, washed with sat. NaCl solution, dried over anhydrous Na_2SO_4, and concentrated to dryness to yield the hard resin as a brown solid (112 mg).

Transformation of hard resin components in a model solution.

The hard resin was dissolved in EtOH (4.0 mg/mL) and an aliquot (50 μL) was added to 1 mL of 10 mM citrate buffer (pH 4.0). The combined solution was stored at 40 °C in the dark and analyzed by HPLC over time. To verify which components in the hard resin were transformed during storage, each of the reference compounds **11a**, **11b**, **12b**, **13b**, **17b**, and **18b** was prepared at a concentration of 50 μg/mL in citrate buffer solution, and then stored and analyzed in the same way.

Isolation of the transformation products.

4′-Hydroxyallocohumulinone (**11a**) (400 mg) was dissolved in EtOH (100 mL) and added to 10 mM citrate buffer (pH 4.0, 2 L). The resulting solution was kept at 40 °C for 2 w, and then 1 M HCl (200 mL) was added and the solution was partitioned with CH_2Cl_2 (500 mL × 3 times). The CH_2Cl_2 layer was washed with sat. NaCl solution, dried over anhydrous Na_2SO_4, and concentrated to dryness to give a yellowish brown oil (291 mg). The oil was dissolved in EtOH and repeatedly subjected to preparative HPLC. The column used was a 150 mm × 10 mm i.d., 5 μm, Alltima C_{18} (Systech, Tokyo, Japan). The LC conditions were as follows: solvent: H_2O/H_3PO_4 (85%), 100/1, (v/v) (solvent A) and MeCN (solvent B), linear gradient consisting of 30% B for 0 → 15 min, 30 to 90% B in 15 → 18 min, and 90% B for 18 → 22 min; flow rate: 4.7 mL/min; detector: 270 nm; column temperature: 40 °C. Nine fractions were recovered based on elution time. Compounds **22a** and **20a** were contained in fractions 1 (t_R 5.5–6.0 min) and 3 (t_R 7.6–8.4 min), respectively. Each eluate was diluted five times with H_2O, adjusted to pH 2.0 with 1 M HCl, and partitioned with CH_2Cl_2 (1/5 volume of the diluted eluate × 2 times). The respective CH_2Cl_2 layer was washed with sat. NaCl solution, dried over anhydrous Na_2SO_4, and concentrated to dryness to yield pure **22a** (3.2 mg) and **20a** (42.0 mg). Compounds **21a** and **23a** were contained in fraction 2 (t_R 6.5–7.4 min) and further purified by repeatedly subjecting them to a second preparative HPLC step. The column used was a 150 mm × 20 mm i.d., 5 μm, L-column 2 ODS (Chemicals Evaluation and Research Institute, Tokyo, Japan). The LC condtions were as follows: solvent: 100 mM NH_4HCO_3 (solvent A) and MeCN (solvent B), isocratic elution at 20% B; flow rate: 9.5 mL/min; detector: 270 nm; column temperature: 40 ˚C. In this preparative HPLC, compounds **21a** and **23a** eluted at 6.4–7.5 min and at 8.6–9.5 min, respectively. Each eluate was immediately diluted twice with H_2O, adjusted to pH 2.0 with 1 M HCl, and partitioned with CH_2Cl_2 (1/5 volume of the diluted eluate × 2 times). Each respective CH_2Cl_2 layer was washed with sat. NaCl solution, dried over anhydrous Na_2SO_4, and

concentrated to dryness to yield pure **21a** (27.5 mg) and **23a** (13.9 mg).

The transformation products (**20b**, **21b**, **22b**, and **23b**) of 4′-hydroxyallohumulinone (**11b**) were prepared and purified in a similar way to **20a**, **21a**, **22a**, and **23a**. In brief, 4′-hydroxyallohumulinone (**11b**, 400 mg) was incubated in 10 mM citrate buffer (pH 4.0, 2 L) for 2 w and partitioned with CH_2Cl_2 after the addition of 1 M HCl (200 mL). The CH_2Cl_2 layer was concentrated to give an oil (367 mg), which was repeatedly subjected to preparative HPLC [column, flow rate, detector, and column temperature identical to those used for the isolation of **20a** and **22a**; solvent: H_2O/H_3PO_4 (85%), 100/1, (v/v) (solvent A) and MeCN (solvent B), linear gradient from 30 to 62% B in 0 → 12 min, 62 to 90% B in 12 → 15 min, and 90% B for 15 → 19 min], and divided into 12 fractions. Compounds **22b** and **20b** were contained in fractions 2 (t_R 6.9 – 7.3 min) and 4 (t_R 9.0 – 9.5 min), respectively. Pure **22b** (3.1 mg) and **20b** (69.4 mg) were recovered from each eluate in the same way as described for **22a** and **20a**. Compounds **21b** and **23b** were contained in fraction 3 (t_R 8.1–8.6 min) and further purified by repeatedly subjecting them to a second preparative HPLC step. The column used was a 50 mm × 20 mm i.d., 5 μm, L-column 2 ODS (Chemicals Evaluation and Research Institute, Tokyo, Japan). The LC conditions were as follows: solvent: 100 mM NH_4HCO_3 (solvent A) and MeCN (solvent B), isocratic elution at 20% B; flow rate: 9.5 mL/min; detector: 270 nm; column temperature: 40 ˚C. In this preparative HPLC, compounds **21b** and **23b** eluted at 3.0–4.0 min and at 4.3–5.3 min, respectively. Pure **21b** (38.5 mg) and **23b** (14.6 mg) were recovered from each eluate in the same way as described for **21a** and **23a**.

Scorpiocohumulinol A (**20a**): Pale yellow oil; $[\alpha]^{20}_D$ ±0 (*c* 0.9, MeOH); HRESIMS (negative) *m/z* 379.1754 $[M - H]^-$ (calcd for $C_{20}H_{27}O_7$, 379.1762); ^1H and ^{13}C NMR data, see Table 7.

Scorpiocohumulinol B (**21a**): Pale yellow oil; $[\alpha]^{20}_D$ ±0 (*c* 0.3, MeOH); HRESIMS (negative) *m/z* 379.1752 $[M - H]^-$ (calcd for $C_{20}H_{27}O_7$, 379.1762); ^1H and ^{13}C NMR data, see Table 7.

Scorpiohumulinol A (**20b**): Yellowish brown, amorphous solid; $[\alpha]^{20}_{D}$ ±0 (*c* 0.7, MeOH); HRESIMS (negative) *m/z* 393.1911 $[M - H]^-$ (calcd for $C_{21}H_{29}O_7$, 393.1919); ^1H and ^{13}C NMR data, see Table 7.

Scorpiohumulinol B (**21b**): Pale yellow oil; $[\alpha]^{20}_{D}$ ±0 (*c* 0.4, MeOH); HRESIMS (negative) *m/z* 393.1913 $[M - H]^-$ (calcd for $C_{21}H_{29}O_7$, 393.1919); ^1H and ^{13}C NMR data, see Table 7.

Dicyclocohumulinol A (**22a**): Pale yellow oil; $[\alpha]^{20}_{D}$ ±0 (*c* 0.2, MeOH); HRESIMS (negative) *m/z* 379.1752 $[M - H]^-$ (calcd for $C_{20}H_{27}O_7$, 379.1762); ^1H and ^{13}C NMR data, see Table 8.

Dicyclocohumulinol B (**23a**): Pale yellow oil; $[\alpha]^{20}_{D}$ ±0 (*c* 0.3, MeOH); HRESIMS (negative) *m/z* 379.1752 $[M - H]^-$ (calcd for $C_{20}H_{27}O_7$, 379.1762); ^1H and ^{13}C NMR data, see Table 8.

Dicyclohumulinol A (**22b**): Pale yellow oil; $[\alpha]^{20}_{D}$ ±0 (*c* 0.2, MeOH); HRESIMS (negative) *m/z* 393.1912 $[M - H]^-$ (calcd for $C_{21}H_{29}O_7$, 393.1919); ^1H and ^{13}C NMR data, see Table 8.

Dicyclohumulinol B (**23b**): Pale yellow oil; $[\alpha]^{20}_{D}$ ±0 (*c* 0.3, MeOH); HRESIMS (negative) *m/z* 393.1913 $[M - H]^-$ (calcd for $C_{21}H_{29}O_7$, 393.1919); ^1H and ^{13}C NMR data, see Table 8.

Results and discussion

Transformation of isolated components during aging in a model solution.

The hard resin prepared from hops stored at 4 ˚C for 3 years was shown to contain a series of α-acid oxides, 4′-hydroxyallohumulinones (**11a–c**) and tricyclooxyisohumulones A (**12a**, **b**) and B (**13a**, **b**) together with xanthohumol (Figure 29A). The constituent profile was similar to that of the hard resin prepared from hops stored at higher temperature to accelerate the oxidation in a study described in chapter 3.

To investigate the compositional changes in the hard resin during beer aging, a model experiment was conducted using an acidic buffer (pH 4.0) to simplify the reaction medium. HPLC analysis of the hard resin after 1 w of storage at 40 ˚C in buffer clearly showed a decrease in 4′-hydroxyallohumulinones (**11a–c**), the appearance of new compounds, and transformation of xanthohumol into isoxanthohumol (Figure 29B). As described in chapter 3, 4′-hydroxyallohumulinones (**11a–c**) were found to transform into 4′-hydroxyallo-*cis*-humulinones (**17a–c**) and *cis*-oxyhumulinic acids (**18a–c**) during the wort boiling process. However, the main compounds generated in the present study did not seem to correspond to **17a–c** or **18a–c**. To verify this assumption, isolated **11a** and **11b** were stored at 40 ˚C in the same buffer and analyzed after 1 w. The HPLC analyses clearly showed that **11a** was transformed mainly into **20a**, **21a**, **22a**, and **23a** (Figure 30A), whereas **11b** was transformed mainly into **20b**, **21b**, **22b**, and **23b** (Figure 30B). Among the reaction products, only trace amounts of **17a** and **17b** were detected, and **18a** and **18b** were not detected. Thus, the degradation of 4′-hydroxyallohumulinones (**11a–c**) during beer aging is different from that during the wort boiling process.

The author also incubated tricyclooxyisohumulones A (**12b**) and B (**13b**), another series of α-acid oxides contained in hop hard resin; however, these compounds were stable and did not decrease in content even after 1 w of storage at 40 ˚C in acidic buffer (Figure 30C and D). Furthermore, 4′-hydroxyallo-*cis*-humulinone (**17b**) and *cis*-oxyhumulinic acid (**18b**), the transformation products of 4′-hydroxyallohumulinone

(**11b**) that form during wort boiling, were evaluated for their stability in acidic buffer. When isolated **17b** was incubated in acidic buffer, some transformation to **18b** was observed; however, **17b** was relatively stable in comparison to **11b** under the experimental conditions (Figure 30E). Similarly, isolated **18b** was incubated, and the result showed very high stability of **18b** under the experimental conditions (Figure 30F).

Taken together, these findings indicate that the transformation of 4′-hydroxyallohumulinones (**11a–c**) accounts mainly for the compositional changes of α-acid oxide derived from stored hard resin during beer aging.

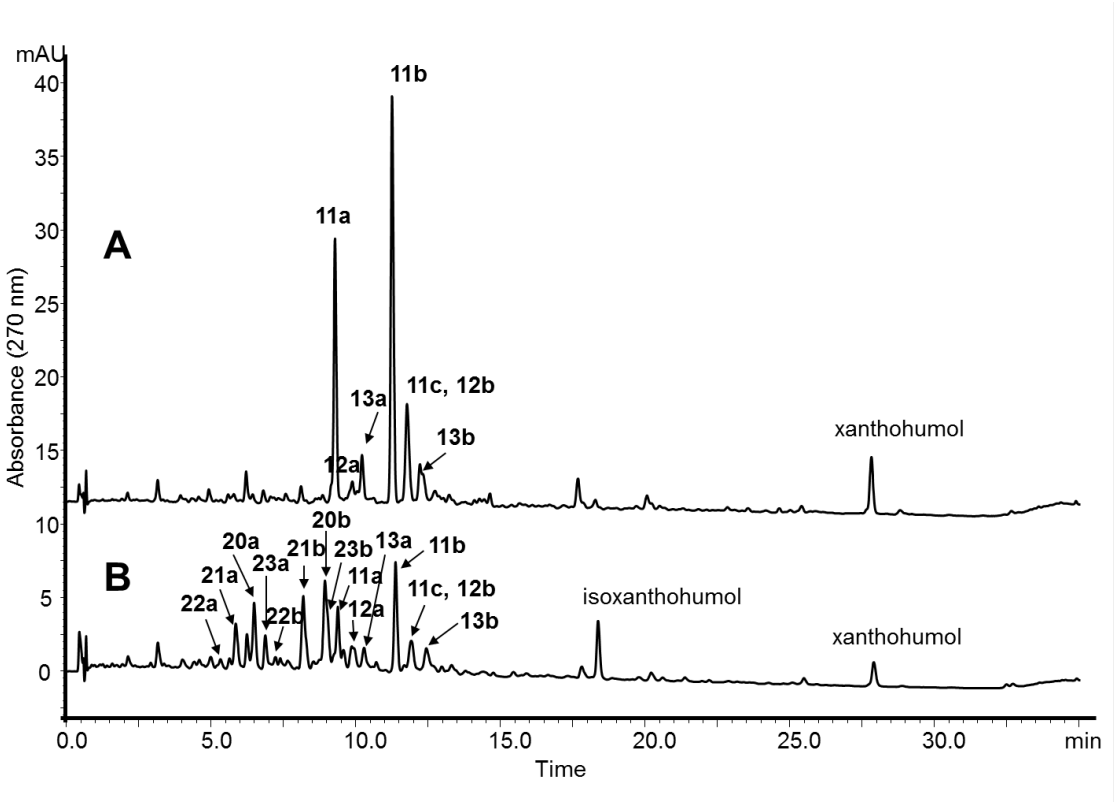

Figure 29. HPLC chromatograms of the hard resin prepared from stored hops (A) before and (B) after incubation in an acidic buffer (pH 4.0) at 40 ˚C for 1 w. The structures of the compounds are given in Figures 17 and 33.

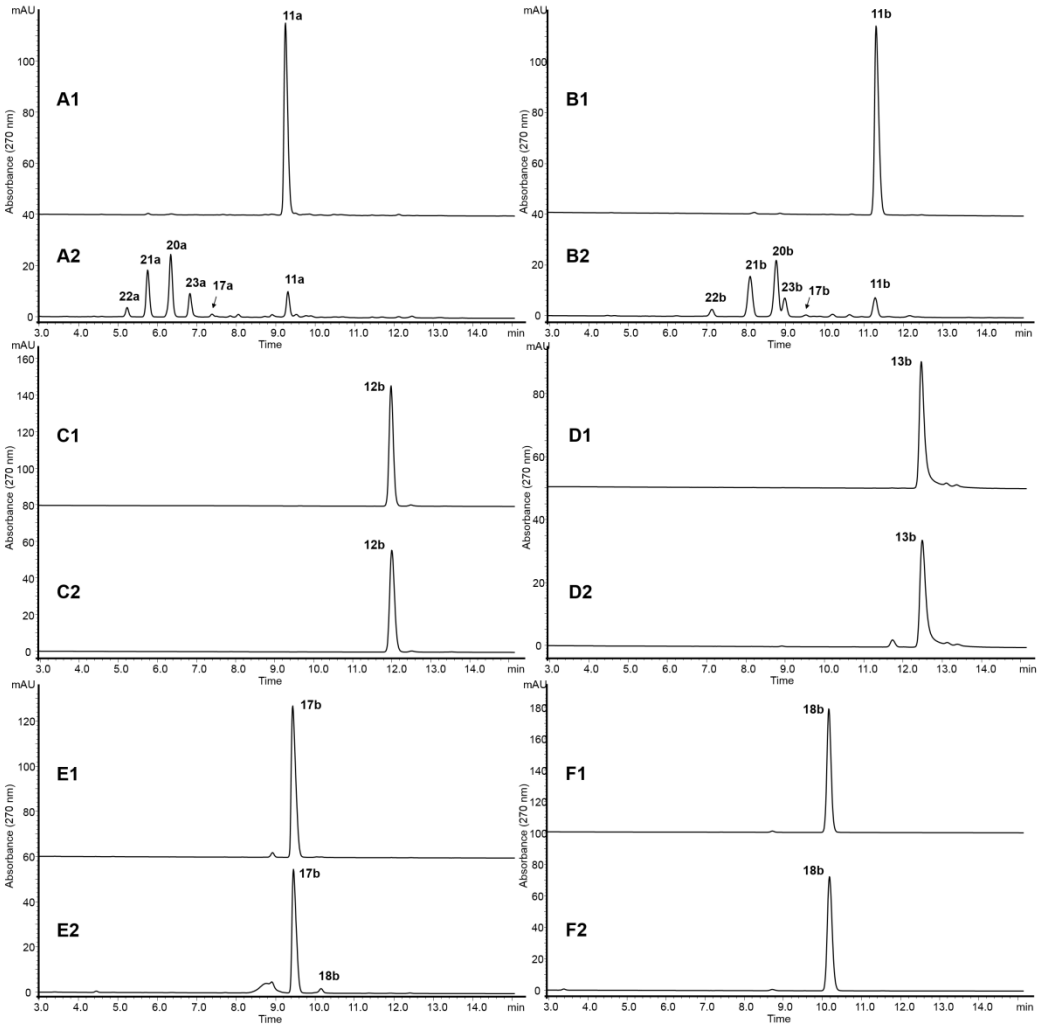

Figure 30. HPLC chromatograms of the reference compounds before and after incubation in an acidic buffer (pH 4.0) at 40 ˚C for 1 w. 4′-Hydroxyallocohumulinone (**11a**): (A1) before and (A2) after incubation. 4′-Hydroxyallohumulinone (**11b**): (B1) before and (B2) after incubation. Tricyclooxyisohumulone A (**12b**): (C1) before and (C2) after incubation. Tricyclooxyisohumulone B (**13b**): (D1) before; and (D2) after incubation. 4′-Hydroxyallo-*cis*-humulinone (**17b**): (E1) before and (E2) after incubation. *cis*-Oxyhumulinic acid (**18b**): (F1) before and (F2) after incubation. The structures of the compounds are given in Figures 17, 21, and 33.

Structural elucidation of the transformation products.

The difference in stability between 4′-hydroxyallohumulinone (**11b**) and 4′-hydroxyallo-*cis*-humulinone (**17b**) in an acidic medium was in agreement with that between *trans*-iso-α-acids and *cis*-iso-α-acids. Among iso-α-acids, only the *trans* isomers are known to form polycyclic compounds via a proton-catalyzed reaction in an acidic medium.[30, 31] As a result, the author considered that 4′-hydroxyallohumulinones (**11a–c**) might be transformed into polycyclic compounds similar to *trans*-iso-α-acids.

To elucidate the structures of the transformation products of 4′-hydroxyallohumulinones, 400 mg samples of isolated **11a** and **11b** were incubated in acidic buffer (pH 4.0) at 40 ˚C for 2 w. The transformation products were purified by using two-phase solvent partition and preparative reverse-phase HPLC, affording **20a** (42.0 mg), **21a** (27.5 mg), **22a** (3.2 mg), and **23a** (13.9 mg) from **11a**, and **20b** (69.4 mg), **21b** (38.5 mg), **22b** (3.1 mg), and **23b** (14.6 mg) from **11b**.

Compound **20a** was obtained as a pale yellow oil. The HRESIMS spectrum and ^{13}C NMR data indicated a molecular formula of $C_{20}H_{28}O_7$, which is identical to that of **11a**. Analysis of the ^{1}H and ^{13}C NMR and HMQC spectra of **20a** in methanol-d_4 strongly suggested that the 2-isobutyryl-3,4,5-trihydroxycyclopent-2-enone structure [C-1 − C-5 (ring A) and C-1‴ − C-4‴] present in the precursor compound **11a** was preserved in **20a** (Table 7, Figure 31). The molecular formula of **20a** required seven indices of hydrogen deficiency (IHD). Four of the seven IHD were accounted by the 2-isobutyryl-3,4,5-trihydroxycyclopent-2-enone structure, and one of the seven IHD was due to a C=C double bond [C-3′ (δ 120.6) and C-4′ (δ 139.6)]. Because **20a** does not possess any other double bonds to account for the last two IHD, it was thought to be a tricyclic compound.

The HMBC correlations of H_3-4″ (δ_H 1.18) and H_3-5″ (δ_H 1.39) to C-3″ (δ_C 82.5) and C-2″ (δ_C 61.9) and the ^{1}H-^{1}H COSY correlation between H-2″ (δ_H 2.80) and H_2-1″ (δ_H 2.08, 2.02) established the connectivity of C-1″ – C-2″ – C-3″ – $2CH_3$ (C-4″and

C-5″), while the HMBC correlations of H-5′ (δ_H 1.48) and H-6′ (δ_H 1.72) to C-4′ and C-3′ and the ^{1}H-^{1}H COSY correlation between H-2′ (δ_H 4.34) and H-3′ (δ_H 5.49) established the connectivity of C-2′ – C-3′ – C-4′– $2CH_3$ (C-5′ and C-6′). A C-2′ – C-1′ – C-4 linkage was indicated from the HMBC correlations of H-3′ to an oxygenated carbon C-1′ (δ_C 91.0) and H-2′ to C-4 (δ_C 83.7), and a C-1′– C-2″– C-1″– C-5 – C-4 linkage was indicated from the HMBC correlation of H-1″ to C-1′, C-4 and C-5 (δ_C 84.2), which confirmed the presence of a cyclopentane ring composed of C-4 – C-5 – C-1″– C-2″ – C-1′ (ring B) (Figure 31). The linkage of C-2′ – C-1′ – C-2″ – C-3″ was also proved by the HMBC correlations described above. The ^{13}C NMR chemical shifts of C-2′ (δ_C 78.8) and C-3″ (δ_C 82.5) (oxygenated carbons) and the non-equivalent ^{13}C NMR chemical shifts of C-4″ (δ_C 25.7) and C-5″ (δ_C 29.9) (dimethyl at C-3″), together with the tricyclic nature of **20a**, confirmed the presence of a furan ring comprising C-2′ – C-1′ – C-2″ – C-3″ (ring C). From these findings, the planar structure of **20a** was established (Figure 31).

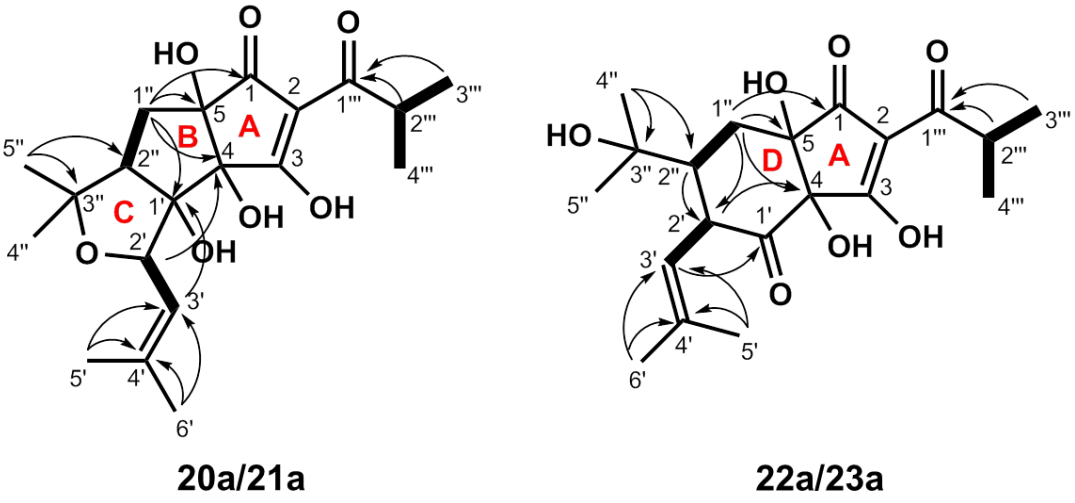

Figure 31. ^{1}H-^{1}H COSY (bold) and selected HMBC (arrow) correlations for compounds **20a/21a** and **22a/23a**.

Table 7. NMR spectroscopic data (400 MHz, methanol-d_4 and pyridine-d_5) for compounds **20a**, **20b**, **21a**, and **21b**[a]

	20a in methanol-d_4		**20b** in methanol-d_4		**21a** in methanol-d_4		**21a** in pyridine-d_5		**21b** in methanol-d_4	
pos.	δ_C, type	δ_H, mult. (*J* in Hz)	δ_C, type	δ_H, mult. (*J* in Hz)	δ_C, type	δ_H, mult. (*J* in Hz)	δ_C, type	δ_H, mult. (*J* in Hz)	δ_C, type	δ_H, mult. (*J* in Hz)
1	200.3, C	-	200.5, C	-	199.2, C	-	202.4, C	-	199.2, C	-
2	111.5, C	-	112.5, C	-	113.3, C	-	111.5, C	-	114.3, C	-
3	197.8, C	-	197.9, C	-	200.6, C	-	202.6, C	-	200.7, C	-
4	83.7, C	-	83.9, C	-	86.3, C	-	83.0, C	-	86.6, CH	-
5	84.2, C	-	84.3, C	-	82.4, C	-	81.0, C	-	82.6, C	-
1'	91.0, C	-	91.1, C	-	93.9, C	-	93.9, C	-	93.9, C	-
2'	78.8, CH	4.34, d (9.1)	78.8, CH	4.33, d (9.1)	79.8, CH	5.05, d (9.1)	79.9, CH	5.70, d (8.7)	79.8, CH	5.05, d (9.1)
3'	120.6, CH	5.49, d (9.1)	120.6, CH	5.49, d (9.1)	121.4, CH	5.40, d (9.1)	124.9, CH	6.13, d (8.7)	121.4, CH	5.40, d (9.1)
4'	139.6, C	-	139.6, C	-	139.2, C	-	134.1, C	-	139.3, C	-
5'	18.5, CH_3	1.48, s	18.5, CH_3	1.50, s	18.8, CH_3	1.76, s	18.8, CH_3	1.85, s	18.8, CH_3	1.76, s
6'	26.2, CH_3	1.72, s	26.27, CH_3	1.73, s	26.6, CH_3	1.79, s	26.3, CH_3	1.60, s	26.6, CH_3	1.79, s
1"	35.4, CH_2	a: 2.08, dd (15.0, 11.5) b: 2.02, dd (15.0, 9.1)	35.4, CH_2	a: 2.07, dd (14.8, 11.2) b: 2.01, dd (14.8, 9.1)	35.0, CH_2	a: 2.38, m b: 1.93, m	37.8, CH_2	a: 2.93, dd (13.1, 7.7) b: 2.53, dd (13.1, 11.7)	34.9, CH_2	a: 2.38, m b: 1.93, m
2"	61.9, CH	2.80, dd (11.5, 9.1)	61.9, CH	2.79, dd (11.2, 9.1)	55.4, CH	1.93, m	55.2, CH	2.39, dd (11.7, 7.7)	55.4, CH	1.93, m
3"	82.5, C	-	82.5, C	-	82.7, C	-	81.8, C	-	82.7, C	-
4"	25.7, CH_3	1.18, s	25.7, CH_3	1.17, s	25.5, CH_3	1.21, s	26.0, CH_3	1.32, s	25.5, CH_3	1.21, s
5"	29.9, CH_3	1.39, s	29.9, CH_3	1.39, s	30.1, CH_3	1.34, s	30.0, CH_3	1.69, s	30.1, CH_3	1.34, s
1"'	207.3, C	-	202.4, C	-	207.1, C	-	202.6, C	-	202.6, C	-
2"'	37.8, CH	3.51, sep (6.8)	48.9, CH_2	a: 2.77, dd (15.0, 7.0) b: 2.69, dd (15.0, 6.9)	37.9, CH	3.58, sep (6.8)	36.7, CH	4.36, sep (6.9)	49.1, CH_2	a: 2.81, dd (15.0, 7.1) b: 2.77, dd (15.0, 6.8)
3"'	17.9, CH_3	1.10, d (6.8)	26.34, CH	2.13, m	18.2, CH_3	1.11, d (6.8)	19.0, CH_3	1.21, d (6.9)	26.3, CH	2.17, m
4"'	18.5, CH_3	1.11, d (6.8)	22.9, CH_3	0.95, d (6.6)	18.3, CH_3	1.13, d (6.8)	19.2, CH_3	1.24, d (6.9)	22.9, CH_3	0.97, d (6.6)
5"'	-	-	22.9, CH_3	0.96, d (6.6)	-	-	-	-	22.9, CH_3	0.97, d (6.6)

[a] Arbitrary numbering according to structures **20a**, **20b**, **21a**, and **21b** shown in Figures 31 and 33.

Compound **21a** was obtained as a pale yellow oil. The HRESIMS spectrum and ^{13}C NMR data together indicated a molecular formula of $C_{20}H_{28}O_7$, which is the same as that of **20a**. Analysis of the ^{1}H and ^{13}C NMR, ^{1}H-^{1}H COSY, HMQC, and HMBC spectra of **21a** in methanol-d_4 and pyridine-d_5 (Table 7) revealed that **21a** possessed the same planar structure as **20a**, and thus **21a** was a stereoisomer of **20a** (Figure 31).

The author investigated the relative configurations of **20a** and **21a**. Because the β-orientations of the hydroxy groups at C-4 and C-5 in both **20a** and **21a** should be preserved from the precursor compound **11a**, the author studied the other three relative configurations (C-1′, 2′, and 2″) in **20a** and **21a** by using NOESY experiments and Chem3D modeling. For both **20a** and **21a**, NOE correlations of H-2′/H_3-4″, H-3′/H_3-5″, and H-2″/H_3-5″ were observed, indicating that H-2′ and H-2″ of the two compounds are located on the opposite side of ring C (Figure 32). Moreover, the strong NOE correlations of H-2′/H-1″a (α-orientation) in **20a** and H-2′/H-1″b (β-orientation) in **21a** suggested that rings B and C in both compounds are *cis*-fused (Figure 32). These findings suggested that the relative configurations of the two compounds were (4β,5β,1′β,2′β,2″β) and (4β,5β,1′α,2′α,2″α).

The ^{1}H chemical shift of H_3-5′ in **20a** was shielded by 0.28 ppm in comparison to **21a**, indicating that the isobutyryl side chain at C-2 in **20a** exists close to the 2-methyl-1-propenyl group at C-2′. This was confirmed by observation of an NOE correlation of H_3-5′/H_3-3‴ only for **20a**, thereby establishing the β-orientation of 1′-OH in **20a**. Thus, the relative configurations of **20a** and **21a** were verified as (4β,5β,1′β,2′β,2″β) and (4β,5β,1′α,2′α,2″α), respectively (Figure 32). Although a structurally similar compound, scorpiohumol, was identified among the degradation products of *trans*-isohumulone,[14] neither compound has been reported previously; therefore, the author named them scorpiocohumulinol A and scorpiocohumulinol B, respectively (Figure 33)

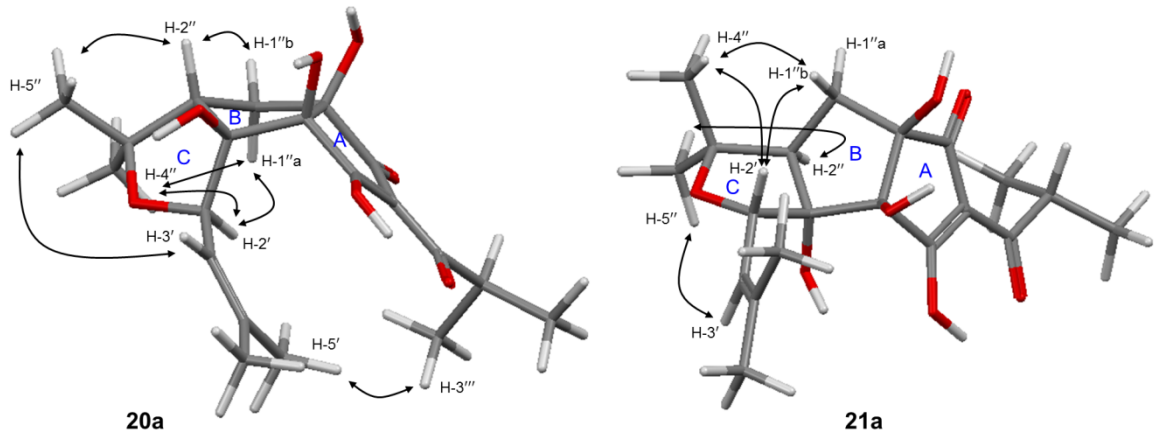

Figure 32. Key NOESY correlations for compounds **20a** and **21a**.

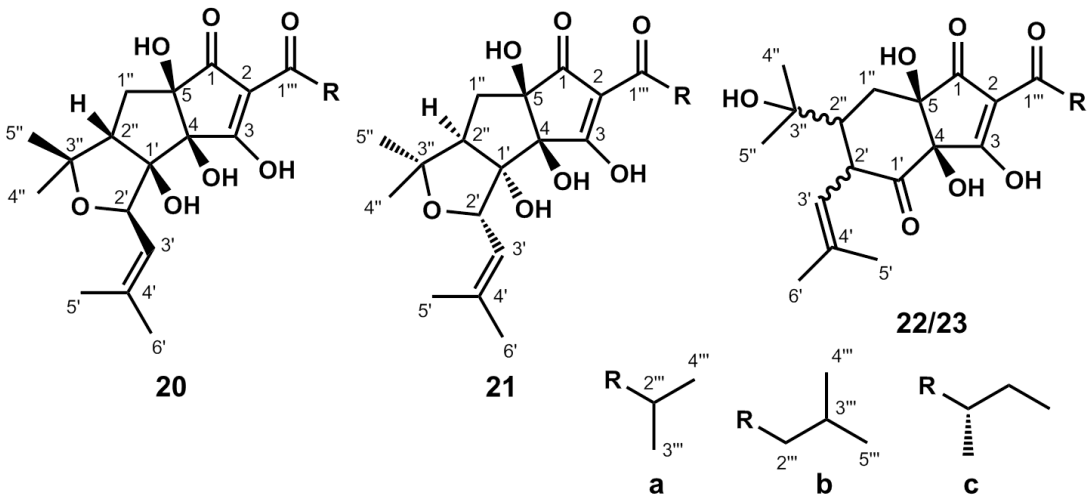

Figure 33. Structures of scorpiohumulinols A: scorpiocohumulinol A (**20a**), scorpiohumulinol A (**20b**), and scorpioadhumulinol A (**20c**); scorpiohumulinols B: scorpiocohumulinol B (**21a**), scorpiohumulinol B (**21b**), and scorpioadhumulinol B (**21c**); dicyclohumulinols A: dicyclocohumulinol A (**22a**), dicyclohumulinol A (**22b**), and dicycloadhumulinol A (**22c**); dicyclohumulinols B: dicyclocohumulinol B (**23a**), dicyclohumulinol B (**23b**), and dicycloadhumulinol B (**23c**).

Compound **20b** was obtained as a yellowish brown, amorphous solid. The HRESIMS spectrum and ^{13}C NMR data indicated a molecular formula of $C_{21}H_{30}O_7$, which is the same as **11b**. Analysis of the ^{1}H and ^{13}C NMR, ^{1}H-^{1}H COSY, HMQC, HMBC, and NOESY spectra established that **20b** possesses an isovaleryl side chain at C-2 instead of the isobutyryl side chain observed in **20a** (Table 7). Thus, **20b** was identified as scorpiohumulinol A, which has not been previously reported (Figure 33).

Compound **21b** was obtained as a pale yellow oil. The HRESIMS spectrum and ^{13}C NMR data indicated a molecular formula of $C_{21}H_{30}O_7$, which is the same as **20b**. Analysis of the ^{1}H and ^{13}C NMR, ^{1}H-^{1}H COSY, HMQC, HMBC, and NOESY spectra established that **21b** possesses an isovaleryl side chain at C-2 instead of the isobutyryl side chain observed in **21a** (Table 7). Thus, **21b** was identified as scorpiohumulinol B, which again has not been previously reported (Figure 33).

Compound **22a** was obtained as a pale yellow oil. The HRESIMS spectrum and ^{13}C NMR data indicated a molecular formula of $C_{20}H_{28}O_7$, which is identical to that of **11a**. Analysis of the ^{1}H and ^{13}C NMR, and HMQC spectra of **22a** strongly suggested that **22a** also possesses the 2-isobutyryl-3,4,5-trihydroxycyclopent-2-enone structure present in **11a** [C-1 – C-5 (ring A) and C-1‴ – C-4‴] (Table 8, Figure 31). The molecular formula of **22a** required seven IHD. Four of the seven IHD were accounted by the 2-isobutyryl-3,4,5-trihydroxycyclopent-2-enone structure, and two of them were due to an olefinic carbon pair [C-3′ (δ 117.6) and C-4′ (δ 138.0)] and another carbonyl carbon [C-1′ (δ 212.8)]. These findings indicated that **22a** possesses a bicyclic structure.

The HMBC correlations of H-4″ (δ_H 1.17) and H-5″ (δ_H 1.24) to C-3″ (δ_C 72.7) and C-2″ (δ_C 57.3), and the ^{1}H-^{1}H COSY correlation between H-2″ (δ_H 2.04) and H_2-1″ (δ_H 2.52, 2.46) established the connectivity of C-1″ – C-2″ – C-3″ – $2CH_3$ (C-4″ and C-5″), while the HMBC correlations of H-5′ (δ_H 1.64) and H-6′ (δ_H 1.78) to C-4′ and C-3′ and the ^{1}H-^{1}H COSY correlation between H-2′ (δ_H 4.13) and H-3′ (δ_H 5.41) established the connectivity of C-2′ – C-3′ – C-4′ – $2CH_3$ (C-5′ and C-6′). The connectivity of C-2′ –

C-2″ was confirmed by the HMBC correlations of H_2-1″ and H-2″ to C-2′ (δ_C 57.4) [the correlation between H-2′ and H-2″ was not observed in the COSY experiment due to the small $J_{2',2''}$ value (<1 Hz)], and the connectivity of C-2′ – C-1′ – C-4 was indicated from the HMBC correlations of H-3′ to the carbonyl carbon C-1′ and H-2′ to C-4 (δ_C 81.7). The HMBC correlations of H_2-1″ to C-1 (δ_C 197.6), C-4, and C-5 (δ_C 77.2) verified the connectivity of C-1″ – C-5 – C-4, thereby establishing the presence of a cyclohexane ring composed of C-4 – C-5 – C-1″ – C-2″ – C-2′ – C-1′ (ring D) in **22a**. Taking these findings altogether established the planar structure of **22a** (Figure 31).

Compound **23a** was obtained as a pale yellow oil. The HRESIMS spectrum and ^{13}C NMR data indicated a molecular formula of $C_{20}H_{28}O_7$, which is the same as that of **22a**. Analysis of the ^{1}H and ^{13}C NMR, ^{1}H-^{1}H COSY, HMQC, and HMBC spectra of **23a** (Table 8) revealed that **23a** possesses the same planar structure as **22a** (Figure 31).

The relative configurations at C-4 and C-5 in both **22a** and **23a** should be preserved from the precursor compound **11a** (β-orientation); however, the author could not obtain information to determine the relative configurations at C-2′ and C-2″ of **22a** and **23a** and only partial relative configurations of them are described here. The author named **22a** and **23a**, which have not been previously reported, as dicyclocohumulinol A and dicyclocohumulinol B, respectively (Figure 33).

Compounds **22b** and **23b** were both obtained as a pale yellow oil. The HRESIMS and ^{13}C NMR data of **22b** and **23b** indicated a molecular formula of $C_{21}H_{30}O_7$, which is the same as that of **11b**. Analysis of the ^{1}H and ^{13}C NMR, ^{1}H-^{1}H COSY, HMQC, and HMBC spectra established that **22b** and **23b** are *n*-congeners of **22a** and **23a**, respectively (Table 8). Thus, **22b** and **23b**, which have not been previously reported, were identified as dicyclohumulinol A and dicyclohumulinol B, respectively (Figure 33).

None of the isolated compounds in this study showed optical activity. Thus, given that the precursors **11a** and **11b** exist as racemic mixtures, all of the isolated compounds were determined to be racemates.

Table 8. NMR spectroscopic data (400 MHz, methanol-d_4) for compounds **22a**, **22b**, **23a**, and **23b**[a]

	22a		**22b**		**23a**		**23b**	
pos.	δ_C, type	δ_H, mult. (*J* in Hz)	δ_C, type	δ_H, mult. (*J* in Hz)	δ_C, type	δ_H, mult. (*J* in Hz)	δ_C, type	δ_H, mult. (*J* in Hz)
1	197.6, C	-	198.0, C	-	200.2, C[b]	-	200.3, C	-
2	112.2, C	-	113.1, C	-	110.3 C	-	111.1, C	-
3	199.5, C	-	199.8, C	-	200.3, C[b]	-	200.9, C	-
4	81.7, C	-	81.8, C	-	81.6, C	-	82.7, CH	-
5	77.2, C	-	77.3, C	-	77.5, C	-	77.8, C	-
1'	212.8, C	-	212.7, C	-	210.2, C	-	210.1, C	-
2'	57.4, CH	4.13, d (9.7)	57.5, CH	4.12, d (9.7)	56.7, CH	3.74, d (8.7)	56.5, CH	3.68, d (8.8)
3'	117.6, CH	5.41, d (9.7)	117.6, CH	5.39, d (9.7)	116.2, CH	5.43, d (8.7)	116.3, CH	5.43, d (8.8)
4'	138.0, C	-	138.0, C	-	139.9, C	-	139.5, C	-
5'	18.5, CH_3	1.64, s	18.5, CH_3	1.63, s	18.6, CH_3	1.57, s	18.6, CH_3	1.53, s
6'	26.6, CH_3	1.78, s	26.27, CH_3	1.78, s	26.3, CH_3	1.77, s	26.2, CH_3	1.77, s
1"	30.1, CH_2	a: 2.52, dd (13.1, 12.3) b: 2.46, dd (13.1, 6.5)	30.1, CH_2	a: 2.51, dd (12.9, 12.9) b: 2.46, dd (12.9, 6.8)	31.7, CH_2	a: 2.73, dd (13.4, 4.4) b: 2.08, dd (14.2, 13.4)	31.5, CH_2	a: 2.75, m b: 2.06, dd (14.1, 14.1)
2"	57.3, CH	2.04, dd (12.3, 6.5)	57.2, CH	2.04, m	55.6, CH	2.22, dd (14.2, 4.4)	55.6, CH	2.28, dd (14.1, 4.7)
3"	72.7, C	-	72.7, C	-	72.4, C	-	72.3, C	-
4"	27.9, CH_3	1.17, s	27.9, CH_3	1.17, s	26.7, CH_3	1.14, s	26.7, CH_3	1.16, s
5"	28.7, CH_3	1.24, s	28.6, CH_3	1.24, s	27.9, CH_3	1.21, s	27.9, CH_3	1.21, s
1'"	206.7, C	-	202.1, C	-	204.1, C	-	198.6, C	-
2'"	37.9, CH	3.51, sep (6.8)	48.7, CH_2	a: 2.74, dd (14.6, 7.0) b: 2.67, dd (14.6, 7.0)	36.4, CH	3.59, sep (6.7)	46.5, CH_2	a: 2.79, dd (13.7, 6.9) b: 2.75, dd (13.7, 7.3)
3'"	18.3, CH_3	1.05, d (6.8)	26.8, CH	2.06, m	18.3, CH_3	1.12, d (6.7)	27.5, CH	2.15, m
4'"	17.8, CH_3	1.07, d (6.8)	22.9, CH_3	0.93, d (6.4)	18.6, CH_3	1.14, d (6.7)	22.9, CH_3	0.97, d (6.6)
5'"	-	-	23.0, CH_3	0.93, d (6.4)	-	-	22.9, CH_3	0.98, d (6.6)

[a] Arbitrary numbering according to structures **22a**, **22b**, **23a**, and **23b** shown in Figures 31 and 33.

[b] Signals interchangeable.

Mechanism of the formation of compounds 20–23 from compound 11.

The above structural elucidation of compounds **20–23** enabled the author to propose a mechanism for their formation (Figure 34). The reaction cascade from compound **11** to compounds **20** and **21** resembles that from hydroxy-*trans*-alloisohumulones to scorpiohumols, which was previously reported as a proton-catalyzed intramolecular nucleophilic cyclization.[14] The reaction starts via protonation of the carbonyl group of the hydroxyisohexenoyl side chain at C-4 in compound **11**, leading to the carbocation intermediate $\mathbf{A_1}$ (Figure 34, route A). Cyclization of $\mathbf{A_1}$ onto the prenyl group at C-5 followed by addition of H_2O to the resultant carbocation would afford the bicyclic intermediate $\mathbf{A_2}$. Upon protonation of the hydroxy group at C-4′ in $\mathbf{A_2}$ followed by elimination of this group as H_2O, the resonance hybrid intermediate $\mathbf{A_3}$ would undergo the second cyclization reaction via the formation of an ether linkage between the hydroxy group at C-3″ and the carbocation at C-2′, leading to compounds **20** and **21**. Given that compounds possessing feasible relative configurations other than compounds **20** and **21** were not isolated or detected, as shown in Figure 30A(2) and B(2), the two cyclization reactions must proceed stereo-selectively under the author's experimental conditions.

In the case of compounds **22** and **23**, an initial protonation reaction presumably occurs at the hydroxy group of the hydroxyisohexenoyl side chain at C-4 in compound **11** (Figure 34, route B). Upon elimination of this group as H_2O, the resonance hybrid intermediate $\mathbf{B_1}$ would undergo the cyclization onto the prenyl group at C-5 to afford the carbocation intermediate $\mathbf{B_2}$. Addition of H_2O would then lead to compounds **22** and **23**. Similar to the cyclization reactions leading to compounds **20** and **21**, the cyclization reaction to afford compounds **22** and **23** must also proceed stereo-preferably because compounds possessing different relative configurations from those of compounds **22** and **23** were not isolated or detected as main products (Figure 30A2 and B2).

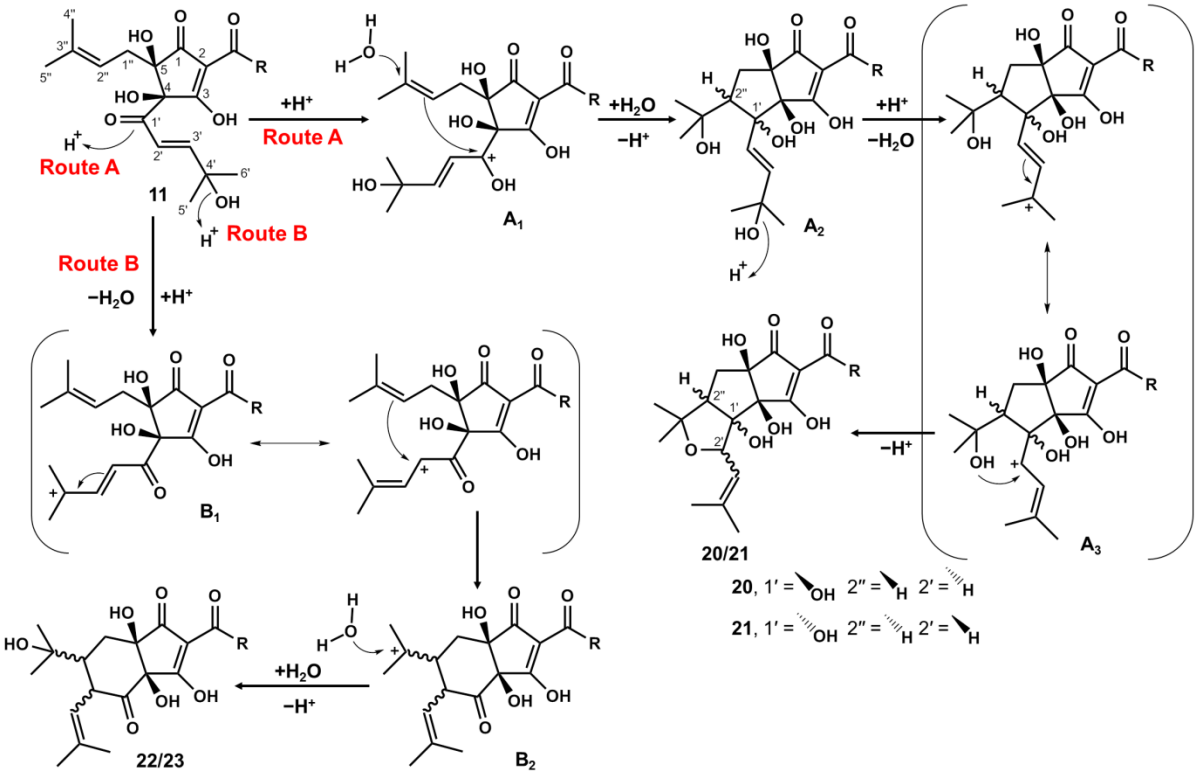

Figure 34. Proposed reaction cascade for the transformation of 4′-hydroxyallohumulinones (**11**) to scorpiohumulinols A/B (**20/21**) and dicyclohumulinols A/B (**22/23**).

Quantitative analyses of compounds 11 and 20–23 during storage in the model solution.

To characterize the compositional changes that occur in stored hard resin during beer aging, the author investigated the time-dependent changes in 4′-hydroxyallohumulinones (**11a** and **11b**) as representative constituents of hard resin derived from stored hops, together with their transformation products, in a model buffer solution (pH 4.0) stored at 40 ˚C. Figure 35 shows the time course of the decrease in 4′-hydroxyallohumulinones and the increase in transformation products. The two 4′-hydroxyallohumulinones (**11a** and **11b**) had decreased by 90% after 1 w and had almost completely transformed after 2 w, whereas the scorpiohumulinols A (**20a** and **20b**) and B (**21a** and **21b**) and the dicyclohumulinols B (**23a** and **23b**) increased and reached

their peak amounts during this period. The scorpiohumulinols B (**21a** and **21b**) that were generated were very stable and did not transform further even after 12 w of storage. The scorpiohumulinols A (**20a** and **20b**) were also stable and decreased only a little during the prolonged storage period. On the other hand, the amount of dicyclohumulinols B (**23a** and **23b**) slowly decreased after reaching a maximum at 2 w, whereas the amount of dicyclohumulinols A (**22a** and **22b**) continuously increased until the 12th week. This indicates that dicyclohumulinols B (**23**) are gradually transformed into dicyclohumulinols A (**22**). A potential reaction from **23** to **22** would be epimerization at C-2′, resulting from either keto-enol tautomerism involving the carbonyl carbon C-1′ or a proton exchange reaction of H-2′. Dicyclohumulinols A (**22**) seem to possess a thermodynamically more stable configuration in comparison to dicyclohumulinols B (**23**). Further studies on the relative configurations of **22** and **23** may lead to a rational explanation of the changes in the ratio of **22** and **23** during storage. In total, the transformation products generated (sum of **20**–**23**) accounted for approximately 70% of the decomposed 4′-hydroxyallohumulinones (**11**).

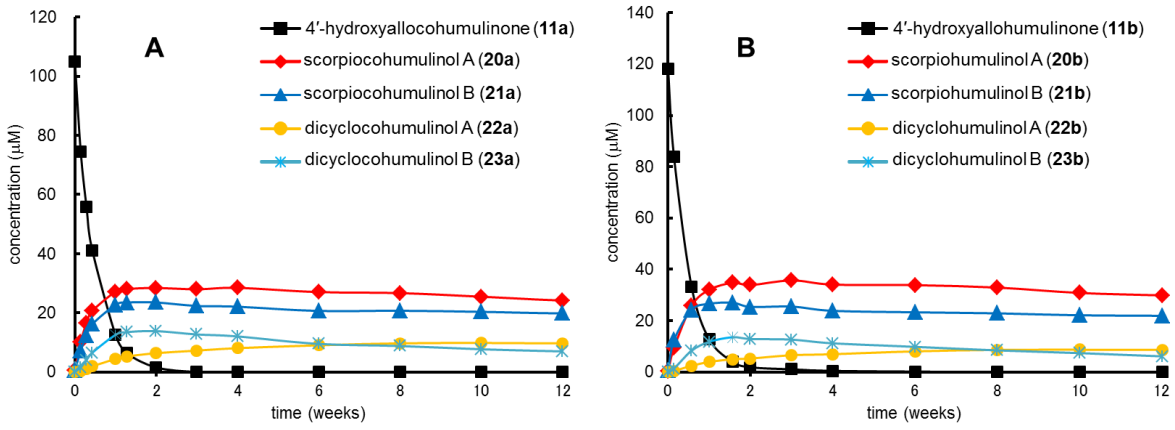

Figure 35. Concentration changes in (A) 4′-hydroxyallocohumulinone (**11a**), scorpiocohumulinol A/B (**20a/21a**), and dicyclocohumulinol A/B (**22a/23a**), and (B) 4′-hydroxyallohumulinone (**11b**), scorpiohumulinol A/B (**20b/21b**), and dicyclohumulinol A/B (**22b/23b**) during incubation in an acidic buffer (pH 4.0) at 40 ˚C for 12 w.

This is the first study to report the time-dependent compositional changes of α-acid-derived oxidation products from the hard resin during beer aging. The author believes that these findings will be extremely valuable both for positively utilizing and controlling the hard resin in hops during brewing, and for evaluating the influence of beer aging on beer properties especially for beer brewed with either hard-resin-enriched hops or extracts.

Summary

The author prepared hard resin from stored hops and investigated its compositional changes in an experimental model of beer aging. The hard resin contained a series of α-acid oxides. Among them, 4′-hydroxyallohumulinones (**11**) were unstable under beer storage conditions, and their transformation induced primary compositional changes of the hard resin during beer aging. The chemical structures of the products, including novel polycyclic compounds scorpiohumulinols A (**20**) and B (**21**) and dicyclohumulinols A

(**22**) and B (**23**), were determined by HRMS and NMR analyses. These compounds were proposed to be produced via proton-catalyzed cyclization reactions of 4′-hydroxyallohumulinones (**11**). Furthermore, they were more stable than their precursor 4′-hydroxyallohumulinones (**11**) during prolonged storage periods. These results will aid understanding of the nature and reactivity of the hard resin in order to realize its true value for brewing.

Chapter 5

Development of preparative and analytical methods of the hop bitter acid oxide fraction and chemical properties of its components

The bitterness quality of beer brewed with stored hops, which contain oxidation products derived from α- and β-acids, has been studied, but the conclusion is disputed.[9, 23, 32, 36-39] Moreover, there are very few published studies on the physiological effects of these oxidation products.[61] In chapters 1 and 2, the author revealed that α-acids are oxidized into humulinones (**6a–c**), 4′-hydroxyallohumulinones (**11a–c**), tricyclooxyisohumulones A (**12a–c**) and B (**13a–c**), and deisopropyltricycloisohumulones (**15a–c**), and that β-acids are oxidized into hulupones (**6a–c**). In chapter 3, the author revealed that 4′-hydroxyallohumulinones (**11a–c**) isomerize into 4′-hydroxyallo-*cis*-humulinones (**17a–c**) and degrade into *cis*-oxyhumulinic acids (**18a–c**) during the wort boiling process. Furthermore, the author revealed that 4′-hydroxyallohumulinones (**11a–c**) isomerize into scorpiohumulinols A (**20a–c**) and B (**21a–c**) and dicyclohumulinols A (**22a–c**) and B (**23a–c**) during beer aging in chapter 4.

Nonetheless, the chemical properties of a large number of other α- and/or β-acid-derived oxidation products remain unknown. In order to evaluate the effects of bitter acid oxides on beer properties as well as their potential health benefits, the chemical structures of the main constituents of bitter acid oxides must be determined. Furthermore, it is essential to develop methods to selectively prepare and analyze the bitter acid oxide fraction, which exclude other hop constituents such as polyphenols, lipids, waxes, and polysaccharides. In addition, understanding chemical properties common to the constituents in whole bitter acid oxides is also helpful in studying the effects of these bitter acid oxides.

Here, the author developed a simple liquid-liquid extraction method to obtain the

total bitter acid oxide fraction from a water extract of stored hops and designated the constituents of this fraction as matured hop bitter acids (MHBA). The chemical properties of MHBA were then thoroughly investigated. A quantitative analytical methodology for whole MHBA was developed and validated and the concentrations of whole MHBA in several commercial beers were investigated using this technique.

Materials and methods

Chemicals and materials.

The following chemicals were obtained commercially: ethylenediaminetetraacetic acid (EDTA), caffeine, H_3PO_4, MeCN, EtOH, and CH_2Cl_2 (Wako Pure Chemicals, Osaka, Japan). Deionized water for chromatography was purified by means of a Milli-Q Gradient A10 system (Millipore, Billerica, MA, USA). An isomerized hop extract and hop pellets were purchased from Hopsteiner (Mainburg, Germany).

Preparation of reference standard compounds.

cis-Iso-α-acids (**3a–c**), *trans*-iso-α-acids (**4a–c**), humulinones (**6a–c**), and hulupones (**5a–c**) were prepared according to a protocol reported in chapter 1. Tricyclooxyisohumulones A (**12b**) and B (**13b**) and deisopropyltricycloisohumulone (**15b**) were isolated from the autoxidation products of humulone as described in chapter 2. 4′-Hydroxyallohumulinones (**11a–c**), 4′-hydroxyallo-*cis*-cohumulinone (**17a**), 4′-hydroxyallo-*cis*-humulinone (**17b**), *cis*-oxycohumulinic acid (**18a**), and *cis*-oxyhumulinic acid (**18b**) were isolated as described in chapter 3. Scorpiocohumulinols A (**20a**) and B (**21a**), scorpiohumulinols A (**20b**) and B (**21b**), dicyclocohumulinols A (**22a**) and B (**23a**), and dicyclohumulinols A (**22b**) and B (**23b**) were prepared as described in chapter 4.

Preparation of a MHBA fraction from stored hops.

Hop pellets (600 g) were stored at 60 °C for 120 h to oxidize α- and β-acids and then extracted with pre-warmed H_2O (50 °C, 6 L) for 1 h. During extraction, the temperature of the extract was maintained at 50 °C. The extract was filtered to remove the debris of hops and then treated with activated charcoal and polyvinylpolypyrrolidone (PVPP) for 2 h. After treatment, the mixture was filtered to separate the extract from activated charcoal and PVPP. The filtrate was heated to 90 °C for 4 h and cooled to room temperature before lyophilizing to yield a pale brown powder as a water extract of stored hops (126 g). A portion (63 g) of this extract was dissolved in H_2O (3 L) and total bitter acid oxides were extracted with CH_2Cl_2 (6 L) after acidifying the solution with 1 N HCl (300 mL). The CH_2Cl_2 layer was dried over anhydrous Na_2SO_4 and evaporated to yield a pale brown, amorphous solid (12.6 g) as a MHBA fraction.

Molecular formula analysis of the MHBA components.

The MHBA fraction was dissolved in EtOH and analyzed using HPLC-PDA-ESI/HRMS to determine the molecular formula of the MHBA components. The HPLC-PDA-HRMS system consisted of an LTQ Orbitrap XL mass spectrometer (ThermoScientific, San Jose, CA, USA) with an Agilent 1200 series binary pump (G1312B), a degasser (G1379B), an autosampler (G1367C), a column compartment (G1316B), and a PDA detector (G1315C) (Agilent, Palo Alto, CA, USA). The LC conditions were as follows: column: 100 × 2.1 mm id, 3 μm, L-column 2 ODS (Chemicals Evaluation and Research Institute, Tokyo, Japan); solvent: 5 mM $HCOONH_4$ (pH 8.5) (solvent A) and MeCN (solvent B), a linear gradient from 10 to 36% B in 0 → 39 min, 36 to 80% B in 39 → 44 min, and 80% B for 44 → 52 min; flow rate: 0.25 mL/min; column temperature: 40 ˚C. The PDA recorded spectra from 190 to 500 nm. The HRMS was operated in negative ionization mode with an ESI source using the following conditions: sheath gas at 50 (arbitrary units), aux gas at 20 (arbitrary units), sweep gas at 0 (arbitrary units), spray voltage at −2.0 kV, capillary temperature at 300 °C, capillary

voltage at −20 V, and tube lens at −70 V. The mass range was from *m/z* 100 to 800 with a resolution of 30000.

Precursor ion scan analysis of the MHBA components.

The MHBA fraction was dissolved in EtOH and analyzed using HPLC-PDA-ESI/MS/MS to investigate the common partial structure of the MHBA components. The HPLC-PDA-MS/MS system consisted of a 4000 Q-Trap mass spectrometer (AB Sciex, Tokyo, Japan) connected to a Shimadzu Prominence UFLC system (Shimadzu, Kyoto, Japan). The LC conditions were the same as described for the HPLC-PDA-ESI/HRMS method. The 4000 Q-Trap mass spectrometer was operated in negative ionization mode with an ESI source for the precursor ion scans of *m/z* 111 (co-homolog) and *m/z* 125 (*n*- and ad-homologs). Nitrogen was used as the turbo gas at 600 °C. Ion source gases 1 and 2 were set to 50 and 70 psi, respectively, N_2 curtain gas was set to 30 psi, and the collision cell gas was set to 7 psi. The ion spray voltage was set to −4500 V, entrance potential (EP) was set to −10 V, and collision cell exit potential (CXP) ramp was set to −41–−7 V. A declustering potential (DP) ramp (−115–−45 V) and collision energy (CE) ramp (−50–−20 V) were used. Q1 and Q3 resolutions were set to unit. The product ion scan of reference standards was performed with the same parameters as described above, except for CE which was set to −50 V. Analyst software version 1.6.1 (AB Sciex, Tokyo, Japan) was used for the experiments.

Acid-base partition experiments of the MHBA components.

The water extract of stored hops (62.5 mg) was dissolved in H_2O (10 mL) and partitioned with CH_2Cl_2 (20 mL) after acidifying the solution with 1 N HCl (1.0 mL). A portion of the CH_2Cl_2 layer (10 mL) was partitioned with 0.1 M NH_4HCO_3 buffer (pH 8.0) (10 mL), and both the aqueous layer and CH_2Cl_2 layer were analyzed by HPLC.

Quantitative HPLC-UV analytical method for whole MHBA.

The following extraction experiments were conducted independently four times. The water extract of stored hops (600 mg) was dissolved in H_2O (250 mL), and the MHBA fraction was extracted with CH_2Cl_2 (500 mL) after acidifying the solution with 1 N HCl (25 mL).The CH_2Cl_2 layer was dried over anhydrous Na_2SO_4 and evaporated to yield a pale brown, amorphous solid.

The obtained respective solid was dissolved in EtOH (0.500 mg/mL) and analyzed by a Prominence UFLC system (Shimadzu, Kyoto, Japan). The analyses were performed using the following conditions: column: 100 × 2.1 mm id, 3 μm, Alltima C_{18} column (Systech, Tokyo, Japan); solvent: H_2O/H_3PO_4 (85%), 1000/0.2, (v/v) containing EDTA (0.02% w/v) (solvent A) and MeCN (solvent B), a linear gradient from 10 to 52% B in 0 → 26.7 min, 52% B for 26.7 → 30 min, 52 to 75% B in 30 → 32.7 min, 75 to 85% B in 32.7 → 36.7 min, and 85% B for 36.7 → 37.7 min; flow rate: 0.6 mL/min; detector: 270 nm; column temperature: 40 ˚C. The injection volume was 3.0 μL.

Baseline drift generated from mobile phase gradient was eliminated by subtracting the chromatogram signals of blank (H_2O) analysis using a baseline correction function of LCsolution software version 1.25 (Shimadzu, Kyoto, Japan). Peaks detected in the region immediately after elution of caffeine and immediately before elution of *trans*-isocohumulone (**4a**) were integrated. The integrated area was quantified as whole MHBA using the calibration curve of tricyclooxyisohumulone (**12b**).

Analytical method validation for whole MHBA in a model beverage.

A bottled carbonated beverage, containing the water extract of stored hops with a final concentration of whole MHBA being around 120 mg/L, was prepared. To evaluate intra- and inter-day precision and reproducibility of quantitative analysis of whole MHBA, the beverage was analyzed (n=6) for six consecutive days. The beverage was degassed by sonication for 15 min and a portion (10 mL) was partitioned with CH_2Cl_2

(20 mL) after acidifying the solution with 1 N HCl (1.0 mL). The two-layered solution was then centrifuged at 6000 *g* for 10 min at 20 ˚C, and a portion (10 mL) of the CH_2Cl_2 layer was collected, dried under N_2 gas, and redissolved in EtOH (1.0 mL). After filtration, this solution was subjected to quantitative HPLC analysis. To evaluate the extraction efficiency of whole MHBA in the analytical procedure, the residual aqueous solution was extracted with CH_2Cl_2 (20 mL) for a second time and the resulting extract was analyzed using the same protocol.

Quantitative analysis of whole MHBA in commercial beers.

Commercially available beers were purchased in a Japanese market. The purchased beers were a selection of both Japanese (A–E) and foreign brands (F–K).

Each beer was degassed by sonication for 15 min and a portion (10 mL) was partitioned with CH_2Cl_2 (20 mL) after acidifying the solution with 1 N HCl (1.0 mL). The two-layered solution was then centrifuged at 6000 *g* for 10 min at 20 ˚C, and a portion (10 mL) of the CH_2Cl_2 layer was collected, dried under N_2 gas, and redissolved in EtOH (1.0 mL). After filtration, this solution was subjected to quantitative HPLC analysis. Iso-α-acid content (sum of **3a–c** and **4a–c**) in the beer was measured simultaneously using ICS-I3 as a calibration standard (American Society of Brewing Chemists, Saint Paul, MN, USA).

Results and discussion

Preparation of a water extract of stored hops and a MHBA fraction.

In this study, the author designated total bitter acid oxides derived from α-, β- and/or iso-α-acids, including structurally unknown constituents, as matured hop bitter acids (MHBA), which showed more hydrophilic properties than iso-α-acids in HPLC analysis (Figure 36). The MHBA fraction could be prepared from a water extract of stored hops as described below in detail.

First, fresh hops were oxidized to transform α- and β-acids into their respective oxidation products, which were then extracted into water. The poorly water-soluble components such as xanthohumol, lipids, and waxes could be excluded in this extraction step, and an extract, containing the oxidation compounds such as 4′-hydroxyallohumulinones (**11a–c**) and tricyclooxyisohumulones A (**12a–c**) and B (**13a–c**), was obtained (Figure 36C). Next, an aqueous solution of the extract was heated. The heating process induced chemical reactions that occur during the wort boiling process, such as transformation of unstable 4′-hydroxyallohumulinones (**11a–c**) into 4′-hydroxyallo-*cis*-humulinones (**17a–c**) and *cis*-oxyhumulinic acids (**18a–c**), as well as potentially other reactions, resulting in the stabilization of the composition of the extract (Figure 36D). Finally, MHBA could be selectively extracted with CH_2Cl_2 from an aqueous solution of the extract after acidification. CH_2Cl_2 was selected as the extraction solvent because the oxidation compounds, which constitute MHBA, were shown to be efficiently extracted with CH_2Cl_2 in the previous study described in chapters 3 and 4. Indeed, CH_2Cl_2 was found to be suitable for the extraction of bitter acid oxides. However, isooctane, which is widely used to extract bitter acids in beer,[83, 84] was unsuitable for the extraction of hydrophilic oxides (Figure 37).

The solid content yield of the water extract from stored hops was about 21% (w/w), and the MHBA fraction accounted for about 20% of the extract. The chemical properties of MHBA as a whole were further investigated.

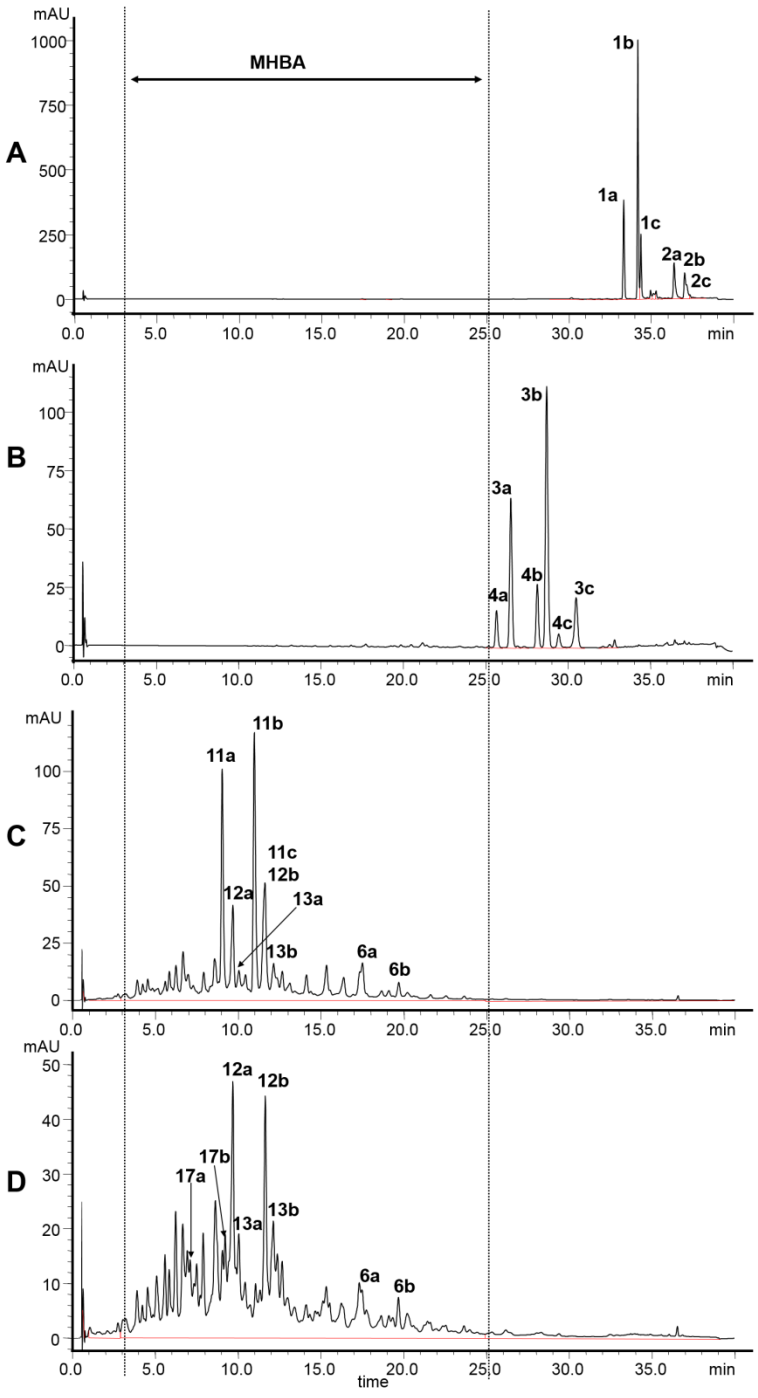

Figure 36. HPLC chromatograms of the (A) EtOH extract of fresh hops, (B) isomerized hop extract, and water extract of hops stored at 60 ˚C for 120 h (C) before and (D) after heating the extract. The chromatograms of (C) and (D) represent the components extractable in CH_2Cl_2 under acidic conditions. Structures of the compounds are given in Figures 1, 17, and 21.

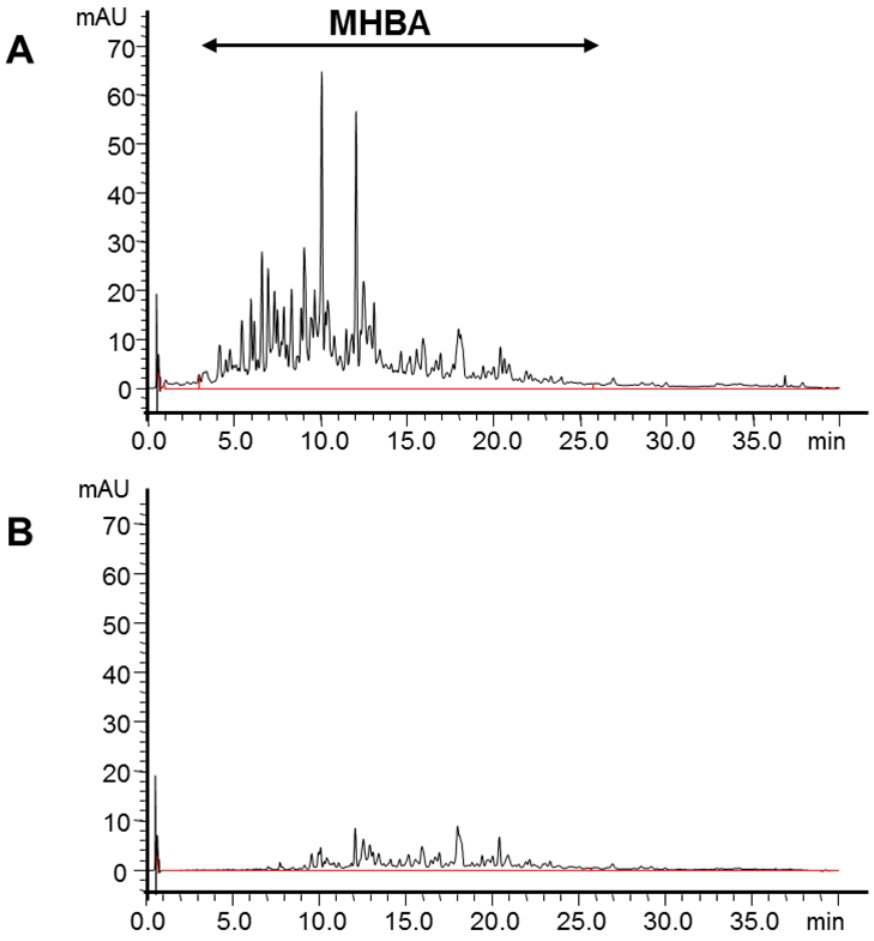

Figure 37. HPLC chromatograms of the constituents extractable in (A) CH_2Cl_2 and (B) isooctane from the acidic aqueous solution of the water extract of stored hops.

Chemical properties of MHBA.

First, the author analyzed the MHBA fraction using HPLC-PDA-ESI/HRMS. The chromatogram at 270 nm and total ion chromatogram (TIC) are shown in Figure 38. Except for some peaks [i.e., peak numbers 85, 95, 98 (cohulupone (**5a**)), and 105 (hulupone (**5b**) and adhulupone (**5c**)) in Figure 38B], which were detected with high intensity by the MS detector in comparison with the UV detector probably because of their especially high efficiency of ionization, the chromatogram at 270 nm (Figure 38A) and TIC (Figure 38B) showed almost the same profile. This result suggested that the

MHBA fraction was composed mostly of substances (i) possessing UV absorption around 270 nm, and (ii) capable of easily forming negative ions in MS. The molecular formulas of the constituents of each peak in Figure 38B indicated by the HRMS data are summarized in Table 9. Humulinones (**6a–c**), 4′-hydroxyallohumulinones (**11a–c**), 4′-hydroxyallo-*cis*-cohumulinone (**17a**), 4′-hydroxyallo-*cis*-humulinone (**17b**), *cis*-oxycohumulinic acid (**18a**), *cis*-oxyhumulinic acid (**18b**), tricyclooxyisohumulones A (**12b**) and B (**13b**), deisopropyltricycloisohumulone (**15b**), hulupones (**5a–c**), scorpiocohumulinols A (**20a**) and B (**21a**), scorpiohumulinols A (**20b**) and B (**21b**), dicyclocohumulinols A (**22a**) and B (**23a**), and dicyclohumulinols A (**22b**) and B (**23b**) were identified in MHBA from direct comparison to the reference standards. It is known that iso-α-acid derivatives are eluted in the order of co-congener, ad-congener, and *n*-congener in ODS HPLC using an alkaline mobile phase.[21, 85] Based on the elution pattern described above and observed *m/z*, 4′-hydroxyallo-*cis*-adhumulinone (**17c**), *cis*-oxyadhumulinic acid (**18c**), tricyclooxyisocohumulones A (**12a**) and B (**13a**), tricyclooxyisoadhumulones A (**12c**) and B (**13c**), deisopropyltricycloisocohumulone (**15a**), deisopropyltricycloisoadhumulone (**15c**), scorpioadhumulinols A (**20c**) and B (**21c**), and dicycloadhumulinols A (**22c**) and B (**23c**)were tentatively identified in MHBA (Table 9). All other structurally unidentified components in MHBA, as far as the author investigated, gave a molecular formula corresponding to the oxidation products of α- and β-acids and related compounds (94% of the components seem to be α-acid oxides and 6% of the components seem to be β-acid oxides) (Table 9). For example, oxygen adducts, water adducts and dehydration products of oxidized α-acids, and compounds produced by oxidative elimination of an acetone (C_3H_6O)[14, 25] and a methylhexenoyl group (C_6H_8O)[13, 14] were detected (Table 9). Thus, MHBA appear to be composed of oxidation products derived primarily from α-acids.

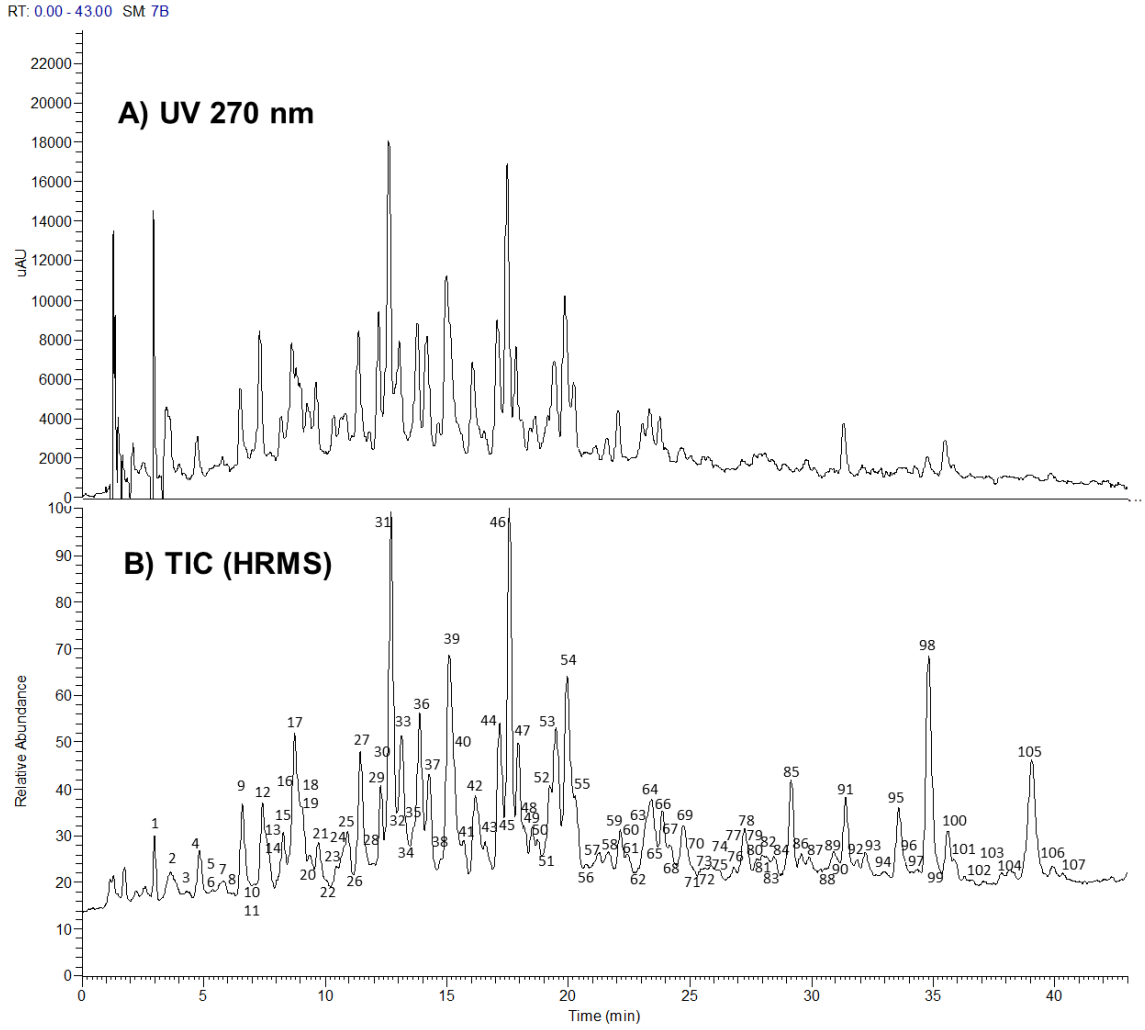

Figure 38. HPLC-PDA-HRMS analysis of the MHBA fraction. (A) Chromatogram of UV at 270 nm, and (B) TIC of HRMS analysis. Observed *m/z* and indicated molecular formula of the constituents of each peak shown in TIC and identified compounds are summarized in Table 9

Table 9. Molecular formula and deduced origin of the MHBA components indicated by HRMS data

peak No.[a]	retention time (min)	observed *m/z*	molecular formula[b]	deduced origin[c]	compound
1	2.98	271.1183	$C_{13}H_{20}O_6$	posthumulone[d] (+O, +H_2O, −methylpentenoyl group)	
	2.98	397.1860	$C_{20}H_{30}O_8$	cohumulone (+2O, +H_2O)	
2	3.61	379.1757	$C_{20}H_{28}O_7$	cohumulone (+2O)	
	3.61	297.1340	$C_{15}H_{22}O_6$	*n*- or adhumulone (+2O, −methylpentenoyl group)	
3	4.36	269.1026	$C_{13}H_{18}O_6$	posthumulone[d] (+2O, −methylpentenoyl group)	
	4.36	381.1911	$C_{20}H_{30}O_7$	cohumulone (+O, +H_2O)	
4	4.80	321.1339	$C_{17}H_{22}O_6$	cohumulone (+2O, −acetone)	
5	5.30	411.2014	$C_{21}H_{32}O_8$	*n*- or adhumulone (+2O, +H_2O)	
	5.30	393.1910	$C_{21}H_{30}O_7$	*n*- or adhumulone (+2O)	
	5.30	335.1493	$C_{18}H_{24}O_6$	*n*- or adhumulone (+2O, −acetone)	
	5.30	379.1754	$C_{20}H_{28}O_7$	cohumulone (+2O)	
6	5.67	285.1340	$C_{14}H_{22}O_6$	cohumulone (+O, +H_2O, −methylpentenoyl group)	
7	5.85	395.1704	$C_{20}H_{28}O_8$	cohumulone (+3O)	
8	6.29	397.1861	$C_{20}H_{30}O_8$	cohumulone (+2O, +H_2O)	
9	6.58	267.1234	$C_{14}H_{20}O_5$	cohumulone (+O, −methylpentenoyl group)	**18a**
10	6.89	393.1912	$C_{21}H_{30}O_7$	*n*- or adhumulone (+2O)	
11	7.19	363.1806	$C_{20}H_{28}O_6$	cohumulone (+O)	
	7.19	381.1914	$C_{20}H_{30}O_7$	cohumulone (+O, +H_2O)	
	7.19	331.1184	$C_{18}H_{20}O_6$	*n*- or adhumulone (+2O, −acetone, −4H)	
	7.19	411.2021	$C_{21}H_{32}O_8$	*n*- or adhumulone (+2O, +H_2O)	
12	7.40	379.1754	$C_{20}H_{28}O_7$	cohumulone (+2O)	**20a**
13	7.56	319.1180	$C_{17}H_{20}O_6$	cohumulone (+2O, −acetone, −2H)	
14	7.74	239.1288	$C_{13}H_{20}O_4$	posthumulone[d] (−methylpentenoyl group, +2H)	
	7.74	395.1707	$C_{20}H_{28}O_8$	cohumulone (+3O)	
	7.74	283.1185	$C_{14}H_{20}O_6$	cohumulone (+2O, −methylpentenoyl group)	
15	8.28	393.1912	$C_{21}H_{30}O_7$	*n*- or adhumulone (+2O)	
	8.28	379.1756	$C_{20}H_{28}O_7$	cohumulone (+2O)	
	8.28	303.1232	$C_{17}H_{20}O_5$	cohumulone (+O, −acetone, −2H)	
16	8.49	251.1285	$C_{14}H_{20}O_4$	cohumulone (−methylpentenoyl group)	
	8.49	335.1494	$C_{18}H_{24}O_6$	*n*- or adhumulone (+2O, −acetone)	
	8.49	321.1337	$C_{17}H_{22}O_6$	cohumulone (+2O, −acetone)	
	8.49	307.1181	$C_{16}H_{20}O_6$	posthumulone[d] (+2O, −acetone)	
	8.49	283.1182	$C_{14}H_{20}O_6$	cohumulone (+2O, −methylpentenoyl group)	
17	8.71	321.1336	$C_{17}H_{22}O_6$	cohumulone (+2O, −acetone)	

Table 9. (continued)

	8.71	379.1754	$C_{20}H_{28}O_7$	cohumulone (+2O)	
	8.71	395.1702	$C_{20}H_{28}O_8$	cohumulone (+3O)	
18	8.91	379.1757	$C_{20}H_{28}O_7$	cohumulone (+2O)	**22a**
19	9.10	335.1495	$C_{18}H_{24}O_6$	*n*- or adhumulone (+2O, −acetone)	
20	9.35	379.1758	$C_{20}H_{28}O_7$	cohumulone (+2O)	
	9.35	409.1863	$C_{21}H_{30}O_8$	*n*- or adhumulone (+3O)	
	9.35	349.1653	$C_{19}H_{26}O_6$	posthumulone[d] (+O) or prehumulone[e] (+2O, −acetone)	
	9.35	307.1548	$C_{17}H_{24}O_5$	cohumulone (+H_2O, −acetone)	
21	9.69	379.1755	$C_{20}H_{28}O_7$	cohumulone (+2O)	**21a**
	9.69	307.1181	$C_{16}H_{20}O_6$	posthumulone[d] (+2O, −acetone)	
	9.69	407.1703	$C_{21}H_{28}O_8$	*n*- or adhumulone (+3O, −2H)	
	9.69	409.1860	$C_{21}H_{30}O_8$	*n*- or adhumulone (+3O)	
22	9.98	269.1390	$C_{14}H_{22}O_5$	cohumulone (+H_2O, −methylpentenoyl group)	
	9.98	379.1755	$C_{20}H_{28}O_7$	cohumulone (+2O)	
	9.98	409.1859	$C_{21}H_{30}O_8$	*n*- or adhumulone (+3O)	
23	10.45	379.1753	$C_{20}H_{28}O_7$	cohumulone (+2O)	
	10.45	395.1703	$C_{20}H_{28}O_8$	cohumulone (+3O)	
	10.45	303.1231	$C_{17}H_{20}O_5$	cohumulone (+O, −acetone, −2H)	
	10.45	411.2014	$C_{21}H_{32}O_8$	*n*- or adhumulone (+2O, +H_2O)	
24	10.71	281.1391	$C_{15}H_{22}O_5$	adhumulone (+O, −methylpentenoyl group)	**18c**[f]
	10.71	379.1757	$C_{20}H_{28}O_7$	cohumulone (+2O)	
	10.71	347.1495	$C_{19}H_{24}O_6$	posthumulone[d] (+O, −2H)	
	10.71	409.1862	$C_{21}H_{30}O_8$	*n*- or adhumulone (+3O)	
	10.71	393.1913	$C_{21}H_{30}O_7$	*n*- or adhumulone (+2O)	
25	10.91	281.1388	$C_{15}H_{22}O_5$	adhumulone (+O, −methylpentenoyl group)	**18c*t***[f]
	10.91	361.1648	$C_{20}H_{26}O_6$	cohumulone (+O, −2H)	
	10.91	363.1803	$C_{20}H_{28}O_6$	cohumulone (+O)	
	10.91	351.1440	$C_{18}H_{24}O_7$	*n*- or adhumulone (+3O, −acetone)	
	10.91	411.2014	$C_{21}H_{32}O_8$	*n*- or adhumulone (+2O, +H_2O)	
	10.91	251.1283	$C_{14}H_{20}O_4$	cohumulone (−methylpentenoyl group)	
	10.91	427.1963	$C_{21}H_{32}O_9$	*n*- or adhumulone (+3O, +H_2O)	
26	11.20	425.1810	$C_{21}H_{30}O_9$	*n*- or adhumulone (+4O)	
27	11.46	281.1389	$C_{15}H_{22}O_5$	*n*-humulone (+O, −methylpentenoyl group)	**18b**
	11.46	379.1755	$C_{20}H_{28}O_7$	cohumulone (+2O)	
	11.46	393.1911	$C_{21}H_{30}O_7$	adhumulone (+2O)	**20c**[f]
28	11.97	393.1911	$C_{21}H_{30}O_7$	adhumulone (+2O)	**20c*t***[f]
	11.97	333.1337	$C_{18}H_{22}O_6$	*n*- or adhumulone (+2O, −acetone, −2H)	
	11.97	281.1026	$C_{14}H_{18}O_6$	cohumulone (+2O, −methylpentenoyl group, −2H)	
	11.97	409.1859	$C_{21}H_{30}O_8$	*n*- or adhumulone (+3O)	
29	12.29	393.1913	$C_{21}H_{30}O_7$	*n*-humulone (+2O)	**20b**

Table 9. (continued)

30	12.54	333.1338	$C_{18}H_{22}O_6$	*n*- or adhumulone (+2O, −acetone, −2H)	
	12.54	379.1755	$C_{20}H_{28}O_7$	cohumulone (+2O)	**23a**
	12.54	363.1806	$C_{20}H_{28}O_6$	cohumulone (+O)	
	12.54	393.1912	$C_{21}H_{30}O_7$	*n*- or adhumulone (+2O)	
	12.54	409.1861	$C_{21}H_{30}O_8$	*n*- or adhumulone (+3O)	
31	12.73	363.1806	$C_{20}H_{28}O_6$	cohumulone (+O)	**12a**
32	12.97	393.1912	$C_{21}H_{30}O_7$	*n*-humulone (+2O)	**22b**
33	13.15	379.1751	$C_{20}H_{28}O_7$	cohumulone (+2O)	**17a**
	13.15	335.1490	$C_{18}H_{24}O_6$	*n*- or adhumulone (+2O, −acetone)	
	13.15	409.1854	$C_{21}H_{30}O_8$	*n*- or adhumulone (+3O)	
34	13.46	305.1388	$C_{17}H_{22}O_5$	cohumulone (+O, −acetone)	**15a**
	13.46	393.1911	$C_{21}H_{30}O_7$	*n*- or adhumulone (+2O)	
	13.46	317.1388	$C_{18}H_{22}O_5$	*n*- or adhumulone (+O, −acetone, −2H)	
35	13.62	361.1649	$C_{20}H_{26}O_6$	cohumulone (+O, −2H)	
	13.62	393.1911	$C_{21}H_{30}O_7$	adhumulone (+2O)	**21c**[f]
36	13.90	335.1494	$C_{18}H_{24}O_6$	*n*- or adhumulone (+2O, −acetone)	
	13.90	237.1129	$C_{13}H_{18}O_4$	posthumulone[d] (−methylpentenoyl group)	
	13.90	393.1911	$C_{21}H_{30}O_7$	adhumulone (+2O)	**21c**[tf]
	13.90	377.1599	$C_{20}H_{26}O_7$	cohumulone (+2O, −2H)	
	13.90	379.1755	$C_{20}H_{28}O_7$	cohumulone (+2O)	
	13.90	411.1653	$C_{20}H_{28}O_9$	cohumulone (+4O)	
37	14.26	393.1906	$C_{21}H_{30}O_7$	*n*-humulone (+2O)	**21b**
	14.26	409.1853	$C_{21}H_{30}O_8$	*n*- or adhumulone (+3O)	
38	14.78	393.1911	$C_{21}H_{30}O_7$	*n*- or adhumulone (+2O)	
	14.78	377.1597	$C_{20}H_{26}O_7$	cohumulone (+2O, −2H)	
39	15.07	363.1806	$C_{20}H_{28}O_6$	cohumulone (+O)	**13a**
40	15.28	393.1909	$C_{21}H_{30}O_7$	*n*- or adhumulone (+2O)	
	15.28	335.1856	$C_{19}H_{28}O_5$	cohulupone (+H_2O)	
	15.28	283.1545	$C_{15}H_{24}O_5$	*n*- or adhumulone (+H_2O, −methylpentenoyl group)	
41	15.72	375.1805	$C_{21}H_{28}O_6$	*n*- or adhumulone (+O, −2H)	
	15.72	361.1649	$C_{20}H_{26}O_6$	cohumulone (+O, −2H)	
	15.72	377.1958	$C_{21}H_{30}O_6$	*n*- or adhumulone (+O)	
	15.72	363.1805	$C_{20}H_{28}O_6$	cohumulone (+O)	
	15.72	263.1284	$C_{15}H_{20}O_4$	*n*- or adhumulone (−methylpentenoyl group, −2H)	
	15.72	317.1388	$C_{18}H_{22}O_5$	*n*- or adhumulone (+O, −acetone, −2H)	
	15.72	393.1910	$C_{21}H_{30}O_7$	*n*- or adhumulone (+2O)	
	15.72	409.1860	$C_{21}H_{30}O_8$	*n*- or adhumulone (+3O)	
42	16.16	393.1910	$C_{21}H_{30}O_7$	adhumulone (+2O)	**17c**[f], **23c**[f]
	16.16	379.1754	$C_{20}H_{28}O_7$	cohumulone (+2O)	**11a**
	16.16	351.1806	$C_{19}H_{28}O_6$	posthumulone[d] (+H_2O)	

Table 9. (continued)

	16.16	411.2015	$C_{21}H_{32}O_8$	*n*- or adhumulone (+2O, +H_2O)	
43	16.70	361.1648	$C_{20}H_{26}O_6$	cohumulone (+O, −2H)	
	16.70	249.1127	$C_{14}H_{18}O_4$	cohumulone (−methylpentenoyl group, −2H)	
	16.70	393.1909	$C_{21}H_{30}O_7$	adhumulone (+2O)	**23c′**[f]
	16.70	391.1753	$C_{21}H_{28}O_7$	*n*- or adhumulone (+2O, −2H)	
	16.70	375.1804	$C_{21}H_{28}O_6$	*n*- or adhumulone (+O, −2H)	
	16.70	379.1753	$C_{20}H_{28}O_7$	cohumulone (+2O)	
	16.70	409.1858	$C_{21}H_{30}O_8$	*n*- or adhumulone (+3O)	
44	17.12	377.1961	$C_{21}H_{30}O_6$	adhumulone (+O)	**12c**
	17.12	393.1910	$C_{21}H_{30}O_7$	*n*- and adhumulone (+2O)	**23b**, **17c′**[f]
	17.12	279.1232	$C_{15}H_{20}O_5$	*n*- or adhumulone (+O, −methylpentenoyl group, −2H)	
45	17.35	361.1650	$C_{20}H_{26}O_6$	cohumulone (+O, −2H)	
	17.35	379.1754	$C_{20}H_{28}O_7$	cohumulone (+2O)	
46	17.57	377.1962	$C_{21}H_{30}O_6$	*n*-humulone (+O)	**12b**
47	17.96	393.1906	$C_{21}H_{30}O_7$	*n*-humulone (+2O)	**17b**
48	18.20	361.1650	$C_{20}H_{26}O_6$	cohumulone (+O, −2H)	
49	18.51	375.1805	$C_{21}H_{28}O_6$	*n*- or adhumulone (+O, −2H)	
	18.51	333.1337	$C_{18}H_{22}O_6$	*n*- or adhumulone (+2O, −acetone, −2H)	
	18.51	251.1285	$C_{14}H_{20}O_4$	cohumulone (−methylpentenoyl group)	
	18.51	319.1545	$C_{18}H_{24}O_5$	adhumulone (+O, −acetone)	**15c**
50	18.75	393.1914	$C_{21}H_{30}O_7$	*n*- or adhumulone (+2O)	
	18.75	391.1758	$C_{21}H_{28}O_7$	*n*- or adhumulone (+2O, −2H)	
	18.75	377.1964	$C_{21}H_{30}O_6$	*n*- or adhumulone (+O)	
	18.75	425.1812	$C_{21}H_{30}O_9$	*n*- or adhumulone (+4O)	
	18.75	349.2016	$C_{20}H_{30}O_5$	*n*- or adhulupone (+H_2O)	
	18.75	363.1809	$C_{20}H_{28}O_6$	cohumulone (+O)	
51	18.91	319.1546	$C_{18}H_{24}O_5$	*n*-humulone (+O, −acetone)	**15b**
52	19.21	263.1286	$C_{15}H_{20}O_4$	*n*- or adhumulone (−methylpentenoyl group, −2H)	
	19.21	363.1809	$C_{20}H_{28}O_6$	cohumulone (+O)	
	19.21	393.1914	$C_{21}H_{30}O_7$	adhumulone (+2O)	**11c**[f]
	19.21	303.1234	$C_{17}H_{20}O_5$	cohumulone (+O, −acetone, −2H)	
	19.21	319.1547	$C_{18}H_{24}O_5$	*n*- or adhumulone (+O, −acetone)	
53	19.55	363.1805	$C_{20}H_{28}O_6$	cohumulone (+O)	
	19.55	377.1960	$C_{21}H_{30}O_6$	adhumulone (+O)	**13c**
	19.55	251.1283	$C_{14}H_{20}O_4$	cohumulone (−methylpentenoyl group)	
	19.55	393.1907	$C_{21}H_{30}O_7$	*n*- or adhumulone (+2O)	
54	19.94	377.1960	$C_{21}H_{30}O_6$	*n*-humulone (+O)	**13b**
	19.94	349.2012	$C_{20}H_{30}O_5$	*n*- or adhulupone (+H_2O)	
	19.94	393.1907	$C_{21}H_{30}O_7$	adhumulone (+2O)	**11c′**[f]
55	20.33	393.1909	$C_{21}H_{30}O_7$	*n*-humulone (+2O)	**11b**

Table 9. (continued)

56	20.72	361.1651	$C_{20}H_{26}O_6$	cohumulone (+O, −2H)
	20.72	377.1963	$C_{21}H_{30}O_6$	*n*- or adhumulone (+O)
	20.72	393.1913	$C_{21}H_{30}O_7$	*n*- or adhumulone (+2O)
57	21.26	349.2012	$C_{20}H_{30}O_5$	*n*- or adhulupone (+H_2O)
	21.26	365.1960	$C_{20}H_{30}O_6$	cohumulone (+H_2O)
	21.26	375.1805	$C_{21}H_{28}O_6$	*n*- or adhumulone (+O, −2H)
	21.26	393.1910	$C_{21}H_{30}O_7$	*n*- or adhumulone (+2O)
	21.26	379.1754	$C_{20}H_{28}O_7$	cohumulone (+2O)
	21.26	407.1702	$C_{21}H_{28}O_8$	*n*- or adhumulone (+3O, −2H)
58	21.66	375.1808	$C_{21}H_{28}O_6$	*n*- or adhumulone (+O, −2H)
	21.66	363.1809	$C_{20}H_{28}O_6$	cohumulone (+O)
	21.66	393.1914	$C_{21}H_{30}O_7$	*n*- or adhumulone (+2O)
59	22.09	375.1807	$C_{21}H_{28}O_6$	*n*- or adhumulone (+O, −2H)
	22.09	393.1913	$C_{21}H_{30}O_7$	*n*- or adhumulone (+2O)
	22.09	395.2068	$C_{21}H_{32}O_7$	*n*- or adhumulone (+O, +H_2O)
	22.09	361.1652	$C_{20}H_{26}O_6$	cohumulone (+O, −2H)
60	22.35	333.1703	$C_{19}H_{26}O_5$	posthumulone[d] (isomerization)
	22.35	263.1286	$C_{15}H_{20}O_4$	*n*- or adhumulone (−methylpentenoyl group, −2H)
61	22.54	375.1808	$C_{21}H_{28}O_6$	*n*- or adhumulone (+O, −2H)
	22.54	349.2015	$C_{20}H_{30}O_5$	*n*- or adhulupone (+H_2O)
	22.54	409.2227	$C_{22}H_{34}O_7$	prehumulone[e] (+O, +H_2O)
	22.54	393.1913	$C_{21}H_{30}O_7$	*n*- or adhumulone (+2O)
62	22.85	361.1649	$C_{20}H_{26}O_6$	cohumulone (+O, −2H)
	22.85	363.1804	$C_{20}H_{28}O_6$	cohumulone (+O)
63	23.08	375.1806	$C_{21}H_{28}O_6$	*n*- or adhumulone (+O, −2H)
64	23.34	377.1961	$C_{21}H_{30}O_6$	*n*- or adhumulone (+O)
	23.34	331.1908	$C_{20}H_{28}O_4$	*n*- or adhulupone (isomerization)
	23.34	343.1543	$C_{20}H_{24}O_5$	cohumulone (−4H)
	23.34	363.1805	$C_{20}H_{28}O_6$	cohumulone (+O)
	23.34	393.1910	$C_{21}H_{30}O_7$	*n*- or adhumulone (+2O)
	23.34	439.2329	$C_{23}H_{36}O_8$	possible minor congener of α-acids[g] (+2O, +H_2O)
65	23.62	361.1653	$C_{20}H_{26}O_6$	cohumulone (+O, −2H)
	23.62	333.1703	$C_{19}H_{26}O_5$	posthumulone[d] (isomerization)
	23.62	391.1759	$C_{21}H_{28}O_7$	*n*- or adhumulone (+2O, −2H)
66	23.86	377.1962	$C_{21}H_{30}O_6$	*n*- or adhumulone (+O)
67	24.09	411.2014	$C_{21}H_{32}O_8$	*n*- or adhumulone (+2O, +H_2O)
	24.09	363.1808	$C_{20}H_{28}O_6$	cohumulone (+O)
	24.09	331.1910	$C_{20}H_{28}O_4$	*n*- or adhulupone (isomerization)
	24.09	317.1391	$C_{18}H_{22}O_5$	*n*- or adhumulone (+O, −acetone, −2H)
	24.09	393.1914	$C_{21}H_{30}O_7$	*n*- or adhumulone (+2O)

Table 9. (continued)

68	24.31	363.1806	$C_{20}H_{28}O_6$	cohumulone (+O)
	24.31	377.1962	$C_{21}H_{30}O_6$	*n*- or adhumulone (+O)
69	24.72	363.1804	$C_{20}H_{28}O_6$	cohumulone (+O)
	24.72	361.1649	$C_{20}H_{26}O_6$	cohumulone (+O, −2H)
	24.72	393.1910	$C_{21}H_{30}O_7$	*n*- or adhumulone (+2O)
70	25.00	375.1805	$C_{21}H_{28}O_6$	*n*- or adhumulone (+O, −2H)
	25.00	379.1754	$C_{20}H_{28}O_7$	cohumulone (+2O)
	25.00	265.1077	$C_{14}H_{18}O_5$	cohumulone (+O, −methylpentenoyl group, −2H)
	25.00	345.1700	$C_{20}H_{26}O_5$	cohumulone (−2H)
	25.00	359.1857	$C_{21}H_{28}O_5$	*n*- or adhumulone (−2H)
71	25.24	361.1651	$C_{20}H_{26}O_6$	cohumulone (+O, −2H)
	25.24	411.2018	$C_{21}H_{32}O_8$	*n*- or adhumulone (+2O, +H_2O)
	25.24	393.1914	$C_{21}H_{30}O_7$	*n*- or adhumulone (+2O)
	25.24	377.1964	$C_{21}H_{30}O_6$	*n*- or adhumulone (+O)
72	25.47	333.2064	$C_{20}H_{30}O_4$	*n*- or adhulupone (+2H)
	25.47	349.1649	$C_{19}H_{26}O_6$	posthumulone[d] (+O)
	25.47	379.1754	$C_{20}H_{28}O_7$	cohumulone (+2O)
	25.47	447.2380	$C_{25}H_{36}O_7$	colupulone (+3O)
73	25.65	393.1913	$C_{21}H_{30}O_7$	*n*- or adhumulone (+2O)
74	25.94	375.1806	$C_{21}H_{28}O_6$	*n*- or adhumulone (+O, −2H)
	25.94	377.1599	$C_{20}H_{26}O_7$	cohumulone (+2O, −2H)
	25.94	361.1651	$C_{20}H_{26}O_6$	cohumulone (+O, −2H)
75	26.20	379.1754	$C_{20}H_{28}O_7$	cohumulone (+2O)
	26.20	421.2223	$C_{23}H_{34}O_7$	possible minor congener of α-acids[g] (+2O)
76	26.83	331.1908	$C_{20}H_{28}O_4$	*n*- or adhulupone (isomerization)
	26.83	349.2013	$C_{20}H_{30}O_5$	*n*- or adhulupone (+H_2O)
	26.83	409.1860	$C_{21}H_{30}O_8$	*n*- or adhumulone (+3O)
	26.83	423.2382	$C_{23}H_{36}O_7$	possible minor congener of α-acids[g] (+O, +H_2O)
	26.83	375.1805	$C_{21}H_{28}O_6$	*n*- or adhumulone (+O, −2H)
77	27.06	347.1857	$C_{20}H_{28}O_5$	cohumulone (isomerization)
	27.06	375.1807	$C_{21}H_{28}O_6$	*n*- or adhumulone (+O, −2H)
	27.06	391.1756	$C_{21}H_{28}O_7$	*n*- or adhumulone (+2O, −2H)
	27.06	409.1861	$C_{21}H_{30}O_8$	*n*- or adhumulone (+3O)
78	27.24	351.1808	$C_{19}H_{28}O_6$	posthumulone[d] (+H_2O)
	27.24	345.1704	$C_{20}H_{26}O_5$	cohumulone (−2H)
	27.24	375.1809	$C_{21}H_{28}O_6$	*n*- or adhumulone (+O, −2H)
	27.24	391.1759	$C_{21}H_{28}O_7$	*n*- or adhumulone (+2O, −2H)
79	27.42	289.1439	$C_{17}H_{22}O_4$	cohumulone (−acetone)
	27.42	333.1700	$C_{19}H_{26}O_5$	posthumulone[d] (isomerization)
	27.42	423.2378	$C_{23}H_{36}O_7$	possible minor congener of α-acids[g] (+O, +H_2O)

Table 9. (continued)

80	27.71	375.1807	$C_{21}H_{28}O_6$	*n*- or adhumulone (+O, −2H)	
	27.71	363.1808	$C_{20}H_{28}O_6$	cohumulone (+O)	
	27.71	331.1546	$C_{19}H_{24}O_5$	posthumulone[d] (−2H)	
	27.71	335.1859	$C_{19}H_{28}O_5$	cohulupone (+H_2O)	
	27.71	393.1913	$C_{21}H_{30}O_7$	*n*- or adhumulone (+2O)	
	27.71	423.2381	$C_{23}H_{36}O_7$	possible minor congener of α-acids[g] (+O, +H_2O)	
	27.71	345.1703	$C_{20}H_{26}O_5$	cohumulone (−2H)	
81	27.97	377.1960	$C_{21}H_{30}O_6$	*n*- or adhumulone (+O)	
	27.97	421.2223	$C_{23}H_{34}O_7$	possible minor congener of α-acids[g] (+2O)	
82	28.20	375.1805	$C_{21}H_{28}O_6$	*n*- or adhumulone (+O, −2H)	
	28.20	357.1699	$C_{21}H_{26}O_5$	*n*- or adhumulone (−4H)	
	28.20	345.1700	$C_{20}H_{26}O_5$	cohumulone (−2H)	
83	28.46	421.2225	$C_{23}H_{34}O_7$	possible minor congener of α-acids[g] (+2O)	
	28.46	377.1964	$C_{21}H_{30}O_6$	*n*- or adhumulone (+O)	
	28.46	365.1965	$C_{20}H_{30}O_6$	cohumulone (+H_2O)	
	28.46	393.1914	$C_{21}H_{30}O_7$	*n*- or adhumulone (+2O)	
84	28.90	345.1703	$C_{20}H_{26}O_5$	cohumulone (−2H)	
	28.90	363.1809	$C_{20}H_{28}O_6$	cohumulone (+O)	
	28.90	375.1808	$C_{21}H_{28}O_6$	*n*- or adhumulone (+O, −2H)	
	28.90	419.2070	$C_{23}H_{32}O_7$	possible minor congener of α-acids[g] (+2O, −2H)	
85	29.18	351.1807	$C_{19}H_{28}O_6$	cohulupone (+O, +H_2O)	
86	29.53	377.1963	$C_{21}H_{30}O_6$	*n*- or adhumulone (+O)	
	29.53	363.1808	$C_{20}H_{28}O_6$	cohumulone (+O)	
87	29.91	375.1805	$C_{21}H_{28}O_6$	*n*- or adhumulone (+O, −2H)	
88	30.44	333.1701	$C_{19}H_{26}O_5$	posthumulone[d] (isomerization)	
	30.44	363.1806	$C_{20}H_{28}O_6$	cohumulone (+O)	
	30.44	279.1233	$C_{15}H_{20}O_5$	*n*- or adhumulone (+O, −methylpentenoyl group, −2H)	
	30.44	377.1962	$C_{21}H_{30}O_6$	*n*- or adhumulone (+O)	
	30.44	431.2432	$C_{25}H_{36}O_6$	colupulone (+2O)	
89	30.93	303.1599	$C_{18}H_{24}O_4$	*n*- or adhumulone (−acetone)	
	30.93	375.1808	$C_{21}H_{28}O_6$	*n*- or adhumulone (+O, −2H)	
	30.93	391.1758	$C_{21}H_{28}O_7$	*n*- or adhumulone (+2O, −2H)	
	30.93	363.1809	$C_{20}H_{28}O_6$	cohumulone (+O)	
90	31.19	393.1912	$C_{21}H_{30}O_7$	*n*- or adhumulone (+2O)	
91	31.40	363.1807	$C_{20}H_{28}O_6$	cohumulone (+O)	**6a**
92	31.91	365.1963	$C_{20}H_{30}O_6$	cohumulone (+H_2O)	
	31.91	359.1858	$C_{21}H_{28}O_5$	*n*- or adhumulone (−2H)	
93	32.22	365.1959	$C_{20}H_{30}O_6$	cohumulone (+H_2O)	
	32.22	359.1855	$C_{21}H_{28}O_5$	*n*- or adhumulone (−2H)	
	32.22	377.1960	$C_{21}H_{30}O_6$	*n*- or adhumulone (+O)	

Table 9. (continued)

94	32.91	349.2014	$C_{20}H_{30}O_5$	*n*- or adhulupone (+H_2O)	
	32.91	377.1962	$C_{21}H_{30}O_6$	*n*- or adhumulone (+O)	
	32.91	437.2174	$C_{23}H_{34}O_8$	possible minor congener of α-acids[g] (+3O)	
	32.91	395.2066	$C_{21}H_{32}O_7$	*n*- or adhumulone (+O, +H_2O)	
	32.91	409.1859	$C_{21}H_{30}O_8$	*n*- or adhumulone (+3O)	
95	33.58	365.1961	$C_{20}H_{30}O_6$	*n*- or adhulupone (+O, +H_2O)	
	33.58	347.1856	$C_{20}H_{28}O_5$	cohumulone (isomerization)	**3a**
	33.58	377.1960	$C_{21}H_{30}O_6$	*n*- or adhumulone (+O)	
96	33.87	359.1856	$C_{21}H_{28}O_5$	*n*- or adhumulone (−2H)	
	33.87	333.1701	$C_{19}H_{26}O_5$	posthumulone[d] (isomerization)	
97	34.13	377.1962	$C_{21}H_{30}O_6$	adhumulone (+O)	**6c**[f]
	34.13	347.1856	$C_{20}H_{28}O_5$	cohumulone (isomerization)	**4a**
	34.13	387.1803	$C_{22}H_{28}O_6$	prehumulone[e] (+O, −4H)	
98	34.77	317.1752	$C_{19}H_{26}O_4$	cohulupone	**5a**
99	35.16	377.1962	$C_{21}H_{30}O_6$	adhumulone (+O)	**6c′**[f]
100	35.60	377.1964	$C_{21}H_{30}O_6$	*n*-humulone (+O)	**6b**
101	35.91	365.1962	$C_{20}H_{30}O_6$	cohumulone (+H_2O)	
102	36.63	347.1857	$C_{20}H_{28}O_5$	cohumulone (isomerization)	
103	37.84	277.1441	$C_{16}H_{22}O_4$	prehumulone[e] (−methylpentenoyl group, −2H)	
	37.84	361.2014	$C_{21}H_{30}O_5$	*n*- and adhumulone (isomerization)	**3b**, **3c**
104	38.25	361.2016	$C_{21}H_{30}O_5$	*n*- and adhumulone (isomerization)	**4b**, **4c**
105	39.04	331.1910	$C_{20}H_{28}O_4$	*n*- and adhulupone	**5b**, **5c**
	39.04	363.1808	$C_{20}H_{28}O_6$	cohumulone (+O)	
106	39.92	379.2119	$C_{21}H_{32}O_6$	*n*- or adhumulone (+H_2O)	
107	40.26	377.1964	$C_{21}H_{30}O_6$	*n*- or adhumulone (+O)	

[a]Shown in Figure 38.

[b]Indicated by observed accurate *m/z*.

[c]Possible reactions to yield the molecule are given in parentheses.

[d]A minor congener of α-acids, which possesses a propanoyl side chain.

[e]A minor congener of α-acids, which possesses an isohexanoyl side chain.

[f]Each of the following compounds exists as two diastereomers: adhumulinone [adhumulinone A (**6c**) and adhumulinone B (**6c′**)]; 4′-hydroxyalloadhumulinone [4′-hydroxyalloadhumulinone A (**11c**) and 4′-hydroxyalloadhumulinone B (**11c′**)]; 4′-hydroxyallo-*cis*-adhumulinone [4′-hydroxyallo-*cis*-adhumulinone A (**17c**) and 4′-hydroxyallo-*cis*-adhumulinone B (**17c′**)]; and *cis*-oxyadhumulinic acid [*cis*-oxyadhumulinic acid A (**18c**) and *cis*-oxyadhumulinic acid B (**18c′**)].

[g]A possible minor congener of α-acids, which possesses an isoheptanoyl side chain.

All the structurally elucidated compounds in MHBA possess a β-tricarbonyl moiety in their structures similar to α-, β- and iso-α-acids (Figures 1, 17, and 21). In the product ion scan of the reference standards using HPLC-ESI/MS/MS, common fragment ions (*m/z* 111 for co-congener and *m/z* 125 for *n*- and ad-congeners) originating from the β-tricarbonyl moiety including the acyl side chains were detected (Figure 39 and Table 10). To check whether all the components in MHBA (including unidentified ones) possess the β-tricarbonyl moiety, precursor ion scans of *m/z* 111 and *m/z* 125 were conducted. The results shown in Figure 40 clearly demonstrate that the MHBA components give fragment ions of *m/z* 111 and *m/z* 125 by MS/MS analysis, suggesting that all the components in MHBA possess a β-tricarbonyl moiety. The behavior of the MHBA components on CH_2Cl_2/H_2O partition (i.e., extractable in CH_2Cl_2 under acidic but not alkaline conditions) also supported the presence of the β-tricarbonyl moiety, which possesses acidic properties (Figure 41).

Taken together, these findings suggest MHBA are mainly composed of α-acid-derived oxides, which possess a common β-tricarbonyl moiety.

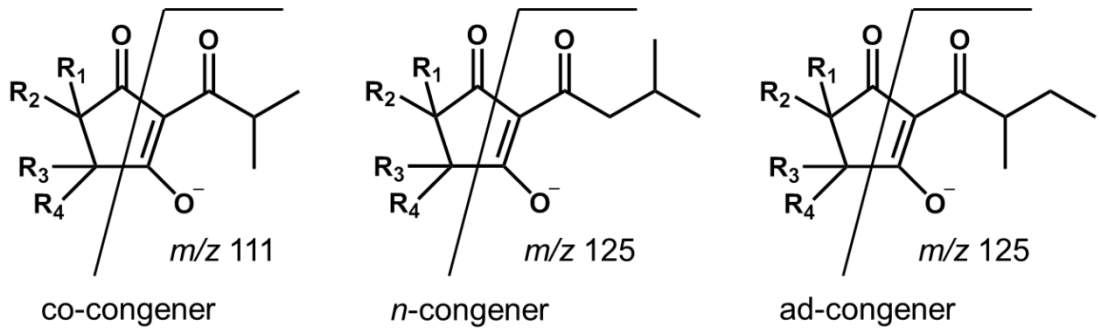

Figure 39. Common fragmentation patterns of iso-α-acid-derivatives by MS/MS analysis.

Table 10. Fragment ions of reference compounds produced by MS/MS analysis

Congener type	Compound	Molecular formula	Molecular ion $[M-H]^-$ (*m/z*)	Major MS^2 ions (*m/z*)[a]
co-	*cis*-isocohumulone (**3a**)	$C_{20}H_{28}O_5$	347	181, 233, 163, 209, 165, **111**, 191, 189, 178, 245
	trans-isocohumulone (**4a**)	$C_{20}H_{28}O_5$	347	181, 233, 209, 207, 235, 163, **111**, 165, 137, 190
	cohumulinone (**6a**)	$C_{20}H_{28}O_6$	363	249, 139, 206, 178, **111**, 191, 165, 163, 277, 167
	4'-hydroxyallocohumulinone (**11a**)	$C_{20}H_{28}O_7$	379	139, 165, 167, 249, 179, 163, 209, 125, 223, **111**
	4'-hydroxyallo-*cis*-cohumulinone (**17a**)	$C_{20}H_{28}O_7$	379	249, 167, 207, 139, 178, 197, 181, **111**, 231, 163
	cis-oxycohumulinic acid (**18a**)	$C_{14}H_{20}O_5$	267	181, 163, **111**, 137, 85, 139, 113, 152, 125, 95
	cohulupone (**5a**)	$C_{19}H_{26}O_4$	317	205, 233, 133, 152, **111**, 219, 180, 191, 137, 165
n-	*cis*-isohumulone (**3b**)	$C_{21}H_{30}O_5$	361	195, 163, 179, **125**, 153, 247, 177, 223, 155, 139
	trans-isohumulone (**4b**)	$C_{21}H_{30}O_5$	361	195, 179, 223, 247, **125**, 163, 153, 221, 177, 191
	humulinone (**6b**)	$C_{21}H_{30}O_6$	377	139, 263, 192, 220, 205, **125**, 165, 211, 163, 181
	4'-hydroxyallohumulinone (**11b**)	$C_{21}H_{30}O_7$	393	139, **125**, 181, 205, 165, 249, 263, 195, 150, 221
	4'-hydroxyallo-*cis*-humulinone (**17b**)	$C_{21}H_{30}O_7$	393	263, 139, 192, 220, 221, 181, **125**, 211, 179, 195
	cis-oxyhumulinic acid (**18b**)	$C_{15}H_{22}O_5$	281	195, 177, 139, **125**, 124, 152, 111, 101, 73, 127
	tricyclooxyisohumulone A (**12b**)	$C_{21}H_{30}O_6$	377	**125**, 377, 245, 275, 285, 207, 149, 201, 188, 175
	tricyclooxyisohumulone B (**13b**)	$C_{21}H_{30}O_6$	377	377, **125**, 188, 293, 165, 231, 245, 275, 303, 174
	deisopropyltricycloisohumulone (**15b**)	$C_{18}H_{24}O_5$	319	**125**, 165, 217, 189, 149, 173, 137, 257, 167, 319
	hulupone (**5b**)	$C_{20}H_{28}O_4$	331	219, 191, 247, 166, 205, **125**, 233, 133, 124, 179
ad-	*cis*-isoadhumulone (**3c**)	$C_{21}H_{30}O_5$	361	195, 191, 223, 179, **125**, 163, 247, 196, 167, 177
	trans-isoadhumulone (**4c**)	$C_{21}H_{30}O_5$	361	195, 223, 221, 179, 191, 177, 247, 196, 178, **125**
	adhumulinone A (**6c**)[b]	$C_{21}H_{30}O_6$	377	263, 139, **125**, 181, 192, 220, 99, 195, 211, 205

Table 10. (continued)

Congener type	Compound	Molecular formula	Molecular ion $[M-H]^-$ (*m/z*)	Major MS^2 ions (*m/z*)[a]
ad-	adhumulinone B (**6c'**)[b]	$C_{21}H_{30}O_6$	377	263, 139, **125**, 181, 211, 179, 163, 220, 191, 121
	4'-hydroxyalloadhumulinone A (**11c**)[b]	$C_{21}H_{30}O_7$	393	139, **125**, 181, 263, 195, 205, 99, 221, 165, 223
	4'-hydroxyalloadhumulinone B (**11c'**)[b]	$C_{21}H_{30}O_7$	393	139, **125**, 181, 263, 195, 165, 223, 205, 221, 192

[a]The fragment ions observed within top 10 intensity are listed in order of intensity.

[b]Adhumulinone and 4'-hydroxyalloadhumulinone exist as two diastereomers, respectively, as desicribed in chapeters 1 and 3.

Notes: The fragment ions characteristic to the β-tricarbonyl moiety (*m/z* 111 for co-congener and *m/z* 125 for *n*- and ad-congeners) are underlined.

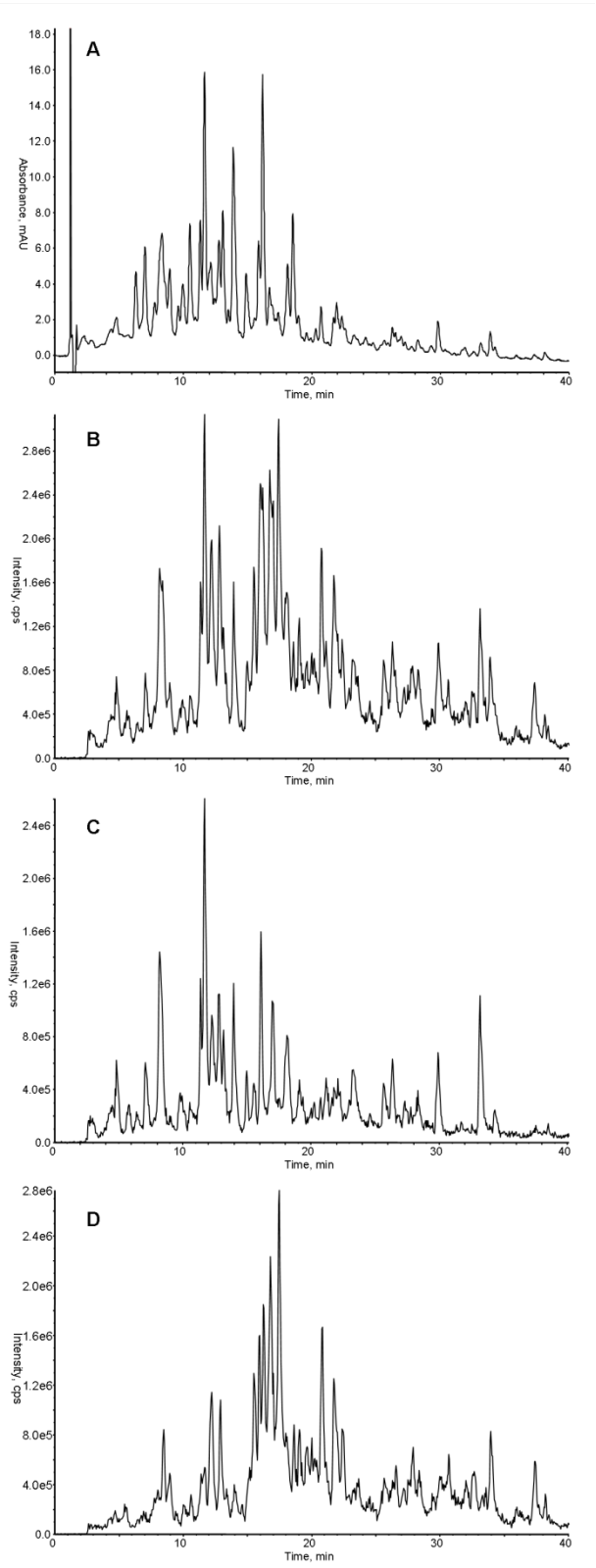

Figure 40. HPLC-PDA-MS/MS analysis of the MHBA fraction.

(A) Chromatogram of UV at 270 nm, (B) TIC of precursor ion scans of *m/z* 111 and 125, (C) chromatogram of precursor ion scan of *m/z* 111, and (D) chromatogram of precursor ion scan of *m/z* 125.

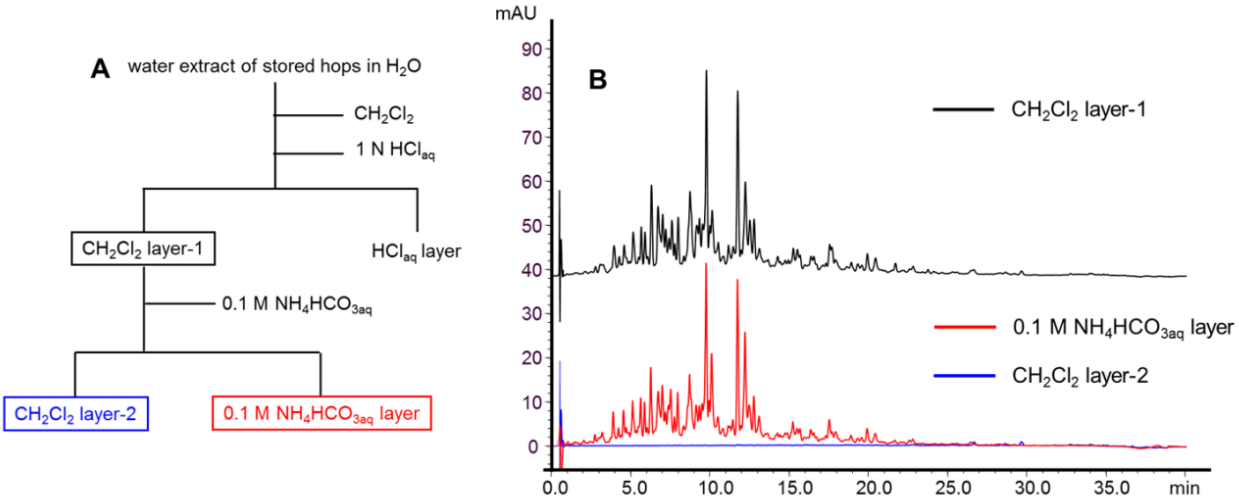

Figure 41. A: Scheme of acid-base partition experiment of the MHBA components. B: HPLC chromatograms of the CH_2Cl_2 layer-1 (partitioned with HCl_{aq}) (black line), CH_2Cl_2 layer-2 (partitioned with 0.1 M NH_4HCO_{3aq}) (blue line), and 0.1 M NH_4HCO_{3aq} layer (red line).

Development of a quantitative analytical method for HPLC analysis of whole MHBA.

Because the UV absorption characteristics of the MHBA components were attributed to the common chromophore (β-tricarbonyl moiety), the difference in the molar absorbance coefficient among the components at 270 nm was assumed to be small.[86] Therefore, the author quantified the total MHBA components using the calibration curve prepared from tricyclooxyisohumulone A (**12b**), which is an abundant (Figure 42) and stable constituent of MHBA as described in chapters 3 and 4.

In the HPLC analysis, the author defines the MHBA elution region as shown in Figure 42 [i.e., from just after the elution of caffeine to just before that of *trans*-isocohumulone (**4a**)]. The caffeine peak was used as an indicator to distinguish the peaks belonging to MHBA from the peaks around the solvent shock, which were not retained by the ODS column. Because the MHBA region was quite broad (i.e., from t_R ~3 min to t_R ~25 min), a correction for baseline drift generated from the solvent gradient was required in order to integrate the total peak area precisely. The baseline drift could be

eliminated by subtracting the chromatogram signals of blank (H_2O) analysis using the analytical software function (Figure 43).

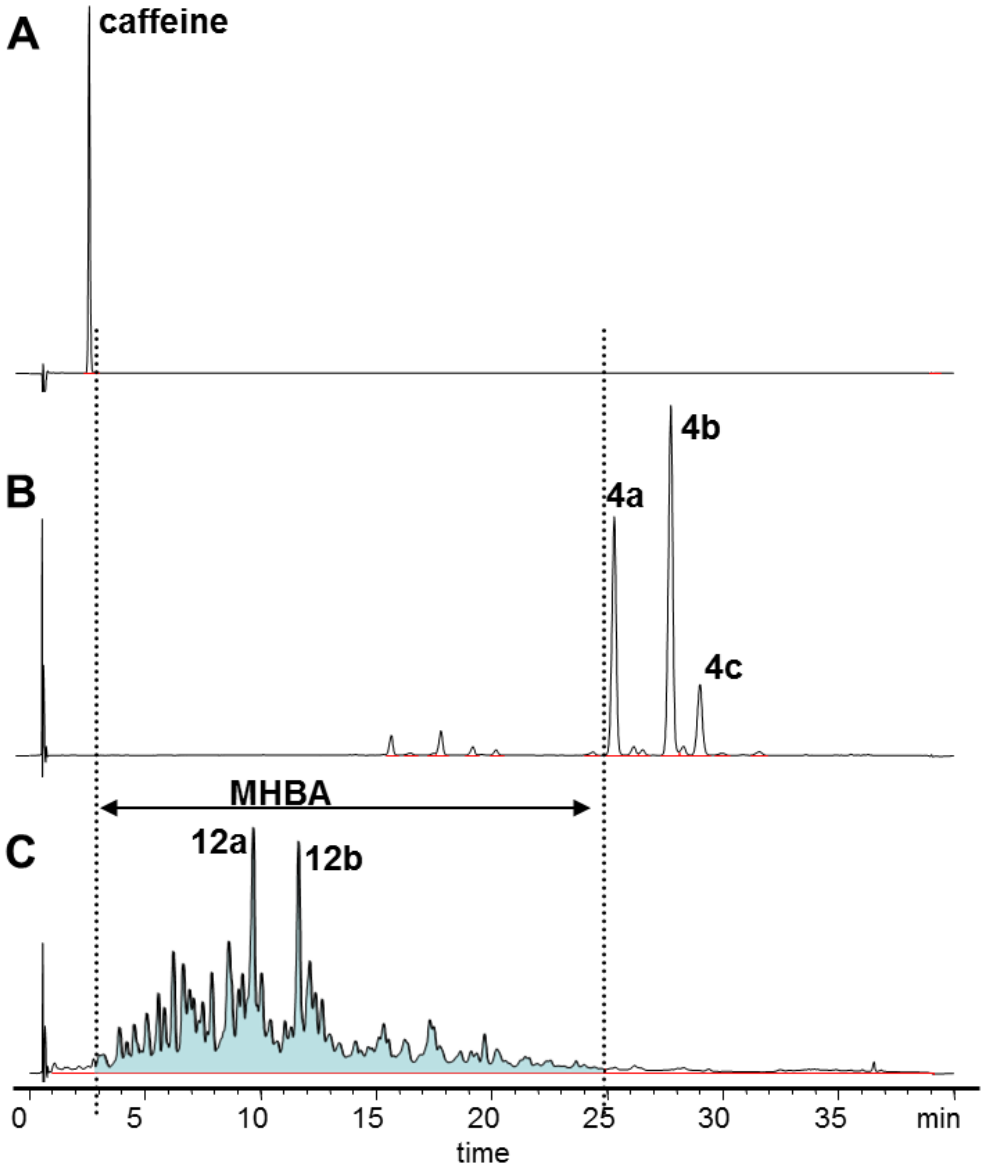

Figure 42. HPLC chromatograms of (A) caffeine, (B) ICS-I3 standard, and (C) the MHBA fraction. ICS-I3 contains mainly *trans*-isocohumulone (**4a**), *trans*-isohumulone (**4b**), and *trans*-isoadhumulone (**4c**). Integrated peak area of whole MHBA is shown in color.

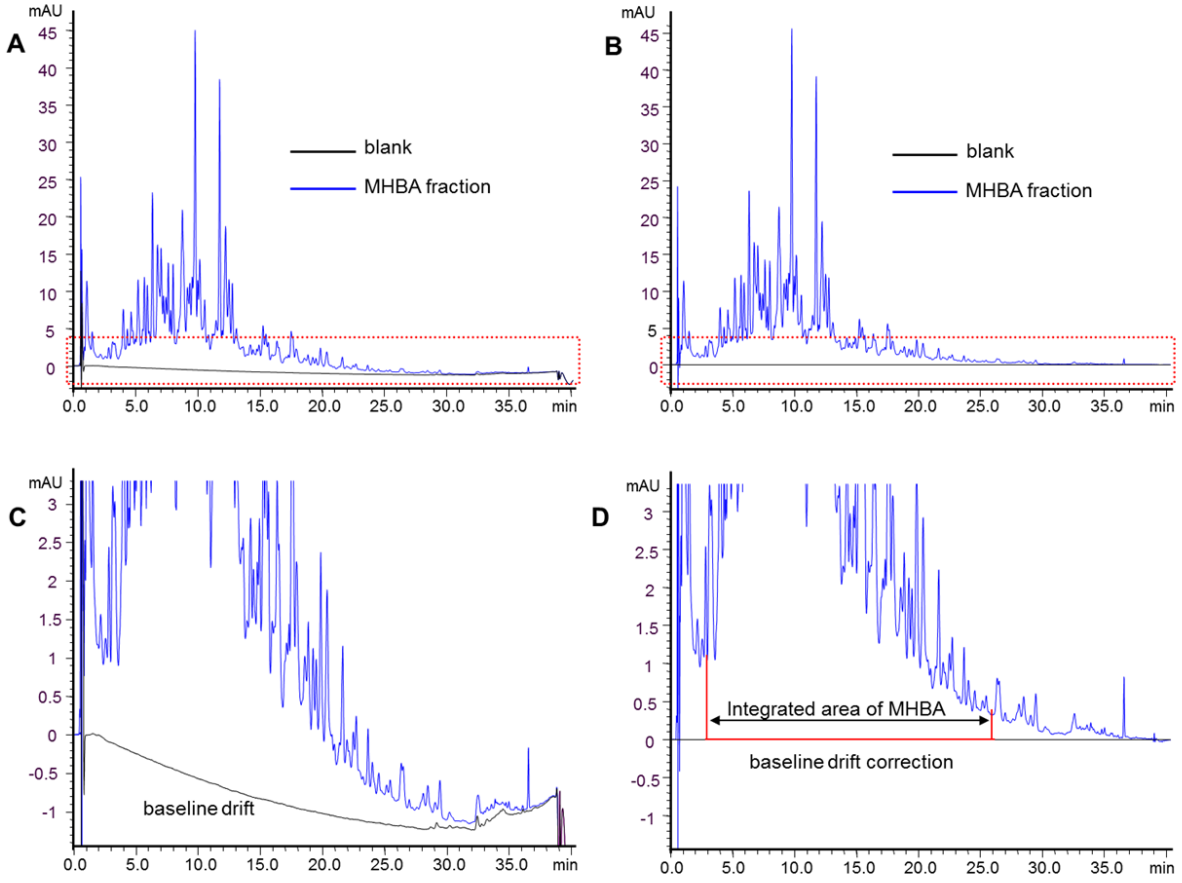

Figure 43. HPLC chromatograms of the blank (H_2O) and MHBA fraction (A) before and (B) after baseline drift correction. HPLC chromatograms of (C) and (D) correspond to the enlarged views of the enclosed regions of (A) and (B), respectively. Integrated peak area of whole MHBA is enclosed by a red line in (D).

The MHBA fraction was prepared independently four times and the whole MHBA content was subsequently determined by HPLC analysis. The quantitative value of MHBA accounted for 95.8% of the solid content of the fraction with few errors [%RSD, 2.05 (n=4)] (Table 11). The almost complete consistency of the solid content and quantitative value obtained by HPLC analysis demonstrated that this analytical method was suitable for the quantitative analysis of whole MHBA.

Table 11. MHBA concentration determined by HPLC analysis of the MHBA fraction

No. of experiment	Yield of the MHBA fraction (mg)[a]	HPLC quantitative value of MHBA (mg/mL)[b]	HPLC quantitative value of MHBA/solid content (%)
1	111	0.469	93.8
2	110	0.491	98.2
3	109	0.482	96.4
4	107	0.473	94.6
Average	109	0.479	95.8
SD	1.80	0.00981	1.96
%RSD	1.65	2.05	2.05

[a]From the water extract of stored hops (600 mg).

[b]Concentration of the solid content of the MHBA fraction in the analyzed solution was 0.500 mg/mL.

Evaluation of the intra- and inter-day analytical precision of whole MHBA.

A model carbonated beverage containing a water extract of stored hops was prepared to evaluate the precision of the author's analytical procedure for the analysis of whole MHBA in a beverage. MHBA in the beverage were extracted with CH_2Cl_2 under acidic conditions and then analyzed by HPLC. To evaluate the extraction efficiency, the residual aqueous solution was extracted with CH_2Cl_2 for a second time. Subsequent analysis showed that the second extract contained very few MHBA components (Figure 44). Indeed, the entire MHBA peak area of the second extract was less than 4% of that of the first extract. Thus, whole MHBA was found to be almost completely extracted in the analytical procedure. The intra- and inter-day precision of the analyses were found to be below 1.55% RSD and 1.10% RSD, respectively (Table 12). These results established that this analytical method had a high degree of precision and reproducibility. Efficient extraction of whole MHBA together with the high level of precision obtained using an external standard method indicate that no internal standard is required for the analysis. Further studies to verify the precision of analysis between laboratories are needed to confirm the versatility of the author's novel analytical method.

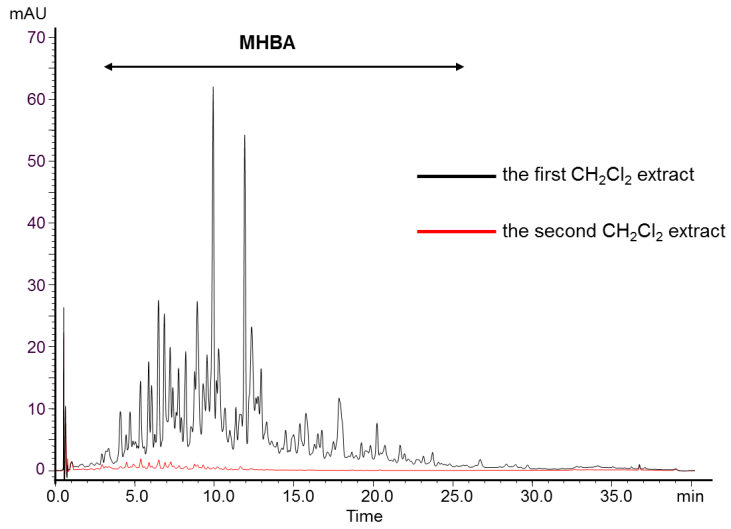

Figure 44. HPLC chromatograms of the first (black line) and second (red line) CH_2Cl_2 extract from the beverage containing MHBA.

Table 12. The intra- and inter-day precision of HPLC analysis of MHBA in a model beverage

		MHBA concentration (mg/L) (average, n=6)	SD	%RSD
Intra-day evaluation	day 1	124	0.527	0.425
	day 2	126	1.36	1.08
	day 3	126	1.18	0.937
	day 4	124	0.628	0.506
	day 5	123	1.29	1.05
	day 6	123	1.91	1.55
Inter-day evaluation		124	1.37	1.10

Quantitative analysis of whole MHBA in commercial beers.

Using the developed analytical method, the author investigated the amount of MHBA in several commercial beers. The MHBA concentration along with the determined iso-α-acid concentration in the beers are summarized in Table 13. The major brands of beer made in Japan (brands A–E) contained 19–38 mg/L MHBA and 16–27 mg/L iso-α-acids. These were all lager type beers. However, beer made in foreign countries (brands F–K) contained 20–210 mg/L MHBA and 3.3–64 mg/L iso-α-acids.

Among them, India Pale Ale (brands G, H, and I) had the highest content of MHBA and iso-α-acids. These results seem reasonable, given that India Pale Ale is brewed with large amounts of hops. Lambic (brands J and K) also showed high concentrations of MHBA, whereas the iso-α-acid concentration was the lowest among the beers analyzed in this study. Because Lambic is manufactured over a long period of time for aging, iso-α-acids are presumably subject to degradation during this period[30, 31, 69] and may indeed be transformed into MHBA components.

Table 13. Concentrations of MHBA and iso-α-acids in commercial beers

Brand	Type of beer	MHBA concentration (mg/L)	Iso-α-acid concentration (mg/L)
A	Lager	19.1	18.3
B	Lager	31.8	23.6
C	Lager	30.4	26.6
D	Lager	24.1	15.7
E	Lager	38.0	26.7
F	Lager	20.1	16.5
G	India Pale Ale	210	62.6
H	India Pale Ale	181	64.0
I	India Pale Ale	152	41.5
J	Lambic	100	3.34
K	Lambic	151	6.39

Unlike the model carbonated beverage, beers contain extracts of malt and other raw materials. The constituents derived from these materials (i.e., other than hops) may co-elute at the MHBA region in the HPLC analysis and the calculated MHBA concentration in beers may be overestimated. Nonetheless, whole MHBA content is certainly reflected in the quantified value because whole MHBA could be extracted by the author's method but not the method using isooctane as extracting solvent (Figure 37). Bittering components, such as iso-α-acids, in beer are usually measured by extracting them with isooctane, and the bitterness unit (BU) is thus calculated using the isooctane extract.[83, 84] It is empirically known that beers with the same BU or iso-α-acid

concentration often differ in their bitterness quality.[9, 23] In these cases, MHBA, which could not be measured by previous techniques, may influence the bitterness quality of the beer. Further studies are needed to clarify the effects of MHBA on beer properties.

In conclusion, it was found that MHBA could be selectively prepared from a water extract of stored hops simply by extraction with CH_2Cl_2 under acidic conditions. Detailed analyses of the chemical properties of MHBA show that they are (i) principally composed of the oxidation products of α-acids, and (ii) possess a common β-tricarbonyl moiety. A quantitative analytical HPLC method for whole MHBA was developed and validated, which enabled the quantification of whole MHBA in a carbonated beverage. All of these findings are helpful for evaluating the effects of MHBA on the properties of beer. Moreover, this technique will be invaluable for examining the bioactivities related to the health benefits of ingesting MHBA. Studies on the health benefits brought about by consuming MHBA are currently in progress.

Summary

The bitter acids in hops and beer, such as α-, β- and iso-α-acids, are known to affect beer quality and display various physiological effects. However, these compounds readily oxidize, and the effect of the oxides on the properties of beer or their potential health benefits are not well understood. In this study, the author developed a simple preparative method for the bitter acid oxide fraction derived from hops and designated the constituents as matured hop bitter acids (MHBA). HPLC-PDA-ESI/HRMS and MS^2 revealed that MHBA are primarily composed of α-acid-derived oxides, which possess a common β-tricarbonyl moiety in their structures similar to α-, β- and iso-α-acids. The author also developed a quantitative analytical method of whole MHBA by HPLC, which showed high precision and reproducibility. Using the author's newly developed method, the concentration of whole MHBA in several commercial beers was evaluated for the first time. The obtained results will promote the study of bitter acid oxides.

REFERENCES

(1) Clark, S. M.; Vaitheeswaran, V.; Ambrose, S. J.; Purves, R. W.; Page, J. E. Transcriptome analysis of bitter acid biosynthesis and precursor pathways in hop (*Humulus lupulus*). *BMC Plant Biol.* **2013**, *13*, 12.

(2) Anonymous. Current review. *J. Inst. Brew.* **1957**, *63*, 281-293.

(3) Krauss, G.; Cook, A. H.; Verzele, M. Recommendations concerning nomenclature of hop resin components. *J. Inst. Brew.* **1969**, *75*, 340-342.

(4) Palamand, S. R.; Aldenhoff, J. M. Bitter tasting compounds of beer. Chemistry and taste properties of some hop resin compounds. *J. Agric. Food Chem.* **1973**, *21*, 535-543.

(5) De Keukeleire, D. Fundamentals of beer and hop chemistry. *Quim. Nova* **2000**, *23*, 108-112.

(6) Eyres, G. T.; Marriott, P. J.; Dufour, J.-P. Comparison of odor-active compounds in the spicy fraction of hop (*Humulus lupulus* L.) essential oil from four different varieties. *J. Agric. Food Chem.* **2007**, *55*, 6252-6261.

(7) Kankolongo Cibaka, M.-L.; Gros, J.; Nizet, S.; Collin, S. Quantitation of selected terpenoids and mercaptans in the dual-purpose hop varieties Amarillo, Citra, Hallertau Blanc, Mosaic, and Sorachi Ace. *J. Agric. Food Chem.* **2015**, *63*, 3022-3030.

(8) Burton, J. S.; Stevens, R. Evaluation of hops. XI. The hard resin and presence of hulupinic acid. *J. Inst. Brew.* **1965**, *71*, 51-56.

(9) Ono, M.; Kakudo, Y.; Yamamoto, R.; Nagami, K.; Kumada, J. Simultaneous analysis of hop bittering components by high-performance liquid chromatography. II. Evaluation of hop deterioration. *J. Am. Soc. Brew. Chem.* **1987**, *45*, 61-69.

(10) Lermusieau, G.; Collin, S. Varietal discrimination of hop pellets. II. Comparison between fresh and aged samples. *J. Am. Soc. Brew. Chem.* **2001**, *59*, 39-43.

(11) Dusek, M.; Olsovska, J.; Krofta, K.; Jurkova, M.; Mikyska, A. Qualitative determination of β-acids and their transformation products in beer and hop using HR/AM-LC-MS/MS. *J. Agric. Food Chem.* **2014**, *62*, 7690-7697.

(12) Jaskula, B.; Kafarski, P.; Aerts, G.; De Cooman, L. A kinetic study on the isomerization of hop α-acids. *J. Agric. Food Chem.* **2008**, *56*, 6408-6415.

(13) Haseleu, G.; Lagemann, A.; Stephan, A.; Intelmann, D.; Dunkel, A.; Hofmann, T. Quantitative sensomics profiling of hop-derived bitter compounds throughout a full-scale beer manufacturing process. *J. Agric. Food Chem.* **2010**, *58*, 7930-7939.

(14) Intelmann, D.; Haseleu, G.; Dunkel, A.; Lagemann, A.; Stephan, A.; Hofmann, T. Comprehensive sensomics analysis of hop-derived bitter compounds during storage of beer. *J. Agric. Food Chem.* **2011**, *59*, 1939-1953.

(15) Takoi, K.; Koie, K.; Itoga, Y.; Katayama, Y.; Shimase, M.; Nakayama, Y.; Watari, J. Biotransformation of hop-derived monoterpene alcohols by lager yeast and their contribution to the flavor of hopped beer. *J. Agric. Food Chem.* **2010**, *58*, 5050-5058.

(16) Kishimoto, T.; Wanikawa, A.; Kagami, N.; Kawatsura, K. Analysis of hop-derived terpenoids in beer and evaluation of their behavior using the stir bar-sorptive extraction method with GC-MS. *J. Agric. Food Chem.* **2005**, *53*, 4701-4707.

(17) Huvaere, K.; Andersen, M. L.; Skibsted, L. H.; Heyerick, A.; De Keukeleire, D. Photooxidative degradation of beer bittering principles: a key step on the route to lightstruck flavor formation in beer. *J. Agric. Food Chem.* **2005**, *53*, 1489-1494.

(18) Schoenberger, C.; Kostelecky, T. 125th anniversary review: the role of hops in brewing. *J. Inst. Brew.* **2011**, *117*, 259-267.

(19) Almaguer, C.; Schoenberger, C.; Gastl, M.; Arendt, E. K.; Becker, T. *Humulus lupulus* - a story that begs to be told. A review. *J. Inst. Brew.* **2014**, *120*, 289-314.

(20) Steenackers, B.; De, C. L.; De, V. D. Chemical transformations of characteristic hop secondary metabolites in relation to beer properties and the brewing process: a review. *Food Chem.* **2015**, *172*, 742-756.

(21) Urban, J.; Dahlberg, C. J.; Carroll, B. J.; Kaminsky, W. Absolute configuration of beer's bitter compounds. *Angew. Chem., Int. Ed.* **2013**, *52*, 1553-1555.

(22) Malowicki, M. G.; Shellhammer, T. H. Isomerization and degradation kinetics of

hop (*Humulus lupulus*) acids in a model wort-boiling system. *J. Agric. Food Chem.* **2005**, *53*, 4434-4439.

(23) Kowaka, M.; Kokubo, E. Composition of bitter substances of hops and characteristics of beer bitterness. *J. Am. Soc. Brew. Chem.* **1977**, *35*, 16-21.

(24) Bishop, L. R.; Whitear, A. L.; Inman, W. R. Scientific basis for beer foam formation and cling. *J. Inst. Brew.* **1974**, *80*, 68-80.

(25) Haseleu, G.; Intelmann, D.; Hofmann, T. Structure determination and sensory evaluation of novel bitter compounds formed from β-acids of hop (*Humulus lupulus* L.) upon wort boiling. *Food Chem.* **2009**, *116*, 71-81.

(26) Haseleu, G.; Intelmann, D.; Hofmann, T. Identification and RP-HPLC-ESI-MS/MS quantitation of bitter-tasting β-acid transformation products in beer. *J. Agric. Food Chem.* **2009**, *57*, 7480-7489.

(27) Rakete, S.; Berger, R.; Boehme, S.; Glomb, M. A. Oxidation of isohumulones induces the formation of carboxylic acids by hydrolytic cleavage. *J. Agric. Food Chem.* **2014**, *62*, 7541-7549.

(28) De Cooman, L.; Aerts, G.; Overmeire, H.; De Keukeleire, D. Alterations of the profiles of iso-α-acids during beer ageing, marked instability of trans-iso-α-acids and implications for beer bitterness consistency in relation to tetrahydroiso-α-acids. *J. Inst. Brew.* **2000**, *106*, 169-178.

(29) Araki, S.; Takashio, M.; Shinotsuka, K. A new parameter for determination of the extent of staling in beer. *J. Am. Soc. Brew. Chem.* **2002**, *60*, 26-30.

(30) Intelmann, D.; Kummerloewe, G.; Haseleu, G.; Desmer, N.; Schulze, K.; Froehlich, R.; Frank, O.; Luy, B.; Hofmann, T. Structures of storage-induced transformation products of the beer's bitter principles, revealed by sophisticated NMR spectroscopic and LC-MS techniques. *Chem. - Eur. J.* **2009**, *15*, 13047-13058.

(31) Intelmann, D.; Demmer, O.; Desmer, N.; Hofmann, T. ^{18}O stable isotope labeling, quantitative model experiments, and molecular dynamics simulation studies on the

trans-specific degradation of the bitter tasting iso-α-acids of beer. *J. Agric. Food Chem.* **2009**, *57*, 11014-11023.

(32) Howard, G. A.; Martin, P. A. Bittering power of stored hops. *J. Inst. Brew.* **1964**, *70*, 424-439.

(33) Rigby, F. L. The practical significance of recent developments in the chemical analysis of hops. *Brew. Dig.* **1958**, 50-59.

(34) Laws, D. R. J. Hop resins and beer flavour V. The significance of oxidized hop resins in brewing. *J. Inst. Brew.* **1968**, *74*, 178-182.

(35) Dresel, M.; Dunkel, A.; Hofmann, T. Sensomics analysis of key bitter compounds in the hard resin of hops (*Humulus lupulus* L.) and their contribution to the bitter profile of pilsner-type beer. *J. Agric. Food Chem.* **2015**, *63*, 3402-3418.

(36) Almaguer, C.; Gastl, M.; Arendt, E. K.; Becker, T. Contributions of hop hard resins to beer quality. *BrewingSci.—Monatsschr. Brauwiss.* **2012**, *65*, 118-129.

(37) Whitear, A. L. Changes in resin composition and brewing behaviour of hops during storage. *J. Inst. Brew.* **1966**, *72*, 177-183.

(38) Aitken, R. A.; Bruce, A.; Harris, J. O.; Seaton, J. C. The bitterness of hop-derived materials in beer. *J. Inst. Brew.* **1970**, *76*, 29-36.

(39) Foster, R. T., II; Weber, K.; Jangaard, N. O. The effect of hop acids transformation on kettle utilization and finished beer flavor and aroma. *Tech. Q. - Master Brew. Assoc. Am.* **1981**, *18*, 109-115.

(40) Cook, A. H.; Howard, G. A.; Slater, C. A. Chemistry of hop constituents. VIII. Oxidation of humulone and cohumulone. *J. Inst. Brew.* **1955**, *61*, 321-325.

(41) Shoolery, J. N.; Verzele, M.; Alderweireldt, F. On the structure of humulinone. *Tetrahedron* **1960**, *9*, 271-274.

(42) Verzele, M.; Anteunis, M.; Alderweireldt, F. Isohumulones. *J. Inst. Brew.* **1965**, *71*, 232-239.

(43) Cook, A. H.; Harris, G. Chemistry of hop constituents. I. Humulinone, a new

constituent of hops. *J. Chem. Soc.* **1950**, 1873-1876.

(44) Verzele, M.; Govaert, F. Humulinone. Its alleged occurrence in hops. *J. Chem. Soc.* **1952**, 3313-3315.

(45) Whitear, A. L.; Hudson, J. R. Hop resins and beer flavor. III. Hop resins in beer. *J. Inst. Brew.* **1964**, *70*, 24-30.

(46) Whitear, A. L. Reversed-phase paper chromatography of hop resins. *Chem. Ind. (London, U. K.)* **1962**, 1464-1465.

(47) Laws, D. R. J.; McGuinness, J. D. Analytical and brewing significance of a tricyclic oxidation product of humulone (tricyclodehydroisohumulone). *J. Inst. Brew.* **1974**, *80*, 174-180.

(48) Ashurst, P. R.; Elvidge, J. A. Hop constituents. XXVIII. Structure of an autoxidation product of humulone. *J. Chem. Soc. C* **1966**, *7*, 675-676.

(49) Van Cleemput, M.; Cattoor, K.; De Bosscher, K.; Haegeman, G.; De Keukeleire, D.; Heyerick, A. Hop (*Humulus lupulus*)-derived bitter acids as multipotent bioactive compounds. *J. Nat. Prod.* **2009**, *72*, 1220-1230.

(50) Karabin, M.; Hudcova, T.; Jelinek, L.; Dostalek, P. Biologically active compounds from hops and prospects for their use. *Compr. Rev. Food Sci. Food Saf.* **2016**, *15*, 542-567.

(51) Shimamura, M.; Hazato, T.; Ashino, H.; Yamamoto, Y.; Iwasaki, E.; Tobe, H.; Yamamoto, K.; Yamamoto, S. Inhibition of angiogenesis by humulone, a bitter acid from beer hop. *Biochem. Biophys. Res. Commun.* **2001**, *289*, 220-224.

(52) Chen, W.-J.; Lin, J.-K. Mechanisms of cancer chemoprevention by hop bitter acids (beer aroma) through induction of apoptosis mediated by fas and caspase cascades. *J. Agric. Food Chem.* **2004**, *52*, 55-64.

(53) Lamy, V.; Roussi, S.; Chaabi, M.; Gosse, F.; Lobstein, A.; Raul, F. Lupulone, a hop bitter acid, activates different death pathways involving apoptotic TRAIL-receptors, in human colon tumor cells and in their derived metastatic cells. *Apoptosis* **2008**, *13*,

1232-1242.

(54) Yasukawa, K.; Takeuchi, M.; Takido, M. Humulon, a bitter in the hop, inhibits tumor promotion by 12-O-tetradecanoylphorbol-13-acetate in two-stage carcinogenesis in mouse skin. *Oncology* **1995**, *52*, 156-158.

(55) Yamamoto, K.; Wang, J.; Yamamoto, S.; Tobe, H. Suppression of cyclooxygenase-2 gene transcription by humulon of beer hop extract studied with reference to glucocorticoid. *FEBS Lett.* **2000**, *465*, 103-106.

(56) Hougee, S.; Faber, J.; Sanders, A.; van den Berg, W. B.; Garssen, J.; Smit, H. F.; Hoijer, M. A. Selective inhibition of COX-2 by a standardized CO_2 extract of *Humulus lupulus in vitro* and its activity in a mouse model of zymosan-induced arthritis. *Planta Med.* **2006**, *72*, 228-233.

(57) Tagashira, M.; Watanabe, M.; Uemitsu, N. Antioxidative activity of hop bitter acids and their analogues. *Biosci. Biotechnol. Biochem.* **1995**, *59*, 740-742.

(58) Tobe, H.; Kubota, M.; Yamaguchi, M.; Kocha, T.; Aoyagi, T. Apoptosis to HL-60 by humulone. *Biosci. Biotechnol. Biochem.* **1997**, *61*, 1027-1029.

(59) Liu, Y.; Gu, X.-h.; Tang, J.; Liu, K. Antioxidant activities of hops (*Humulus lupulus*) and their products. *J. Am. Soc. Brew. Chem.* **2007**, *65*, 116-121.

(60) Yajima, H.; Noguchi, T.; Ikeshima, E.; Shiraki, M.; Kanaya, T.; Tsuboyama-Kasaoka, N.; Ezaki, O.; Oikawa, S.; Kondo, K. Prevention of diet-induced obesity by dietary isomerized hop extract containing isohumulones, in rodents. *Int. J. Obes. (Lond)* **2005**, *29*, 991-997.

(61) Sasaoka, N.; Sakamoto, M.; Kanemori, S.; Kan, M.; Tsukano, C.; Takemoto, Y.; Kakizuka, A. Long-term oral administration of hop flower extracts mitigates alzheimer phenotypes in mice. *PLoS One* **2014**, *9*, e87185/1-e87185/12, 12 pp.

(62) Intelmann, D.; Haseleu, G.; Hofmann, T. LC-MS/MS quantitation of hop-derived bitter compounds in beer using the ECHO technique. *J. Agric. Food Chem.* **2009**, *57*, 1172-1182.

(63) James, P.; Tynan, T.; McMurrough, I.; Byrne, J. Preparation, purification and separation by high performance liquid chromatography of humulinic acids, dehydrohumulinic acids, and hulupones. *J. Inst. Brew.* **1990**, *96*, 137-141.

(64) Hughes, P. S. Preparative regime for the purification of bitter acids derived from hops (*Humulus lupulus* L.). *J. Chromatogr., A* **1996**, *731*, 327-330.

(65) Alderweireldt, F.; Verzele, M.; Anteunis, M.; Dierckens, J. The isomerization products of humulone. *Bull. Soc. Chim. Belg.* **1965**, *74*, 29-40.

(66) Howard, G. A.; Slater, C. A. Chemistry of hop constituents. XII. The structure of humulinone. *J. Chem. Soc.* **1958**, 1460-1462.

(67) Stevens, R.; Wright, D. Evaluation of hops. X. Hulupones and the significance of β acids in brewing. *J. Inst. Brew.* **1961**, *67*, 496-501.

(68) De Keukeleire, D.; Siaens, E.; Verzele, M. Regiospecific singlet oxygen oxidation of (-) R-tetrahydrohumulone and hexahydrocolupulone. *Bull. Soc. Chim. Belg.* **1976**, *85*, 293-304.

(69) Intelmann, D.; Hofmann, T. On the autoxidation of bitter-tasting iso-α-acids in beer. *J. Agric. Food Chem.* **2010**, *58*, 5059-5067.

(70) Verzele, M.; De Keukeleire, D. In *Chemistry and Analysis of Hop and Beer Bitter Acids*; Elsevier: Amsterdam, The Netherlands. **1991**, pp. 90.

(71) de Almeida, N. E. C.; Homem-de-Mello, P.; De Keukeleire, D.; Cardoso, D. R. Reactivity of beer bitter acids toward the 1-hydroxyethyl radical as probed by spin-trapping electron paramagnetic resonance (EPR) and electrospray ionization-tandem mass spectrometry (ESI-MS/MS). *J. Agric. Food Chem.* **2011**, *59*, 4183-4191.

(72) Winkelmann, K.; Heilmann, J.; Zerbe, O.; Rali, T.; Sticher, O. New phloroglucinol derivatives from *Hypericum papuanum*. *J. Nat. Prod.* **2000**, *63*, 104-108.

(73) Winkelmann, K.; Heilmann, J.; Zerbe, O.; Rali, T.; Sticher, O. Further prenylated bi- and tricyclic phloroglucinol derivatives from *Hypericum papuanum*. *Helv. Chim. Acta*

2001, *84*, 3380-3392.

(74) Waertgen, K.; Wichtl, M. Tricyclooxyisohumulone: a new autoxidation product of humulone. *Planta Med.* **1991**, *57*, 498-499.

(75) Yin, S.; Wang, X.-N.; Fan, C.-Q.; Liao, S.-G.; Yue, J.-M. The first limonoid peroxide in the meliaceae family: Walsuronoid A from *Walsura robusta*. *Org. Lett.* **2007**, *9*, 2353-2356.

(76) Manzo, E.; Ciavatta, M. L.; Melck, D.; Schupp, P.; de Voogd, N.; Gavagnin, M. Aromatic cyclic peroxides and related keto-compounds from the *Plakortis* sp. component of a sponge consortium. *J. Nat. Prod.* **2009**, *72*, 1547-1551.

(77) De Potter, M. D. K., D. Tricyclo-oxy- and tricyclo-hydroperoxycolupulones. *Bull. Soc. Chim. Belg.* **1978**, *23*, 108-112.

(78) European Brewery Convention (EBC). Methods: 7.5 Bitter substances in hops and hop products: Lead conductance value and total resin, soft resin and hard resin, In *Analytica-EBC*; Fachverlag Hans Carl: Nürnberg, Germany, 2008.

(79) Stevens, J. F.; Taylor, A. W.; Clawson, J. E.; Deinzer, M. L. Fate of xanthohumol and related prenylflavonoids from hops to beer. *J. Agric. Food Chem.* **1999**, *47*, 2421-2428.

(80) Dierckens, J.; Verzele, M. Oxidation products of humulone and their stereoisomerism. *J. Inst. Brew.* **1969**, *75*, 453-456.

(81) Furihata, K.; Seto, H. J-Resolved HMBC, a new NMR technique for measuring heteronuclear long-range coupling constants. *Tetrahedron Lett.* **1999**, *40*, 6271-6275.

(82) Morvai, M.; Nagy, T.; Kocsis, A.; Szabo, L. F.; Podanyi, B. Effect of oxygen substituents on two- and three-bond carbon-proton spin-spin coupling constants. *Magn. Reson. Chem.* **2000**, *38*, 343-359.

(83) Howard, G. A. Institute of brewing analysis committee estimation of the bitterness of beer. *J. Inst. Brew.* **1968**, *74*, 249-251.

(84) Anonymous. Bitterness units of beer and wort. *J. Am. Soc. Brew. Chem.* **1996**, *54*, 186-187.

(85) Vanhoenacker, G.; De Keukeleire, D.; Sandra, P. Analysis of iso-α-acids and reduced iso-α-acids in beer by direct injection and liquid chromatography with ultraviolet absorbance detection or with mass spectrometry. *J. Chromatogr. A* **2004**, *1035*, 53-61.
(86) Verzele, M.; Steenbeke, G.; Verhagen, L. C.; Strating, J. Improved analysis by liquid chromatography of iso-alpha acids. *J. High Resolut. Chromatogr.* **1990**, *13*, 826-831.

List of publications

Chapter 1

Taniguchi, Y.; Matsukura, Y.; Ozaki, H.; Nishimura, K.; Shindo, K. Identification and quantification of the oxidation products derived from α-acids and β-acids during storage of hops (*Humulus lupulus* L.). *J. Agric. Food Chem.* **2013**, *61*, 3121-3130.

DOI: 10.1021/jf3047187

Chapter 2

Taniguchi, Y.; Taniguchi, H.; Matsukura, Y.; Kawachi, Y.; Shindo, K. Structural elucidation of humulone autoxidation products and analysis of their occurrence in stored hops. *J. Nat. Prod.* **2014**, *77*, 1252-1261.

DOI: 10.1021/np4008427

Chapter 3

Taniguchi, Y.; Taniguchi, H.; Yamada, M.; Matsukura, Y.; Koizumi, H.; Furihata, K.; Shindo, K. Analysis of the components of hard resin in hops (*Humulus lupulus* L.) and structural elucidation of their transformation products formed during the brewing process. *J. Agric. Food Chem.* **2014**, *62*, 11602-11612.

DOI: 10.1021/jf504394h

Chapter 4

Taniguchi, Y.; Yamada, M.; Taniguchi, H.; Matsukura, Y.; Shindo, K. Chemical characterization of beer aging products derived from hard resin components in hops (*Humulus lupulus* L.). *J. Agric. Food Chem.* **2015**, *63*, 10181-10191.

DOI: 10.1021/acs.jafc.5b04138

Chapter 5

Taniguchi, Y.; Matsukura, Y.; Taniguchi, H.; Koizumi, H.; Katayama, M. Development of preparative and analytical methods of the hop bitter acid oxide fraction and chemical properties of its components. *Biosci. Biotechnol. Biochem.* **2015**, *79*, 1684-1694.

DOI: 10.1080/09168451.2015.1042832

Acknowledgments

The author wishes to express his sincere thanks to Professor Naoki Mori, Division of Applied Life Sciences, Graduate School of Agriculture, Kyoto University, for his kind guidance and encouragement.

The author is deeply grateful to Professor Kazutoshi Shindo, Department of Food and Nutrition, Faculty of Human Sciences and Design, Japan Women's University, for his valuable advice and guidance throughout this work.

The author gratefully thanks to Dr. Keiji Deuchi, General Manager of Central Laboratories for Key Technologies, KIRIN Co., Ltd., Dr. Yutaka Konishi, Dr. Toshihiro Komeda, and Dr. Tomoyuki Kadota for providing the author with the opportunity of writing this thesis and for their kind support. The author would like to express his appreciation to Mr. Mikio Katayama, Research Laboratories for Health Science & Food Technologies, KIRIN Co., Ltd., for providing the author with the opportunity of researching hop chemistry.

The author is indebted to Ms. Yasuko Matsukura, Ms. Harumi Taniguchi, Ms. Makiko Yamada, Ms. Hiromi Ozaki, Dr. Koichi Nishimura, Mr. Yasuji Kawachi, Dr. Hideki Koizumi, and Dr. Kazuo Furihata for their collaboration and valuable discussions. The author thanks to Dr. Kazuaki Ohara and Ms. Yumie Morimoto-Kobayashi for useful discussions.

Thanks are due to all the members of Central Laboratories for Key Technologies and Research Laboratories for Health Science & Food Technologies, KIRIN Co., Ltd., for their helpful support and assistance. The author wishes to thank KIRIN Co., Ltd., for permission to present this study.

Finally, the author wishes to express his deep gratitude to his family for their encouragement and support.

Yoshimasa Taniguchi